DEPARTMENT OF TRANSPORTATION

Evaluation and Refinement of Minnesota Queue Warning Systems

John Hourdos, Principal Investigator
Civil, Environmental, and Geo- Engineering
University of Minnesota

MARCH 2023

Research Report
Final Report 2023-05

To request this document in an alternative format, such as braille or large print, call 651-366-4718 or 1-800-657-3774 (Greater Minnesota) or email your request to ADArequest.dot@state.mn.us. Please request at least one week in advance.

Technical Report Documentation Page

1. Report No.	2.	3. Recipients Accession No.	
MN 2023-05			
4. Title and Subtitle Evaluation and Refinement of Minnesota Queue Warning Systems		5. Report Date March 2023 6.	
7. Author(s) John Hourdos and Jake Robbennolt		8. Performing Organization Report No.	
9. Performing Organization Name and Address Department of Civil, Environmental, and Geo- Engineering University of Minnesota 500 Pillsbury Dr SE Minneapolis, MN 55455		10. Project/Task/Work Unit No. CTS #2019027 11. Contract (C) or Grant (G) No. (c) 1003325 (wo) 84	
12. Sponsoring Organization Name and Address Minnesota Department of Transportation Office of Research & Innovation 395 John Ireland Boulevard, MS 330 St. Paul, Minnesota 55155-1899		13. Type of Report and Period Covered 14. Sponsoring Agency Code	
15. Supplementary Notes http://mdl.mndot.gov/			

16. Abstract (Limit: 250 words)

This study evaluates the first and a second implementations of the MN-QWARN queue warning algorithm developed by Hourdos et al. (1). This algorithm was developed to detect specific crash prone conditions created by traffic oscillations (shockwaves) on freeway systems. The MN-QWARN system was specifically calibrated for the freeway studied in Hourdos et al. (1) and was moved to a new location with minimal calibration. This evaluation found that the right-side model had a detection rate of 25% and a false alarm rate of 36%. The left-side model had a detection rate of 64% and a false alarm rate of 23%. We also note high over-warning rates on both lanes. Based on these findings, we recommend recalibrating the MN-QWARN algorithm at this location to examine improvements in performance.

17. Document Analysis/Descriptors	18. Availability Statement		
Traffic safety, Queuing, Warning systems, Algorithms, Crashes	No restrictions. Document available from: National Technical Information Services, Alexandria, Virginia 22312		
19. Security Class (this report) Unclassified	20. Security Class (this page) Unclassified	21. No. of Pages 115	22. Price

EVALUATION AND REFINEMENT OF MINNESOTA QUEUE WARNING SYSTEMS

FINAL REPORT

Prepared by:

John Hourdos and Jake Robbennolt

Department of Civil, Environmental, and Geo- Engineering
University of Minnesota

MARCH 2023

Published by:

Minnesota Department of Transportation
Office of Research & Innovation
395 John Ireland Boulevard, MS 330
St. Paul, Minnesota 55155-1899

ACKNOWLEDGMENTS

This work was supported by the Minnesota Department of Transportation (MnDOT). The authors would like to thank Garrett Schreiner, Brian Kary, Jesse Larson, and Douglas Lau of MnDOT for their assistance in this project. The authors would also like to thank Gordon Parikh and Derek Lehrke, formerly of the Minnesota Traffic Observatory University of Minnesota, for helping record video data and maintaining the data collection infrastructure.

TABLE OF CONTENTS

LIST OF FIGURES

LIST OF TABLES

EXECUTIVE SUMMARY

In 2017, a MnDOT-funded project developed and field-tested two Queue Warning systems that followed different philosophies regarding rear-end collision safety. The first system's philosophy followed the premise that freeway rear-end collisions tend to occur in extended stop-and-go traffic or at end-of-queue locations. The second Queue Warning system, later named MN-QWARN, was based on the hypothesis that not all congestion events are dangerous but there are certain traffic conditions that are crash prone regardless of whether they result in standing queues or not. Such crash prone conditions (CPC) can be isolated, fast moving, shockwaves involving only a small number of vehicles in the deceleration-stop-acceleration cycle. For such conditions, a much denser detection infrastructure is needed. One location where such conditions have been identified and which resulted in more than 100 crashes per year was the westbound section of I-94 in downtown Minneapolis, Minnesota. In this location, the Minnesota Traffic Observatory (MTO) has had a permanent Field Lab since 2002. Based on the framework proposed by Dr. Hourdos (56), this effort approaches the topic from the quantification of traffic flow to the multi-layer system design along with different approaches including the traffic assessment modeling and the development of control algorithms. The 2017 project focused mainly on the development of the MN-QWARN system and initial evaluation covering a short period of time.

The project described in this report had two major objectives. The first objective was to capitalize on the extensive surveillance and data collection infrastructure of the MTO to conduct a long-term evaluation of the MN-QWARN system as developed and deployed in the 2017 project. The second objective involves the fact that, following 2018, the original deployment site underwent a massive reconstruction aimed at, among other goals, a geometric solution to the high-crash problem. In anticipation of changes in congestion patterns due to the construction and in the interest of evaluating the transferability of the MN-QWARN system, the second objective involved the deployment of the system in a new site on the same roadway, approximately 0.75 miles upstream.

The MNQWARN system was first implemented in the right lane of a 1.7-mile-long freeway segment of westbound Interstate 94 (I-94 WB) near downtown Minneapolis, where the event frequency prior to the system's installation was 11.9 crashes per million vehicles traveled (MVT) and 111.8 near crashes per MVT. Machine vision detectors (MVDs) installed on a nearby rooftop captured the real-time vehicle data. The data were delivered to a server running the main control algorithm at the MTO via its communication network. The control algorithm assessed the "dangerousness" of the given traffic conditions and responded with a warning result based on a multi-metric traffic evaluation model and a control-reasoning heuristic.

MNQWARN was monitored during the three phases of the field implementation. Phase 1 lasted from March 1, 2016, to April 30, 2016, and involved the operation of the system in silent mode, meaning the sign was not activated but alarms were recorded. During this phase, the system's ability to operate correctly and reliably were tested and minor adjustments were made in the system parameters. Phase 2 lasted from May 1, 2016, to June 1, 2016, and involved full system operation as well as the introduction of a heuristic test to reduce the time it took the alarm to shut off at the end of the day when traffic returned to free flow. Phase 3 lasted from June 2, 2016, to August 31, 2016, and involved the full

operation of the system with no further changes or fine-tuning. The system continued running through August 31, 2018, with sporadic minor outages. The results presented in this report were gathered between June 2016 and August 2018. To determine the effectiveness of the system, video captured by MTO's rooftop station was watched by Undergraduate Research Assistance (UGRA) from the period of April 2016 to August 2018. During the reduction process, a shift in the data being captured by the UGRA occurred to ensure all aspects of the effectiveness of the system were being considered. All the events observed during the evaluation period were tabulated and sorted based on whether the drivers involved were warned or not warned about CPCs before the event, and if the drivers were not warned, the events were separated by the reason the system failed to warn them.

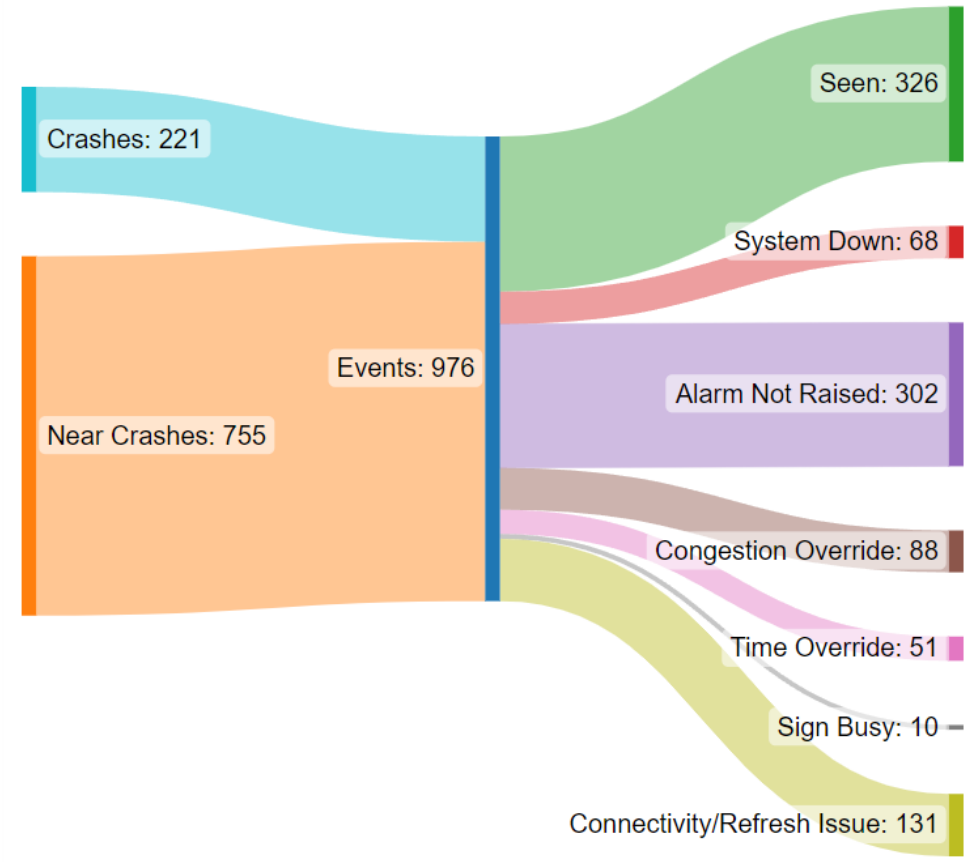

A second implementation of MN-QWARN aimed to test the transferability of the system. To take advantage of the extensive data collection and surveillance infrastructure of the MTO I94 Field Lab paired with the expectation of severe congestion upstream of the original test section due to the four-year-long reconstruction project, the project targeted the area over Hiawatha Ave as the second system evaluation site. Two new MTO traffic detection and monitoring stations were deployed and a specially installed MnDOT NIT pole for use in this project was instrumented and integrated into the MTO I-94 Field Lab system. These stations, described by their approximate location on the road, were the 11th Ave Solar station, the Median station, and the Hiawatha NIT pole station. The new implementation of the MN-QWARN algorithm used a changeable message sign at the far upstream end of the corridor

where there was also a Minnesota Department of Transportation (MNDOT) vehicle speed detector reporting 30-second average vehicle speed data.

Initial investigation in this project revealed that the two sides of the road experienced fundamentally different traffic-flow conditions. This fact required a dual, parallel implementation of the system with separate algorithms operating on the right and left lanes of the road. Alarms activated the following appropriate messages on the CMS: Slow Traffic Ahead Left Lanes, Slow Traffic Ahead Right Lanes, or Slow Traffic Ahead All Lanes.

The location of the second deployment had far fewer crashes than the original implementation and evaluation, making the earlier methodology difficult to replicate. There were not enough crashes or near crashes along this stretch of road to draw strong conclusions without waiting several years. For this reason, a new methodology for finding a ground truth of dangerous conditions was developed. A new methodology for the estimation of hypothetical vehicle trajectories given the sparce detector data available was used. Known vehicle trajectories can be ranked in categories based on their speed and deceleration rates to determine whether the respective drivers should have been warned. The methodology presented here is scalable and can be applied to any road section. However, for the purposes of this report, we examine the 2665-ft segment of roadway on I-94 in Minneapolis, where the queue warning system is deployed.

To rate the performance of the MN-QWARN algorithm, we define 4 major categories of events based on the ratings of each hypothetical vehicle. The first category (G) and most common is when drivers did not need to be warned and were not warned. The second category is when drivers were warned when they needed to be warned (Y). Both these cases are examples of successful operation of the algorithm. The third case is a failure of the system when the alarm was not raised but a warning was needed (N). This category corresponds to a missed alarm.

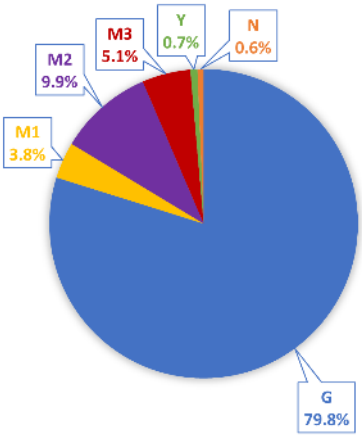

System Performance Left

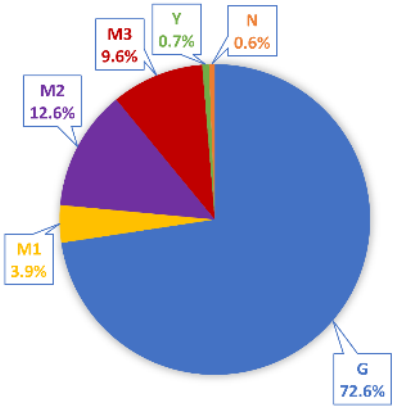

System Performance Middle

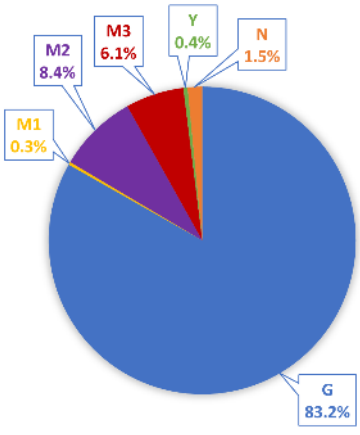

System Performance Right

Finally, the last category (M) is when drivers were warned and did not need to be. The latter is also split into three separate cases. M1 denotes when the driver was warned but should not have been because vehicles were going slowly under the sign and continued to move slowly throughout the study area (less

than 20 mph). M2 is when the driver was warned when decelerating to a stop in the study area but not at a high enough rate to be dangerous. Finally, M3 is when a vehicle's speed never dropped below 30 mph in the study area. This is the most important case to avoid since it erodes driver trust in the sign. To simplify the equations below, we define $M = M1 + M2 + M3$.

The evaluation metrics based on the hypothetical trajectories are helpful but are often on too fine of a time scale for a sign that is only updated every 30 seconds and an algorithm intended to warn groups of vehicles, not individual drivers. For this reason, it is important to group these trajectories into "events" made up of several dangerous trajectories. This is done using a heuristic process to determine the most important time periods each day for the sign to be on.

Once groups have been created, they can be categorized based on their relationship with alarms. A Missed group means the alarm did not come on within 5 minutes before or after the group. A Missed – Early Alarm means the alarm would not have been seen by any drivers in the group but was on and ended within 5 minutes of the beginning of the group. Similarly, a Missed – Late Alarm means the alarm came on within 5 minutes of the end of the group. Hit – Off Early means part of the group saw the alarm, but it went off before some vehicles at the end of the group saw it. Hit – On Late means the end of the group saw the alarm but not the beginning of the group. Hit – Short Alarm means the alarm came on late and went off early and Hit – Long Alarm means the alarm come on early and went off late. These events are categorized in Figure 5-3.

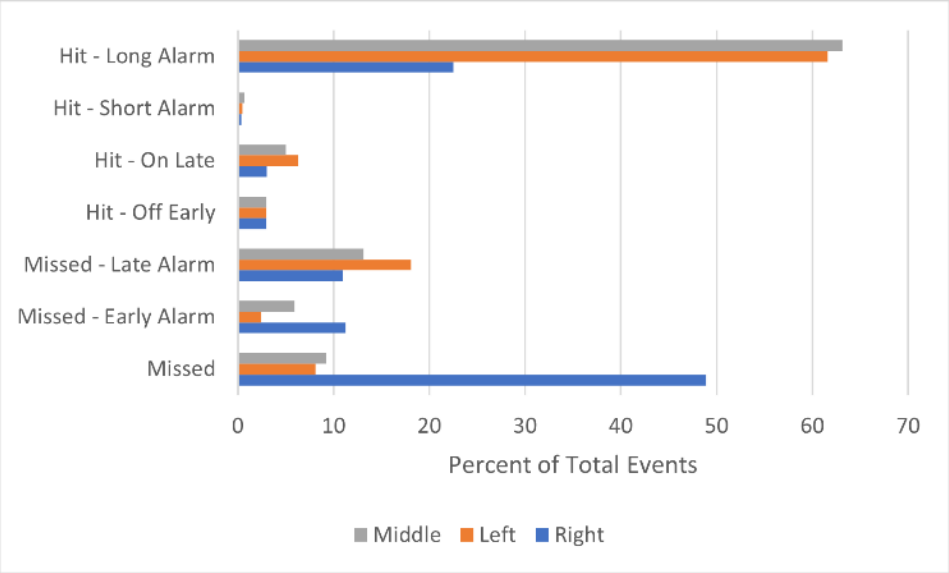

Result	Left	Middle	Right
Under-Warning	0.34%	0.28%	0.69%
Over-Warning	24%	26%	10%
Modified Over-Warning	21%	24%	8%

CHAPTER 1: INTRODUCTION

In 2016, US officials reported the occurrence of 7.2 million total motor vehicle crashes, including 34,439 fatalities (102). According to the Minnesota Department of Transportation (MnDOT), the average cost of a single crash was $7,200 when it involved only property damage, $87,000 to $600,000 when it involved injury, and as high as $11.1 million when the crash was fatal (103). In 2017, the Minnesota Department of Public Safety (DPS) reported 11,487 crashes occurred on freeways. These crashes accounted for the death of 31 people and the injury of 3,367 people (33).

Benefits to studying crashes and crash prevention systems include reduction of user costs such as delay, improved safety, and operation and maintenance savings. Recently, Chatterjee and Davis (22) confirmed that freeway rear-end events are the most frequently occurring capacity-reducing incidents on freeways and tend to occur when stopping shockwaves form. By developing a model for rear-end crash conditions and verifying it with video recordings of crash events, the study determines that drivers with reaction times longer than their following headways can be considered unsafe.

A MnDOT funded project (61) that ended in 2017 aimed to develop and field test two Queue Warning systems following different philosophies regarding rear-end collision safety. The first system's philosophy followed the premise that freeway rear-end collisions tend to occur in extended stop-and-go traffic or at end-of-queue locations. The second Queue Warning system, later named MN-QWARN, was based on the hypothesis that not all congestion events are dangerous but there are certain traffic conditions that are crash prone regardless of whether they result in standing queues or not. Such crash prone conditions (CPC) can be isolated, fast moving, shockwaves involving only a small number of vehicles in the deceleration-stop-acceleration cycle. For such conditions, a much denser detection infrastructure is needed. One location where such conditions have been identified and that has resulted in more than 100 crashes per year was the westbound section of I-94 in downtown Minneapolis, Minnesota. In this location, the Minnesota Traffic Observatory (MTO) has had a permanent Field Lab since 2002. Based on the framework proposed by Dr. Hourdos (56), this effort approaches the topic from the quantification of traffic flow to the multi-layer system design along with different approaches including the traffic assessment modeling and the development of control algorithms. The 2017 project, focused mainly on the development of the MN-QWARN system and an initial evaluation covering a short period of time.

The project described in this report had two major objectives. The first objective was to capitalize on the extensive surveillance and data collection infrastructure of the MTO to conduct a long-term evaluation of the MN-QWARN system as developed and deployed in the 2017 project. The second objective involved the fact that, following 2018, the original deployment site underwent a massive reconstruction aimed at, among other goals, a geometric solution to the high-crash problem. In anticipation of changes in congestion patterns due to the construction and in the interest of evaluating the transferability of the MN-QWARN system, the second objective involved the deployment of the system in a new site on the same roadway, approximately 0.75 miles upstream.

In the rest of this chapter, a thorough literature review of existing queue warning solutions is presented. Chapter 2 covers the results of the long-term evaluation of MN-QWARN in its original deployment. Chapter 3 describes the effort involved in the new deployment of the system and is followed by results from the one-year evaluation. Originally the project plan prescribed a two-year evaluation period, but the COVID-19 pandemic practically nullified the effort during the first year (2020).

1.1 WHAT IS A QUEUE WARNING SYSTEM?

A Queue Warning system attempts to detect when incidents may occur on the roadway and alert drivers to prevent them. Queue Warning systems come in many different forms, from fixed or variable message signage (Infrastructure only) to Connected Vehicle Vehicle2Vehicle (V2V) and/or Vehicle2Infrastructure (V2I) warnings. Queue Warning systems make use of a variety of detection systems and algorithms to inform drivers of the presence of downstream congestion, or otherwise crash prone conditions. Drivers can then anticipate hard braking, slow down, avoid erratic behavior, and ultimately reduce queueing-related conditions.

1.2 CRASH PRONE TRAFFIC CONDITIONS

Although crashes can happen any time there is a disturbance on the roadway, research has shown (56) that there are Crash Prone traffic Conditions (CPCs) that are associated with collisions, specifically rear-end collisions. Discerning what factors influence crash rates and the way in which they do so has been the aim of many research projects. Qiu and Nixon (112) reviewed the effects of weather on the likelihood of a crash. Kopelias et al. (74) studied how the combined effects of geometric, operational, and weather factors influence crash frequencies.

Traffic on urban freeways, however, tends to react differently to those factors. Golob and Recker (44) found that although collision with objects and the crashes of multiple vehicles are more frequent on wet roads, rear-end crashes are more likely to occur on dry roads with good visibility. They proposed that these rear-end crashes are highly correlated to large differences in individual speed like those seen in “stop-and-go” traffic. Such traffic conditions are often referred to as traffic shockwaves or traffic oscillations. These oscillations can be isolated and fast moving, involving only a small number of vehicles in the deceleration-stop-acceleration cycle. Zheng et al. (141) studied the effects of traffic oscillations on freeway crashes where they found that traffic oscillations and congestion are highly correlated to freeway crashes.

1.3 CRASH PREDICTION MODELS

Various crash-prediction models (7,16,108,97,96) have been developed using the aforementioned CPC risk factors. In such models, crash probability is used as a measure of the likelihood of a crash. Significant association has been shown between crash probability and traffic conditions. Hourdos et al. (56) utilized crash probability to detect real-time CPCs on a freeway in Minneapolis, MN. While different approaches to apply crash-prediction models in real-time environments have been proposed and simulated (1,118,25,2,75), implementation of such models into real-time systems is still rare.

1.4 DETECTION OF DOWNSTREAM CONGESTION

Existing event-based data collection about traffic can be leveraged to detect downstream congestion and alert drivers to be aware of their surroundings and driving behavior. Data from roadway units such as the SMART-Signal systems installed in MnDOT detector cabinets can be placed into an algorithm designed to "see" a queue as it travels to the position of a detector. Although traffic states from detectors upstream and downstream of the queue occurrence position give some implication of the jam, it can be risky to predict the occurrence of queue before it reaches a detector because such prediction easily generates false alarms. Algorithms developed to monitor queues this way must account for this by monitoring the queues as they are seen by detectors, rather than capturing the occurrence time and location of every queue flagged.

1.5 MNDOT QUEUE WARNING SYSTEMS

In Minnesota, three Queue Warning systems have been developed and field tested. Two such systems were implemented in 2016 in an effort to reduce incidents on heavily crashed and near-crashed sections of I-94 and I-35 in Minneapolis (56). This current project is an evaluation and refinement of one of these systems. Original results are discussed below. The third system is not officially referred to as a queue warning system, as it follows an indirect method in delivering the warning to the drivers. The Smart Work Zone Speed Notification (SWZSN) system was originally envisioned as an alternative to a previous Advisory Speed Limit system MnDOT had developed (63) but for the purposes of this report, it bears all the qualifications for a queue warning system as it is based on a method for detecting congestion and deliver a warning to drivers.

1.5.1 CPC Queue Warning (MN-QWARN)

In the summer of 2016, a CPC Queue Warning system was put into place on I-94, testing the hypothesis that not all congestion events are dangerous, but certain traffic conditions are Crash Prone whether they result in standing queues or not. The CPC Queue Warning system was based on identifying CPCs and relaying them to drivers through warning signage. I-94 was chosen to deploy the system due to CPCs resulting in more than 100 crashes per year. The geometry of the site was such that the majority of those crashes were rear-end, as it was not a merge zone (56). Figure 1-1 shows the CPC Queue Warning system architecture.

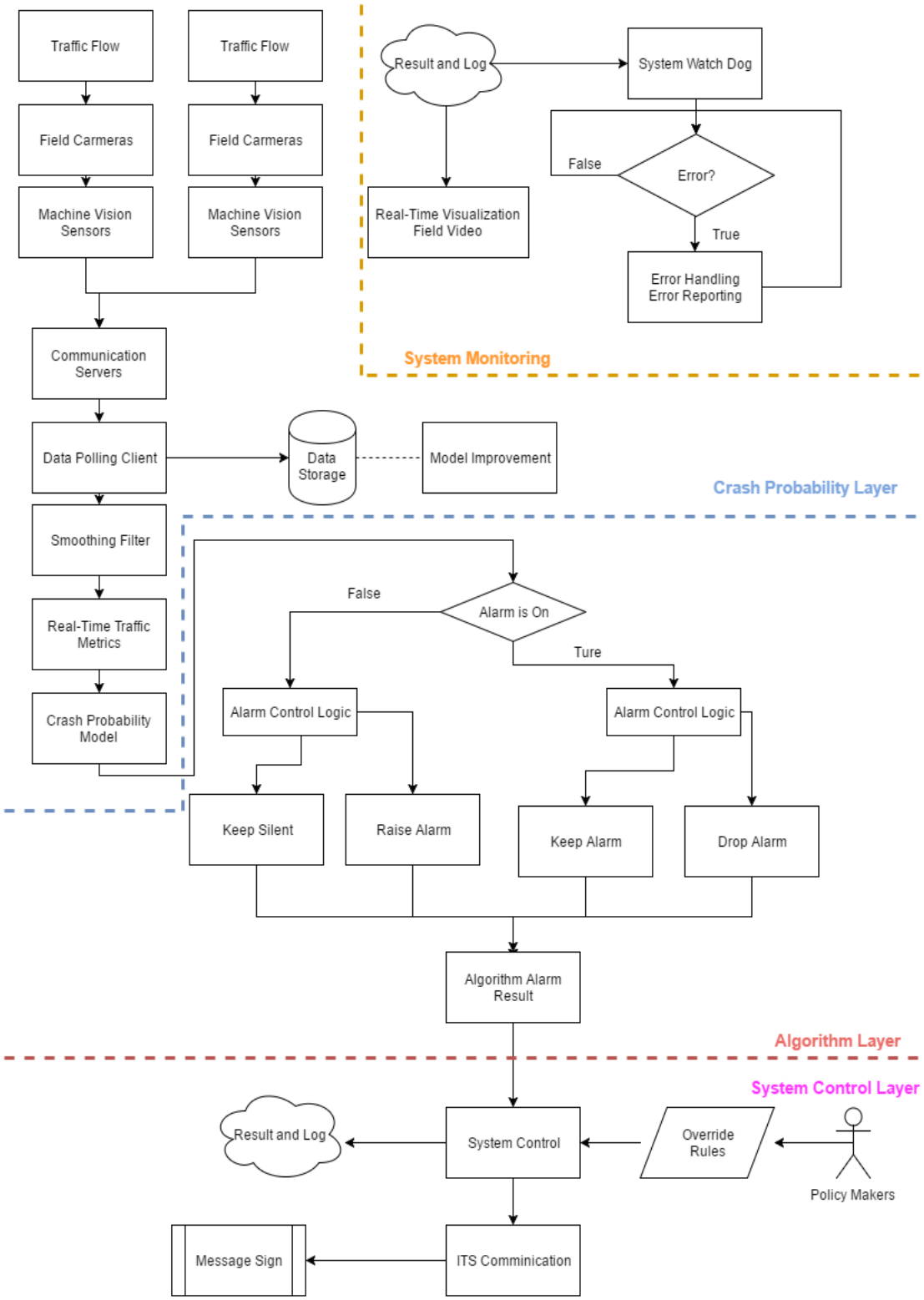

Figure 1-1 CPC Queue Warning System Architecture

As shown in Figure 1-1, the CPC Queue warning followed a three-layer design. The crash probability layer collected real-time individual vehicle measurements and processed them to remove noise. The filtered data then passed to the crash-probability model to assess the likelihood of a crash. This crash likelihood along with additional traffic information, such as speeds and headways, were passed to the second layer, the algorithm layer. In this layer, the algorithm decided if a warning message should be generated by comparing the crash probability with preset thresholds and real-time traffic conditions. A decision of whether to raise or drop the alarm was generated and passed to the third layer, system control, in which requirements from policy makers were applied to modify the result before delivering it to the Intelligent Lane Control Sign (ILCS) in the field.

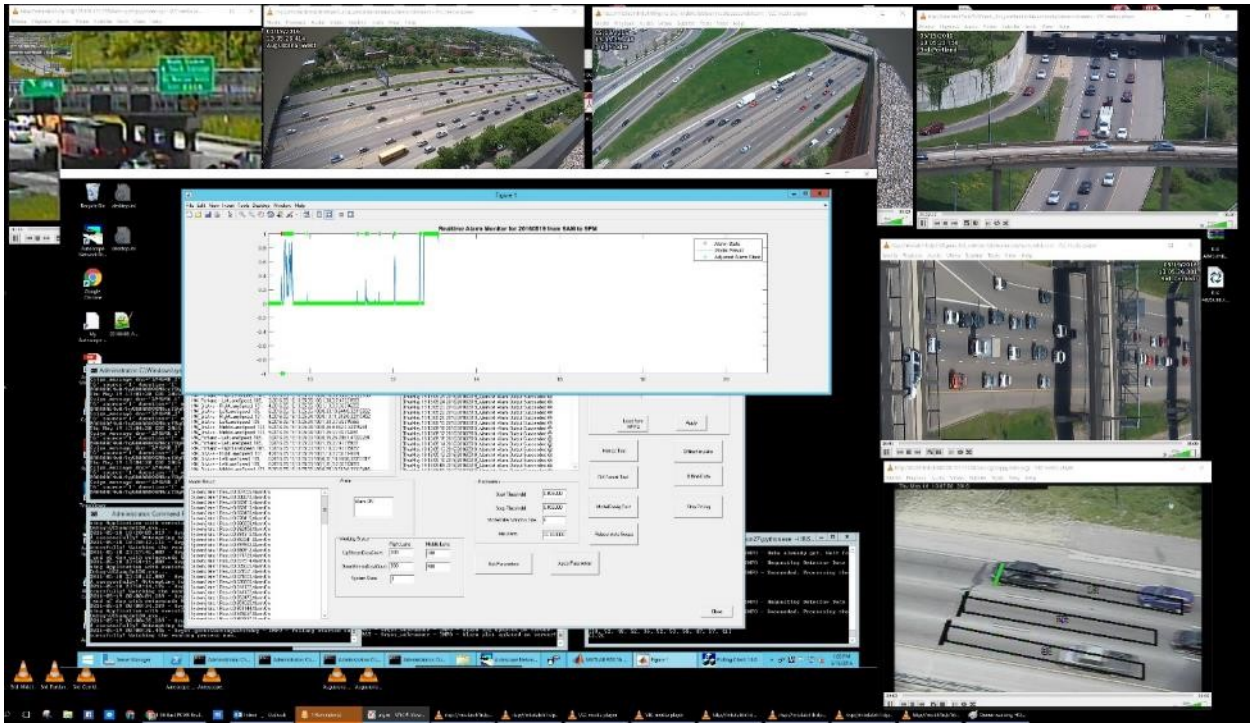

Figure 1-2 Control Interface of the Real-Time I-94 Queue Warning System

Over a three-month evaluation period, the CPC Queue Warning system was shown to reduce crashes by 22% and near-crash events by 54%. Issues such as restrictions on the time of day the system could operate, other messages overriding the Queue Warning signs, and drivers misinterpreting signage due to the choice of message displayed or even simply not seeing the message due to gantry placement warrant further study of the effectiveness of the system (56).

1.5.2 I-35W Queue Warning

On I-35W, a different Queue Warning Algorithm (MI-QWARN) system was put into place, testing the hypothesis that freeway rear-end collisions tend to occur in extended stop-and-go traffic or at end-of-queue locations. The MI-QWARN system read real-time information from five sets of MnDOT's SMART-Signals and used the data to determine if a queue was forming.

The algorithm looks at two types of shockwaves: queuing shockwave, described by the position of the last queued vehicle, and discharge shockwave, described by the position of the first vehicle waiting to be discharged. Figure 1-3 shows the estimation of density and flow rate between detectors during a shockwave.

Figure 1-4 shows the queue estimation algorithm's architecture. The first step of the algorithm identifies the occurrence and termination of a queue at detector locations. This can be identified by looking at vehicle occupancy time; if a vehicle has occupied a detector for ten seconds, it is safe to say the vehicle is stopped in a queue. However, relying solely on occupancy time may miss some queues, as drivers may maintain following distances greater than detector length, resulting in a blank detection area. In that case, vehicles are queued, but no occupancy time can be seen. Another issue arising when implementing the algorithm in the real world is that the value of occupancy time is only archived after the vehicle leaves the detector; in order to estimate the queue in a timely manner, the algorithm cannot wait until the vehicle occupying the detector for an abnormally long period of time leaves to begin computing. The algorithm compensates for this by examining speeds of past vehicles, the gap since the last vehicle left the detector and the occupancy time of the last vehicle. To determine the true end of the queue, rather than a false end created by stop-and-go traffic a similar methodology is used.

The difference between the arriving times of consecutive vehicles gave the headway for these two vehicles and taking the occupation time out of the headway gave the gap between these two vehicles.

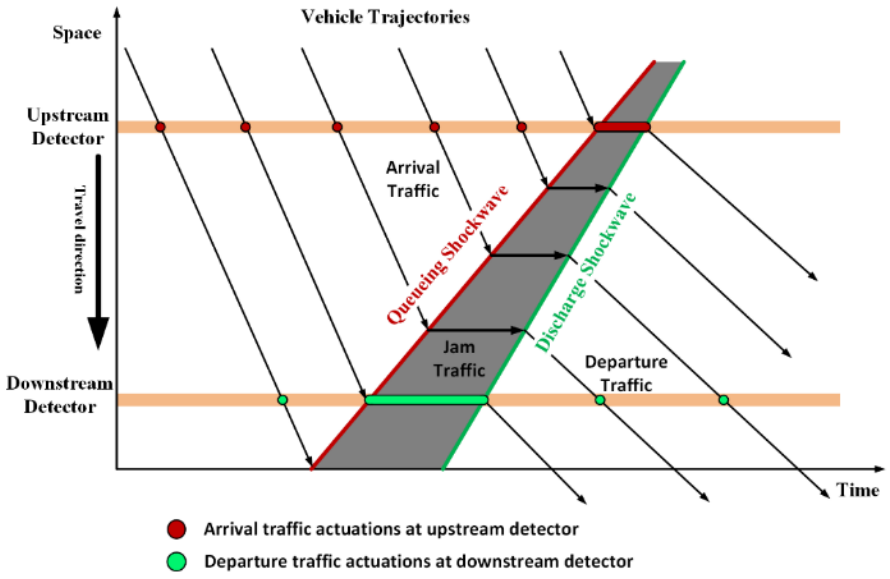

Figure 1-3 Estimation of density and flow rate

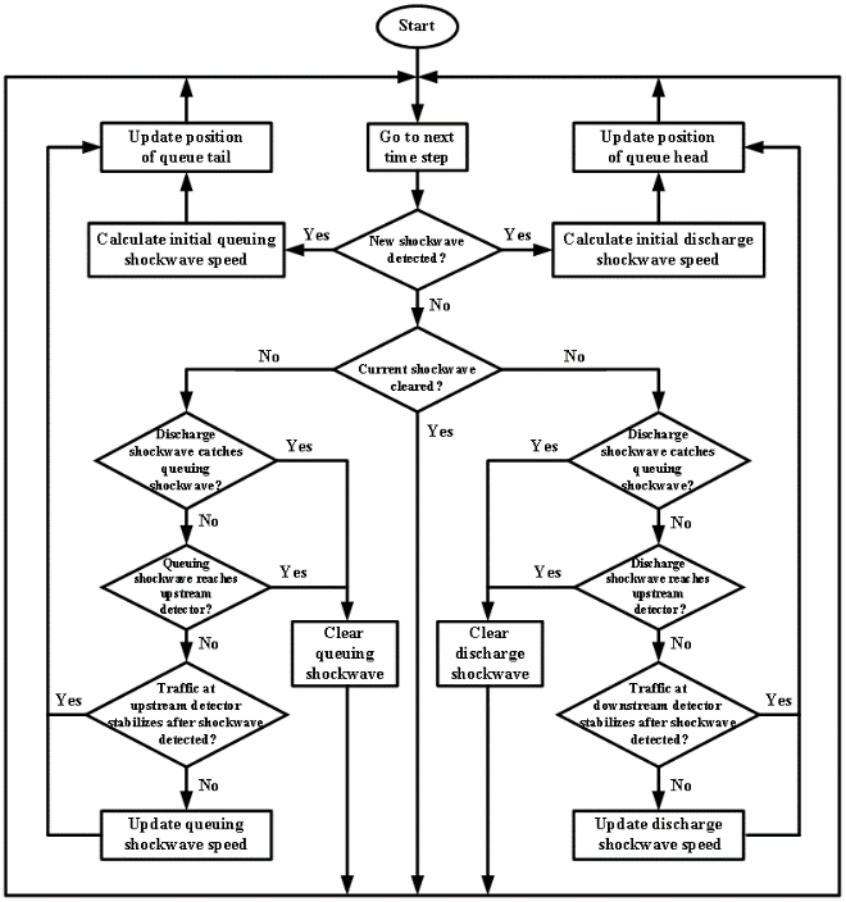

Figure 1-4 Flowchart of the I-35W Queue Estimation Algorithm

To ensure the system performed as intended, it carefully monitored what type of queue was detected as forming. Queues reaching from detector-to-detector point were flagged in the system, while queues starting in-between detector locations were examined more closely. Queues not propagating downstream to detectors were omitted by the algorithm due to their limited influence in space and time, and possibility of raising false alarms. Queues flagged in the system sent a request to display warning messages on the ILCS along the roadway.

The queue warning system for the I-35W site is shown in Figure 1-5. Real-time high-resolution vehicle actuation data were collected from three detector stations, namely S12, S14 and S15, and archived in the SMART-Signal server database. The queue warning software was developed to retrieve these data, estimate the queue length every second based on the algorithm proposed in Section 3.5.1, and then decide when and where to show the message of “SLOW TRAFFIC AHEAD”. The messages were read by the Intelligent Roadway Information System (IRIS) from MnDOT and then displayed on the corresponding ILCS located upstream of S12.

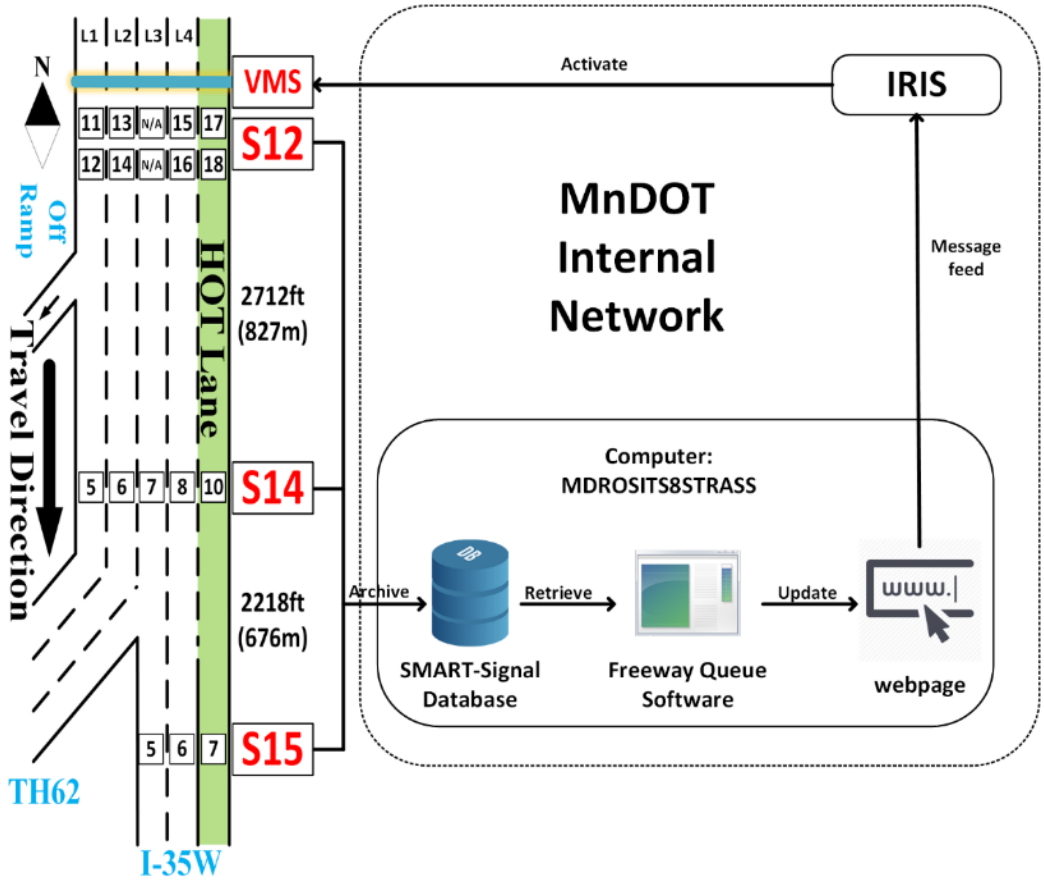

Figure 1-5 System structure

Note that the queue estimation and decision to show the warning messages are done on a lane-by-lane basis. Generally, the traffic states of each lane (except HOT lane) are monitored separately at downstream detector stations S14 and S15. If a stopped queue is detected and the estimated queue length exceeds a certain threshold on any lane, the warning message will be activated on the ILCS of that lane. Considering the fact that vehicles in some lanes may change lanes together (e.g., Lane 1 and Lane 2 to the direction of TH62), warning messages on these lanes are shown together if the queue length is long enough on any of the lanes. Once the downstream queue is discharged, the warning messages will be turned off. If queues spill back to S12, the system will also stop giving the warning message on the corresponding lane so as to avoid confusing drivers that have already joined the queue.

A snapshot of the software is shown in Figure 1-6. The upper middle pane of the software interface shows the current time. A static map of the place of interest is shown in the middle pane. The middle left and middle right panes show real-time traffic information including the timestamp, occupancy time, headway, gap, and speed of each vehicle passing by the corresponding detector station. The lower left and lower right panes show the estimated queue length when under queuing conditions. There are four black boards (ILCS) on the upper part of the software with each one corresponding to one lane (HOT lane is not included). The left two ILCSs (Lane 1 and Lane 2) correspond to the left lanes that merge onto

TH62 direction. The rightmost ILCS (Lane 4) corresponds to the lane that goes to I-35W direction. The ILCS on Lane 3 corresponds to the lane that can either exit onto TH62 or stay on I-35W.

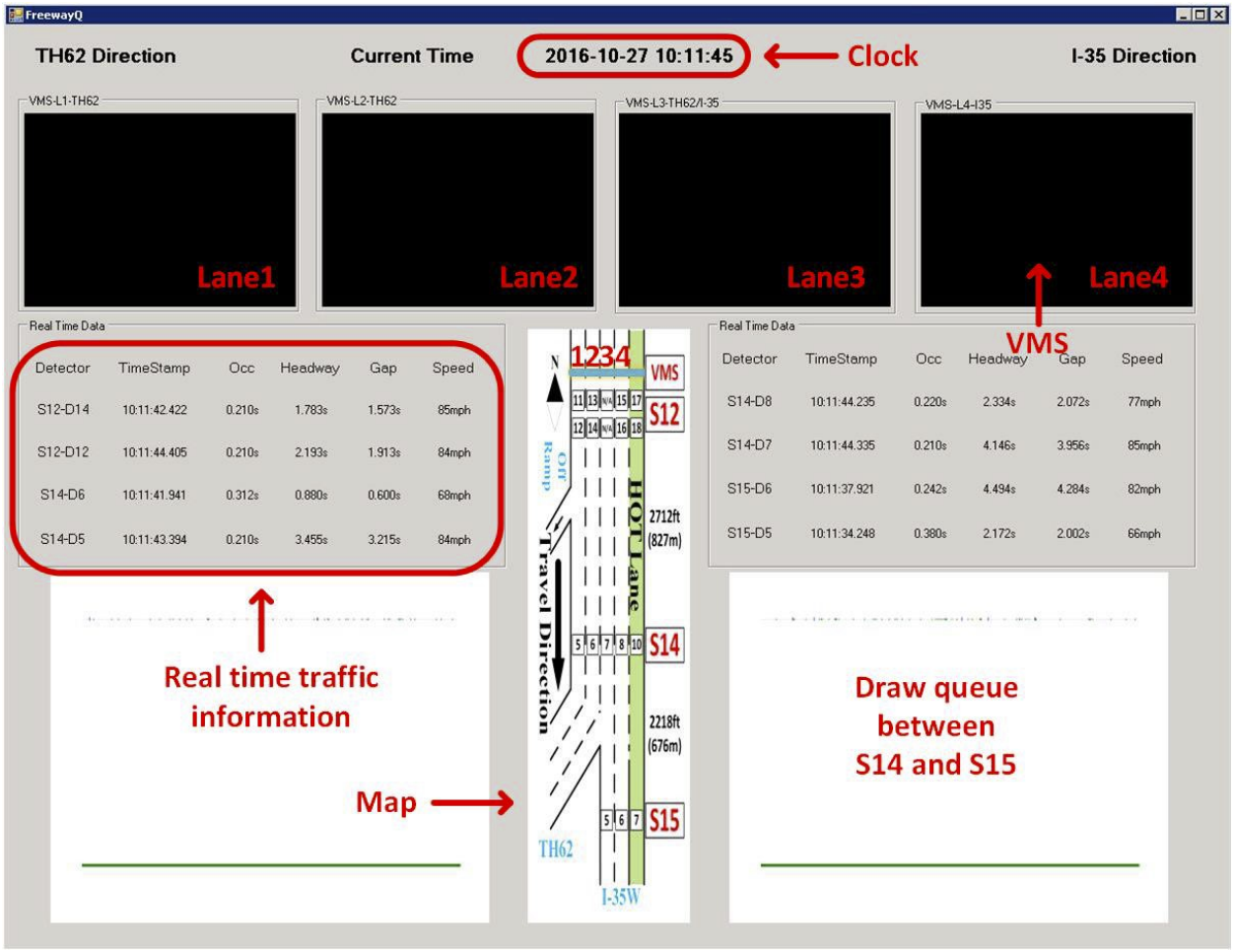

Figure 1-6 A snapshot of the developed software

The system resulted in smoothing of the traffic flow by reducing the speed variance at downstream locations, as well as speed difference between upstream and downstream. In general, they found that travelers responded to the message “SLOW TRAFFIC AHEAD”. However, the evaluation period for this system was only three weeks, and no meaningful data could be gathered on the influence of the system on crash rates (56).

1.5.2.1 Agency Overrides

Both the MI-QWARN and MN-QWARN queue warning systems were affected by agency overrides at the time of deployment. The overrides were intended to limit possible overexposure of drivers to the warning by what was, at the time of implementation, an unproven system. They consisted of a time override and a congestion override. The time override prevented the ILCS from being turned on, regardless of the alarm status before noon or after 8 p.m. The congestion override also prevented the sign from being turned on when five consecutive 30- second average speed measurements at the loop

detector near the farthest upstream sign are below 25 mph. This override was intended to reduce driver overexposure to the warning by not displaying a warning when drivers are already travelling slowly.

1.5.3 Smart Work Zone Speed Notification (SWZSN) system

Although not a "queue warning" system like the CPC and MQWA, the SWZSN system aimed to alert drivers approaching a work zone generated downstream congestion and queueing. SWZSN does this by informing drivers of the speed of the downstream segment using a type of portable ILCS, Portable Changeable Message Signs (PCMS). The hypothesis was that drivers, knowing the speed up to 1 mile downstream will preferably slow down early or at least be alert of the queue and perform smoother decelerations avoiding rear-end collisions. MTO recorded video of the SWZSN in action to determine if the system was functioning. Cameras were moved in 2017 to optimize the performance of data extraction. Figure 1-8 shows the work zone with SWZSN controlled PCMS trailers marked, as well as MTO camera positions and coverage in 2016 and 2017.

During the first year of the systems operation, based on empirical analysis of the messages generated, the project team identified discrepancies in the Speed Notification Algorithm, mostly in the form of unreasonable or delayed messages. The Regional Traffic Management Center never officially disclosed the logic used in the system, so it was difficult to know if any changes were implemented during the second year of the system's operation (2017). Regardless, during the 2017 construction season the operation experienced a significant reduction in the earlier identified problematic operation. It is possible that although the algorithm didn't change, the utilized Wavetronix speed sensors MnDOT deployed were providing better speed measurements.

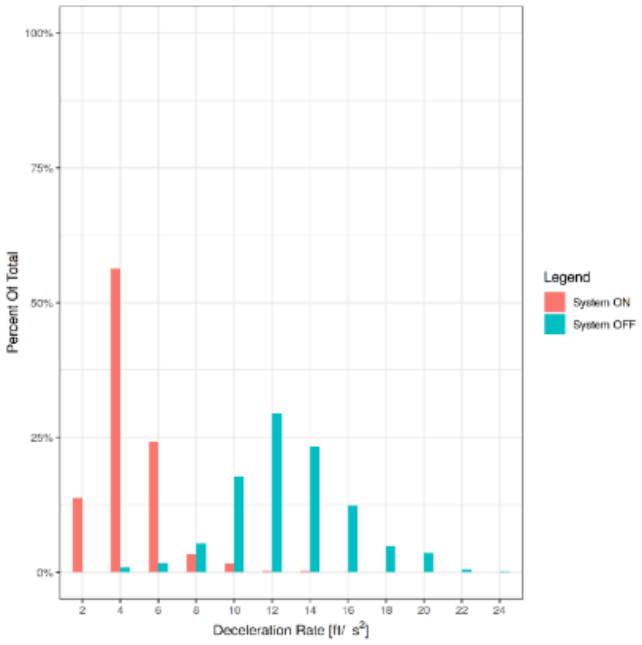

Figure 1-7 Decelerations at the Johnson Pkwy Station. Reduced Lane Work Zone Layouts.

Figure 1-8 SWZSN Work zone with PCMS trailers, camera stations, and radio links

Overall, the Speed Notification system resulted generally in beneficial reductions of selected decelerations by the drivers. In situations where the messages communicated to the drivers were consistent and accurate, reductions of more than 30% (Figure 1-7) in the selected deceleration rates were observed. Unfortunately, several cases where counterproductive or misleading messages were communicated to the drivers, prompting relative increases to the selected deceleration rates to be observed.

The most important observation, stemming from both positive and negative influences, is that the Speed notification system is noticed by the drivers and results in a statistically significant influence in driving behavior. This is much more of a result than many other driver warning systems have achieved, and it suggests that downstream speed notification, as opposed to advisory speed limits, is an effective traffic control tool. The particular speed estimation and message generation algorithm could be improved to reduce the occurrences of misleading and counterproductive message combination.

1.6 REAL-TIME FUNCTIONALITY

To make real-time queue warning systems such as the MN-QWARN, MI-QWARN, and SWZSN systems work, vehicle queue length estimation must be as accurate and close to real time as possible. Drivers must be warned to slow down, either with specific advisory speed limits or displays about incidents on the roadway or queues ahead through Intelligent Lane Control Signs. Note, ILCS is not an industry standard term. ILCS, as defined by MnDOT, specifically refers to one full-matrix electronic sign over each lane of traffic, spaced approximately every half-mile. However, with the lack of a proper industry term encompassing a dynamic driver message system, this report will use ILCS throughout. This literature review now shifts focus to both queue length estimation and ILCS.

1.6.1 Freeway queue length estimation

Real-time prediction of the queue length on freeway is of great help for the development of advanced freeway traffic management systems. Since the 1960's (40,99,132,45), the importance of managing vehicle queue length to reduce vehicle delay and prevent spillover, especially at signalized intersections, has been long recognized and studied (30,31,13,21,91,92,93). Meanwhile, vehicle queue estimation on freeway aiming to improve the freeway capacity and avoid rear-end accidents continues to receive much attention.

1.6.1.1 Basic Methodology on Queue Length Estimation

Essentially, two basic approaches have been developed to estimate queue length, namely the cumulative traffic input-output methods and the shockwave methods.

The first type of queue length estimation models is based on the analysis of cumulative traffic counts at both the input and output to a link (131,99,116,41,18,9,117,119,124,128). Such models are commonly used to describe traffic queuing process. However, according to Michalopoulos et al. (90), they are not sufficient for "obtaining the spatial distribution of queue lengths in time". Another obvious limitation of

such models is that they are able to estimate the queuing states only when the queue length does not exceed beyond the input detectors. These drawbacks limit the application of such type of models.

The second type of model is analyzing vehicle queue based on the feature of traffic shockwaves. The shockwave analysis takes the traffic flow as a continuous flow on road and studies the characteristics of it. A shockwave, also known as the kinematic wave, is the interface between any two traffic states with different characteristics (flow rate, speed and/or density). The shockwave theory provides a powerful tool for analyzing the evolution of traffic condition in a time-space diagram, especially during the formation and dissipation of highway bottleneck. One of the anchors of shockwave analysis is the traffic flow model. Lighthill and Whitham (81) and Richards (114) independently developed the first dynamic traffic flow model (LWR model). This LWR model describes traffic on a link using a conservation law and an equilibrium relation between density and flow, better known as the fundamental diagram (FD). Kinematic wave models have been widely used to study traffic dynamics on road links both analytically and numerically. Later, the original LWR model was extended in different directions to incorporate more realistic details. A more complete review of the traffic flow model and shockwave analysis is found in Maerivoet and De Moor (89).

1.6.1.2 Recent Work on Vehicle Queue Length Estimation

In particular, this part will review some recent works on vehicle queue analysis for intersections and freeway bottlenecks.

On the intersection vehicle queue estimation side, Hiribarren and Herrera (51) proposed a real-time traffic state estimation model utilizing vehicle trajectory data. Similarly, Cheng et al. (26) proposed a method of queue length estimation for signal control using probe vehicle trajectories. Instead of using traffic flow model, Comert and Cetin (29) developed a queue estimation method based on conditional probability and Bayes' rule.

Regarding vehicle queue on freeways, researchers put much effort on the queue analysis at freeway work zones. Jiang (68) applied shockwave analysis to estimate traffic delay and vehicle queue length at freeway work zones. Karim and Adeli (69) computed the queuing delay and vehicle queue length using a deterministic traffic flow model after calculating the freeway work zone's capacity. Later, Ghosh-Dastidar and Adeli (43) presented a microsimulation model based on neural network for the queue length estimation at freeway work zones. A more comprehensive review on vehicle queue length estimation at freeway work zones could be found in Weng and Meng (133). Beyond the vehicle queue analysis at work zones, Wu et al. (135) estimated queue length on freeway on-ramps. Similarly, the Kalman filter method was applied in Sheu et al. (120) to estimate real-time delays and queues in the presence of freeway incidents.

Qom et. al (112) recently tested two new queue estimation methods based on input and output to a link using point detectors. The first method estimates queue length between two detectors by using linear interpolation between the travel time measurements when the link is fully queued versus when no queue is present. The second method divides a segment with a partial queue into two segments, where the first is assumed to be similar to upstream traffic and the second is similar to downstream conditions.

The length of each segment is calculated based on AVI speed data. These methods have implications for both off-line and real-time applications.

1.6.1.3 Vehicle Queue Length Estimation Methods Using High-Resolution Data

Most research on estimating vehicle queue utilizes aggregated data. For instance, Skabardonis and Geroliminis (121) proposed a method to estimate intersection queue length using aggregated loop detector data in 30-s intervals. Some use probe vehicles' trajectory data, as presented above. Few of them really fully utilized the high-resolution data. This is partially because high-resolution traffic data was not available until recently.

Using the high-resolution event-based field data obtained from the SMART-Signal system, Liu et al. (85) developed a real-time queue length estimation method for congested signalized intersections. One of the appeals of this work is that this method is capable of estimating the length of queues that exceed the location of upstream queue detectors. In particular, the high-resolution data was used to identify the "break points" (time and location of traffic flow pattern changes), which contributed significantly to the long queue estimation. Then, simple shockwave theory was applied to study the dynamics of traffic flow. The field test showed accurate outcomes from this method in terms of queue length estimation at intersections. As an application of this method, Liu and Ma (84) proposed a virtual vehicle probe model to estimate the time-dependent travel time. Though the objective was to estimate the travel time, queue length at the intersection was estimated in advance in order to accurately calculate the vehicle probe's travel speed. The field test at an 11-interseciton arterial corridor along France Avenue in Minneapolis, MN demonstrated that the proposed model can generate accurate time-dependent travel times under various traffic conditions.

Based on these works, a shockwave profile model (SPM) for traffic flow was proposed in Wu and Liu (136) which filled the research gap of implementing traffic flow model in signalized urban arterial. The SPM model is particularly suitable for simulating traffic flow on congested signalized arterials especially with queue spillover problems where the steady-state periodic pattern of queue build-up and dissipation process may break down. Field tests of the SPM model show that it can successfully identify the queue length, queue spillover occurrences and the dynamics of the vehicle queue for a three-intersection arterial on Trunk Highway 55, MN.

However, it is not straightforward to extend the queue estimation algorithm from arterial to freeway. First, most queues on arterial are caused by traffic signals. They have fixed cyclic pattern that starts from a stop line at the beginning of a red period. Therefore, if the signal status is available, the onset of the queue can be immediately detected by a stop bar detector. A similar pattern exists for queues on freeway on-ramps (134), but it cannot be expected on freeway mainlines. The start of a stopped queue on freeway is not predictable; it can be anywhere, at any time (36). Second, the speed of discharge shockwave is almost constant for a specific approach of an intersection because the traffic state downstream of the queue at the beginning of discharge is always empty (85). On the other hand, freeway queues may begin to discharge under various downstream traffic conditions. Last, the impact of lane changes can be omitted for queues on arterial because vehicles are forbidden to change lanes when getting close to intersections. However, for most freeway segments, vehicles can change lanes as long as they do not impede others.

1.6.1.4 Remarks on Vehicle Queue Length Estimation

Based on the review above, most of the previous research works focused on vehicle queue length estimation at signalized intersections and particular locations (e.g., work zones and ramps) on freeways. Fewer of them are dedicated to the more general analysis of freeway vehicle queue. The research gap in the theoretical analysis of freeway queue formation, evolution and dissipation using high-resolution data is even more obvious. The difficulty to capture the dynamics of freeway traffic maneuver is one obstacle ahead of such analysis. Another difficulty is lack of field data, especially the high-resolution data. Realizing the research gap and opportunity, developing methods to identify the freeway vehicle queue's formation, evolution and dissipation processes using high-resolution data collected from the continuation of this project will contribute significantly both in theory and in practice.

1.6.2 Intelligent Lane Control Signals

In the case that a queue on freeway is predicted and/or identified, informing drivers about the downstream queue and preparing them for the changes of traffic status is necessary for freeway traffic management. ILCS can be utilized to display warning messages and guide drivers to adjust speed to avoid potential rear-end collision and improve the freeway performance. In the following, the effectiveness of freeway ILCS systems and the response from drivers to such systems, both from simulation results and field tests, are reviewed.

1.6.2.1 Simulation and Survey Studies

Chatterjee et al. (23) conducted a survey on drivers' response to variable message signs (ILCS). It was found from the questionnaires that, though only 1/3 of drivers saw the information, 1/5 of them would change their route choices. Many research works reported that drivers' behavior could be more influenced by speed advisory and lane changing signs (comparing with the route changing messages). For instance, Hassan et al. (49) investigated drivers' response to different ILCS messages and then claimed that the message of "Caution-fog ahead-reduce speed" was the one with the best effect. This work was done with driving simulation software.

Khan (71) developed an infrastructure-based queue-end warning system which automatically estimates the queue length and displays messages on portable ILCS in order to reduce rear-end collisions. However, the exact messages on boards were not specified. This work was tested in simulation. It is noted that the warning system was deployed at freeway work zones thus the location of the queue remained fairly constant. Whether the developed approach can handle other forms of queues on freeway is not clear. Lee and Abdel-Aty (74) conducted a study including 86 participants who drove a 5-mile section of freeway on a driving simulator. The participants were exposed to warning messages as well as speed limit messages. Simulation results yielded that when warning messages or speed limits were displayed, participants generally drove at a uniform speed. Their research findings also indicated that warning messages were beneficial in reducing speed variation and removing congestion and could potentially reduce crash risk on freeways.

1.6.2.2 Examples of Real ILCS System Implementation

In addition to simulation and survey studies, field tests of such variable message systems were also conducted. A large-scale real-time driver warning system called the Caltrans Automated Warning System (CAWS) was installed on Interstate 5 and State Route 120 near Stockton, California and started to work in 1996 (87,88,20). CAWS displays various messages and signs to inform drivers about the approaching traffic condition and advised speed. Messages are designed for conditions with different visibilities and purposes. By comparing the data from both the study direction (the direction of freeway without a warning system, I-5 North) and the control direction (the direction of freeway with a warning system, I-5 South), it showed that the number of crashes was reduced after the installation of the warning systems.

A newer Active Traffic Management System (ATMS) incorporating ILCS was implemented in 2015 on a stretch of I-66 in Northern Virginia, a major commuter route to and from Washington, D.C. (65). This system used Advisory Variable Speed Limits (AVSLs), a Queue Warning system, lane use advisories, and Hard Shoulder Running (HSR), all disseminated to drivers via ILCS. Overall, they saw statistically significant improvement of traffic flow during off peak weekday hours, and travel time and travel time reliability improvement of 10% to 14%. Most of these benefits came from HSRs, but AVSL was only active for 1.5 months, which was not enough time to gather empirical evidence. Also of note, this system uses aggregate INRIX data, not high-resolution real-time data.

Wrapson et al. (134) studied the effectiveness of different types of signs. By measuring the vehicle speed in a 32mph zone, it suggested that even only displaying the average speed of neighboring vehicles without giving a specific speed advisory or warning the drivers that their speeds were being measured could significantly reduce the vehicle speed. Harder et al. (48) also studied driver response to various signage; they found drivers responded more quickly to signage including chevrons or diagonal arrows than to words. The diagonal arrow was the most effective at encouraging drivers to move over, being visible from 266 feet on average. Signs regarding speed limits were not as effective, with participants slowing down as they reached variable message signing with advisory speeds, but ultimately passing the 35mph speed limit display at an average speed of 38.7 mph. Bertini et al. (15) tested their automatic speed limit advisory system at bottlenecks along a section of German freeway, which decreased the speed limit before bottleneck activation as a means of managing traffic density. A strong correlation between speed limit and information messages and actual traffic dynamics on the Autobahn was found.

Another notable effort in the development and deployment of crash prone traffic condition detection and alert systems is currently active in Japan (104). Under the Advanced cruise-assist Highway System (AHS) program, two systems relevant to this research are currently in the field deployment and evaluation stage. The first one is an automated roll-over alert system. The system is comprised of several sensors providing information on individual vehicle speed, height, and weight. It estimates the probability that a vehicle might roll-over in the approaching sharp curve. If this probability is greater than a pre-defined threshold, message signs and radio signals will alert the specific driver of the danger and require the driver to slow down. This system is based on simple physical models which determine the roll-over probability and is mainly aimed to prevent large truck crashes. The second system

developed under the AHS program is more relevant to the scope of this research. This automated driver alert system aims at rear-end crash prevention at roadway sections with special geometric designs and limited visibility (e.g., sharp curve). In general, the logic of the system is straightforward: if there is a queue in the predefined position or any other lane obstruction, the warning mechanism is activated and then sends alert messages to drivers.

A common application for dynamic ILCS and queue-warning systems is on work zones where the reduced capacity of the roadway cannot accommodate normal traffic volumes. Two systems designed for this application employ several sensors along the road upstream of the construction zone to detect the location of the upstream end of the queue. The first queue-warning system (71) uses live radar detection data from two sensors (one immediately upstream of the work area and one at the end of the work area) to extrapolate the location of the back of the queue. The location of the back of the queue is then displayed on a portable changeable message sign (PCMS) at the location of the upstream sensor. The second queue-warning system (71) uses up to eight speed sensors spread out over seven miles to detect queues. The system warns drivers approaching the work zone of any queues present through several upstream PCMSs. Texas Department of Transportation used the eight-sensor system in a 96-mile project and found it lowered crash rates by as much as 47% when compared to an estimate of what they would have been had the system not been deployed.

For metropolitan areas where congestion is commonplace, slightly different approaches with queue warning and ILCS are often employed. One system in Houston, TX (108) uses MVDs to measure the speeds of vehicles approaching the area in which congestion generally occurs. When the system detects three consecutive vehicles with speeds lower than 25 mph, lights flash above a warning sign. Pesti et al. report decreases of 2% to 6% in vehicle conflicts when this queue warning system is in place. Another queue warning system deployed on a congestion-prone freeway is in Eugene, OR (32). The system measures freeway occupancy using three side-fire, dual-beam traffic detectors. When the freeway vehicle occupancy exceeds thresholds established by the Oregon Department of Transportation (ODOT), warnings are displayed on the Portable Changeable Message Signs (PCMSs) until the occupancy no longer exceeds the threshold along with a minimum display time of 5 minutes. The system is reported to have decreased the crash rate by over 35%, but no current research has been published.

1.6.2.3 ILCS Applications in Minnesota

In addition to the two Queue Warning sites evaluated and refined in this project, other ILCS systems have been implemented in the state of Minnesota. For example, the project of “Accident Prevention Based on Automatic Detection of Accident Prone Traffic Conditions” (56) hangs displays permanently over the traffic lanes on key segments of I-94 and I-35W. Staff members at MnDOT’s Regional Transportation Management Center (RTMC) monitor the flow of traffic through closed-circuit video cameras and sensors embedded in the pavement. When an incident occurs, RTMC staff programs the ILCS units to display a series of messages directing drivers away from blocked lanes. A rich crash database was created and analyzed to investigate crash related traffic events and contribution factors such as weather, individual vehicle speed and headways, etc.

Another project, “Development of Real-time Traffic Adaptive Crash Reduction Measures for the Westbound I-94/35W Commons Section”, (62) utilized 3D virtual reality to help design a warning system. Traffic data was collected from a high crash zone on I-94. This project visualized and analyzed the crash data using a micro-simulation method and highlighted gaps in technology and knowledge which hampered existing and future research projects with similar objectives. One of the gaps pointed out was that the two most widely used data sources, video data and GPS data, are not accurate enough for online microsimulation purposes. High-resolution event-based data collected from the real time queue warning systems may help bridge this gap.

Two additional projects regarding MnDOT’s usage of ILCS have been completed by the MTO. The first study, done in 2014, called “Investigation of the Impact of the I-94 ATM System on the Safety of the I-94 Commons High Crash Area” (63), examined data both before and after variable message signing was placed along the highest crash and near-crash site of I-94. The signage warned drivers to reduce their speeds gradually as they traveled downstream, generating a forward moving shockwave intended to weaken or absorb backward moving congestion shockwave. Based on the loop detector data and speed-based shockwave analysis performed by MTO, no significant change in driver behavior was noted anywhere along the corridor due to variable message signing. Shockwaves were generated at similar rates and propagated at similar speeds in both the before and after periods of study, signaling no improvement to safety.

The second study, done in 2016, “Evaluation of the Effectiveness of ATM Messages Used During Incidents” (63), examined the ILC system on I-94 westbound in downtown Minneapolis, the same corridor studied in 2014. This study focused on the strength of various usages of ILCS in addition to inducing or directing a desirable lane selection behavior from drivers. Specifically, the study examined impacts of ILCS on driving behavior during non-recurrent congestion. This study found that ILCS for incident management specifically had a significant effect on driver behavior, especially in prompting proper lane selection under capacity reducing incidents.

In terms of specific scenarios of ILCS use, the 2016 research showed that specific sign configurations induce more lane changes than others. For example, the Use Caution sign has a relatively weak effect on lane changes especially in comparison to stronger messages like Merge, Lane Closed Ahead (LCA) and Lane Closed (LC). Perhaps intuitively, the Merge chevron sign seems to be the strongest sign for inducing lane changes upstream of an incident. The research has also shown that the combination of LCA followed by a Merge chevron on successive gantries is most effective, supporting Harder et al.’s conclusion (48). The analysis as well as the empirical evidence show that the visual presence of first responders like FIRST and State Patrol vehicles has an observable positive effect on lane change behavior but not as effective as instructions on an ILCS. Although the presence of first responders is a direct confirmation of the incident presence, it does not provide information to the drivers on which lane to choose. Generally, the combination of directed information along with the confirmation from the presence of units on scene is most effective.

The 2016 study also showed that ILCS operation in heavy congestion—particularly in stop and go conditions—becomes ineffective. As stated in the report, “a lane selection system stops being effective

when lane changes are impossible" (63), but further than that, ILCS was shown to empty the lane an incident occurred in well upstream. This leads to wasted storage space by emptying the lane early, worsening upstream congestion. Therefore, ILCS to induce lane changes ahead of an incident can become ineffective and also detrimental under stop-and-go conditions. A better strategy may be to turn off the ILCS messages or change them from a prompt to change lanes to something else, especially if a first responder is already on the scene.

1.6.2.4 Remarks on ILCS

Both simulation and field studies have shown positive impacts of ILCS system on the safety of freeway. Additionally, ILCS systems also improve the mobility of the freeway traffic flow by helping drivers stabilize their speed, eliminate stop-and-go movements, and choose the proper lane during incidents. Another lesson learned from the literature is that different signs carrying different information will have different levels of effectiveness on different groups of drivers. Sending out information with the best results requires well designed signs and messages. However, ILCS can be ineffective if used in heavy congestion, stop-and-go traffic, or when directing drivers to change lanes too far ahead of incidents.

1.7 CONCLUDING REMARKS

Through CPC detection, queue length estimation, and ILCS implementation, the I-94 and I-35W Queue Warning systems sought to create and refine algorithms to detect either CPCs or roadway queues and warn drivers. The original projects were hindered by project timing and implementation difficulties, as well as agency restrictions on relaying messages to drivers, though they delivered promising initial reduction of crashes and smoother traffic flow. The continuation of these two projects and incorporation of new and existing research on CPCs, driver warnings, and queue estimation as well as similar active queue warning systems, will determine if they are successful.

CHAPTER 2: EVALUATION OF MN-QWARN FOR THE PERIOD 2016 TO 2018 (PORTLAND AVE)

2.1 MN-QWARN BACKGROUND

The MN-QWARN system is based on the hypothesis that not all congestion events are dangerous but there are certain traffic conditions that are crash prone regardless of whether they result in standing queues or not. Such CPCs can be isolated, fast-moving shockwaves, involving only a small number of vehicles in the deceleration-stop-acceleration cycle. For such conditions, a dense detection infrastructure is needed. The MN-QWARN system was implemented along the westbound section of I-94 in downtown Minneapolis, due to the high number of crashes experienced there (more than 100 per year). The Minnesota Traffic Observatory has had a permanent Field Lab in this location since 2002.

Based on the framework proposed by Dr. Hourdos (4), this system approaches the topic from the quantification of traffic flow to the multi-layer system design along with different approaches including traffic assessment modeling and the development of control algorithms. This approach utilizes individual vehicle measurements including individual vehicle speeds and time headways, as the major type of data for the system operation. The prototype of a CPC detection-based queue warning system was developed by a research team lead by Dr. John Hourdos at the University of Minnesota.

2.2 MN-QWARN IMPLEMENTATION

The MNQWARN system was implemented in the right lane of a 1.7-mile-long freeway segment of westbound Interstate 94 (I-94 WB) near downtown Minneapolis where the event frequency prior to the system's installation was 11.9 crashes per million vehicles traveled (MVT) and 111.8 near crashes per million vehicles traveled (MVT). Machine Vision Detectors (MVDs) installed on a nearby rooftop captured the real-time vehicle data. The data were delivered to a server running the main control algorithm at the Minnesota Traffic Observatory (MTO) via MTO's communication network. The control algorithm assesses the "dangerousness" of the given traffic conditions and responds with a warning result based on a multi-metric traffic evaluation model and a control-reasoning heuristic.

2.2.1 Study Site and Available Data

To best study crashes, conditions must be observed and measured before, during, and shortly after an actual event. This requirement translates to a need for continuous monitoring and data collection at a location that maximizes the probability of capturing crashes on camera.

In the Minneapolis-Saint Paul Metropolitan Area (Twin Cities), I-94 connects the two cities and is the major freeway corridor connecting the two banks of the Mississippi River in the region. The site of this study is a segment with a length of 1.7 miles on I-94 WB near downtown Minneapolis. This segment of I-94 is near the exit of I-35W, the west branch of Interstate 35 that runs through Minneapolis. The close proximity to the downtown area results in a large traffic volume merging in and out these two freeways. The combination of such a large vehicle volume and great degree of merging often destabilizes traffic on

this freeway segment thereby causing shockwaves where drivers need to reduce their speed in a short time and space or, when drivers fail to decrease their speed quickly enough, rear-end crashes. According to MnDOT records, this segment had the highest crash rate in the entire Minnesota freeway system. In 2002, the site exhibited 4.81 crashes per million vehicle miles (MVM) – equivalent to approximately one crash every two days – while the network average is 0.96 crashes per MVM. During the PM peak period, the aforementioned site exhibited an average of 15.43 crashes/MVM whereas the entire I-94 freeway experienced only 3.29 crashes/MVM (81)]. Fatalities and severe injuries are very rare since the prevailing speed during CPCs is relatively low. The majority of crashes result only in property damage.

Figure 2-1 Aerial view of implementation site.

The crash-prone section of I-94 WB runs parallel to I-35W and short ramps allow transfers between freeways (Figure 2-1). The freeways and cross streets are labeled. The changeable message boards are denoted by the red circles and the high-volume on-ramp is enclosed by the green rectangle. The site includes two on-ramps, three off-ramps, three main lanes, and two 3,000-foot auxiliary lanes – one in each of the two areas where weaving is common (just downstream of the green rectangle and between the two red circles in Figure 2-1). Weaving is excessive where high volumes enter from the ramp (outlined by the green rectangle in Figure 2-1) which combines traffic from Minnesota State Highway 65 (MN 65) and the downtown business center to the north with I-94. In addition to the traffic volume entering the rightmost lane from the ramp, many drivers on I-94 merge right in order to be in or near the rightmost lane in anticipation of the two off-ramps downstream of Lasalle Ave. During periods of congestion, shockwaves generally originate when vehicles merge onto I-94 from the aforementioned ramp and cause vehicles in the rightmost lane to brake. If conditions are sufficiently dense, one vehicle entering from the ramp can initiate a chain reaction of vehicles braking that grows into a shockwave that causes increasingly intense braking as it moves upstream. Due to vertical and horizontal curves, vehicles between Chicago Ave and Portland Ave have limited forward sight distance. Drivers' inability to see a shockwave approaching forces them to rely heavily on their reaction time to avoid rear-ending the vehicle ahead.

In 2002, for the purposes of projects related to intelligent transportation systems (ITS), a traffic detection and surveillance laboratory was established as part of the Minnesota Traffic Observatory (MTO) at the University of Minnesota. Hourdakis et al. (*53*) report details of the site instrumentation and capabilities. Because the site is close to the downtown area, nearby high-rise buildings allowed for the installation of several cameras and MVDs overlooking the roadway. While most of the sensors are not

utilized by the queue warning system, they provide the means of collecting detailed observations and determining ground truth.

As shown in Table 2-1, different types of data were used across this study. Individual vehicle measurements of speed and time headway were used for the operation of the system and aggregated traffic speed data from loop detectors serve for system adjustment and system evaluation. In order to collect the necessary individual vehicle data cost-effectively and unobtrusively, MVDs were utilized (Figure 2-2). Due to the high concentration of conflict events at the test site, only two such sensors stations were necessary, one placed at the location of the most frequent crashes (right) and the second approximately 750 feet downstream (left). The two stations were deployed between 3rd Ave and MN 65 and between MN 65 and Portland Ave.

Table 2-1 Summary of data types and purpose

Data	Type	Source	Purpose
Aggregated Traffic Data	Real-Time	Loop Detector	Additional input for system adjustment
Aggregated Traffic Data	Historical	Loop Detector	Developing of system evaluation methodology
Individual Vehicle Measurements	Real-Time	MVD	The main input of the system
Individual Vehicle Measurements	Historical	MVD	Algorithm and system design and development
Traffic Event Data	Historical	Video	System evaluation methodology development, algorithm and system development

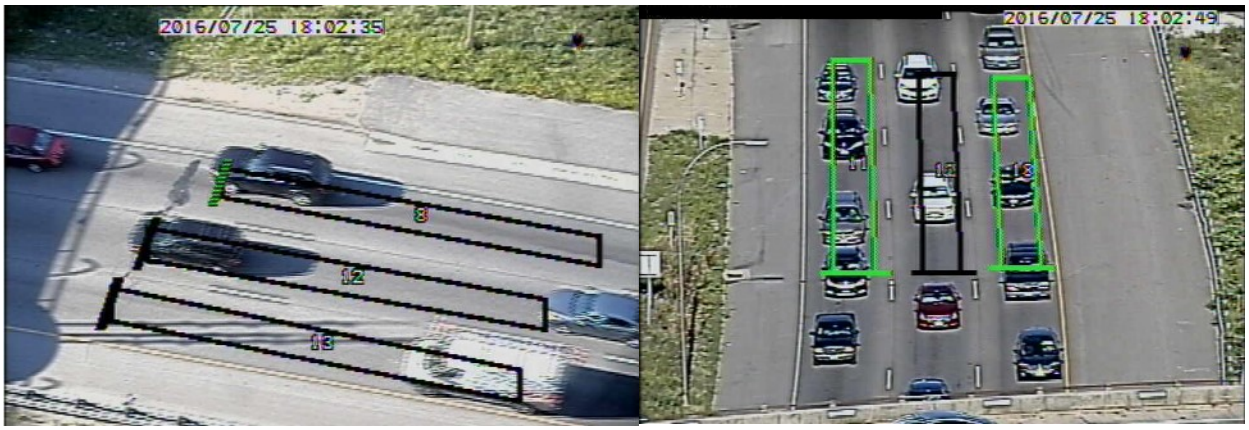

Figure 2-2 Machine Vision Sensors

This study also utilized MnDOT in-pavement loop detectors to provide 30-second volume and occupancy data to provide additional information for system adjustment from policymakers. Five surveillance cameras were also employed: four atop a high-rise building to capture vehicle conflict events between 3rd Ave and Chicago Ave on video and one atop a pole to capture live video of the MnDOT changeable message boards at the 11th Ave gantry (rightmost red circle in Figure 2-1). Video from all five cameras was captured and saved digitally from 9 a.m. to 8 p.m. every day. Vehicle data from the loop detector is collected 24 hours a day, 7 days a week whereas the individual vehicle measurements were only collected between 7 a.m. and 8 p.m. each day. Traffic event data extracted from these surveillance videos were used to measure the performance of the proposed system in a real-world context.

For illustration, figure 2-3 shows the Field Lab rooftop stations which are mounted and connected to power.

2.2.2 Detecting and Reacting to CPCs

Beginning in the summer of 2016, MNQWARN was active. MNQWARN is a CPC Queue Warning system, based on identifying CPCs and relaying them to drivers through warning signage. As discussed previously, the instrumented section of I-94 was specifically chosen to deploy the system due to CPCs resulting in more than 100 crashes per year. The geometry of the site was such that the majority of those crashes were rear-end, as it was not a merge zone. Figure 2-4 shows the CPC Queue Warning system architecture as implemented in MNQWARN.

To capture traffic data, live video from the existing camera detector stations was merged with data from in-pavement loop detectors. The algorithm described Figure 2-4 utilized this data to create a rear-end collision warning system. The system would prompt the ILCS units to display warning messages for drivers, such as Prepare to Stop, Slow Traffic Ahead, and Traffic Ahead 10 MPH.

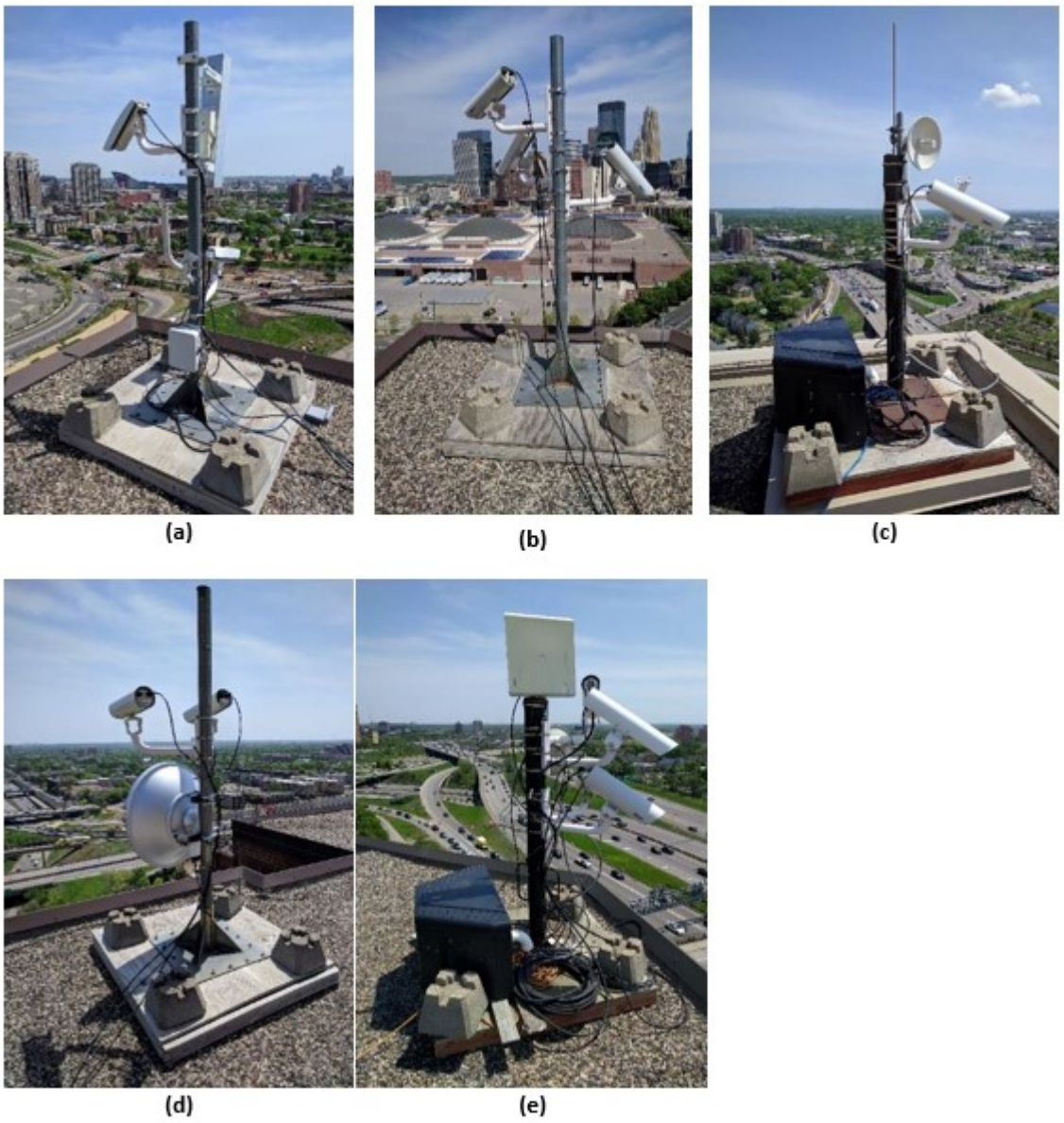

Figure 2-3 Rooftop stations (a)-(b) along 3rd , (c) Cedar Ave, (d) 3rd Ave and (e) Augustana

As shown in Figure 2-4, MNQWARN followed a three-layer design. The crash probability layer collected real-time individual vehicle measurements and processed them to remove noise. The filtered data then passed to the crash-probability model to assess the likelihood of a crash. This crash likelihood along with additional traffic information, such as speeds and headways, were passed to the second layer, the algorithm layer. In this layer, the algorithm decided if a warning message should be generated by comparing the crash probability with preset thresholds and real-time traffic conditions. A decision of whether to raise or drop the alarm was generated and passed to the third layer, system control, in which requirements from policy makers were applied to modify the result before delivering it to the Intelligent Lane Control Sign (ILCS) in the field.

Specifically, as part of the terms for the deployment of the system, two overrides were included and the preexisting MnDOT signs' refresh rate was kept. Two sets of Intelligent Lane Control Signs (ILCSs) are used to communicate the warnings to the drivers. The overrides are intended to limit possible overexposure of drivers to the warning by what was, at the time of implementation, an unproven system and consist of a time override and a congestion override. The time override prevents the sign from being turned on, regardless of the alarm status before noon or after 8 p.m. The congestion override also prevents the sign from being turned on when five consecutive 30- second average speed measurements at the loop detector near the farthest upstream sign are below 25 mph. This override is intended to reduce driver overexposure to the warning by not displaying a warning when drivers are already travelling slowly. The rate at which the sign is updated is a result of the sign being part of the MnDOT Twin Cities metro-wide network. Initial activation can vary from a few seconds to one minute, depending on the synchronization between the independent queue warning system and the traffic operations system that controls the signs. This delay amplifies short gaps in the alarm activation.

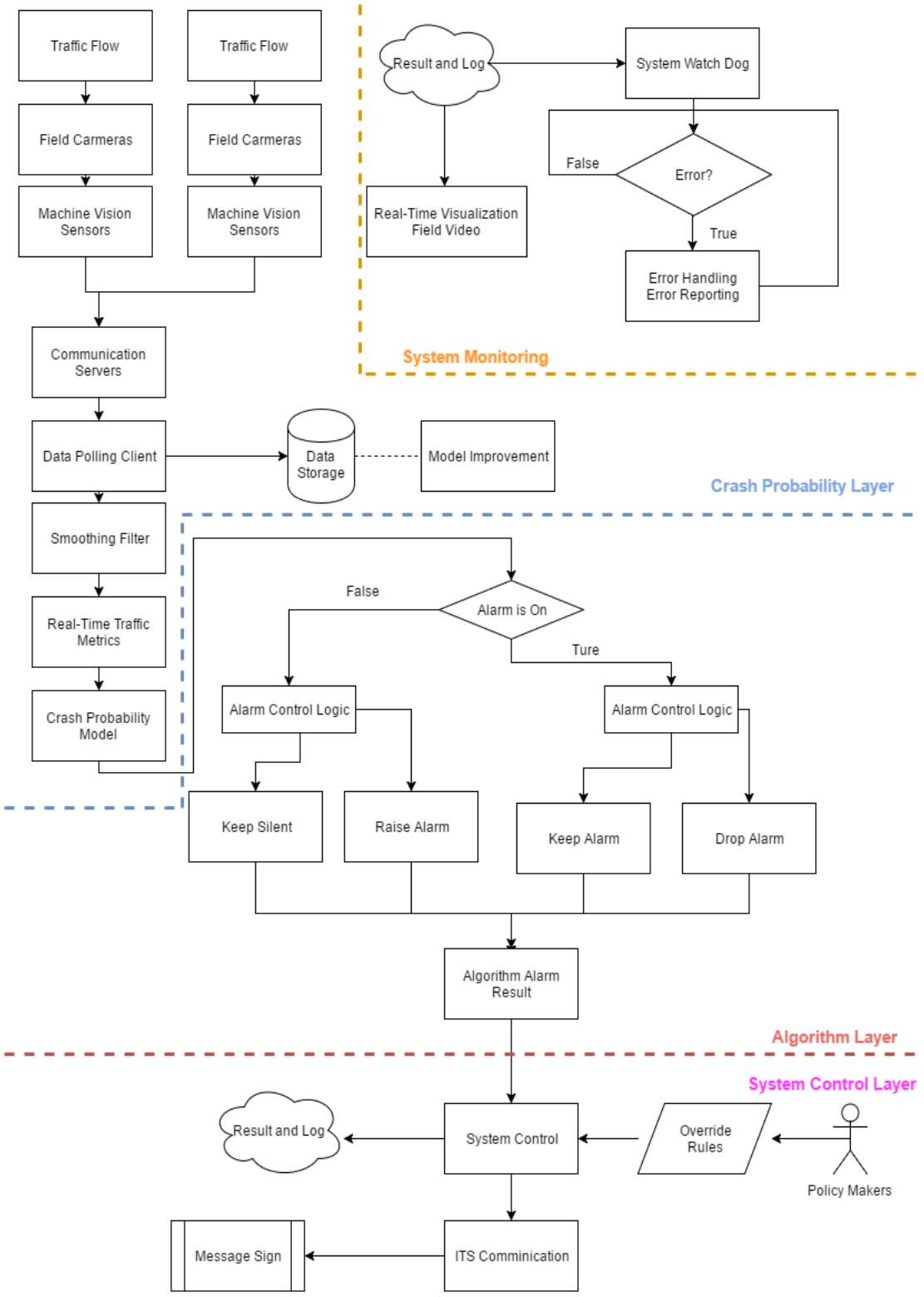

Figure 2-4 MNQWARN System Architecture

For more details of the MNQWARN's CPC system architecture and calibration, please see the 2017 MNQWARN report "Development of a Queue Warning System Utilizing ATM Infrastructure System Development and Field-Testing" (60).

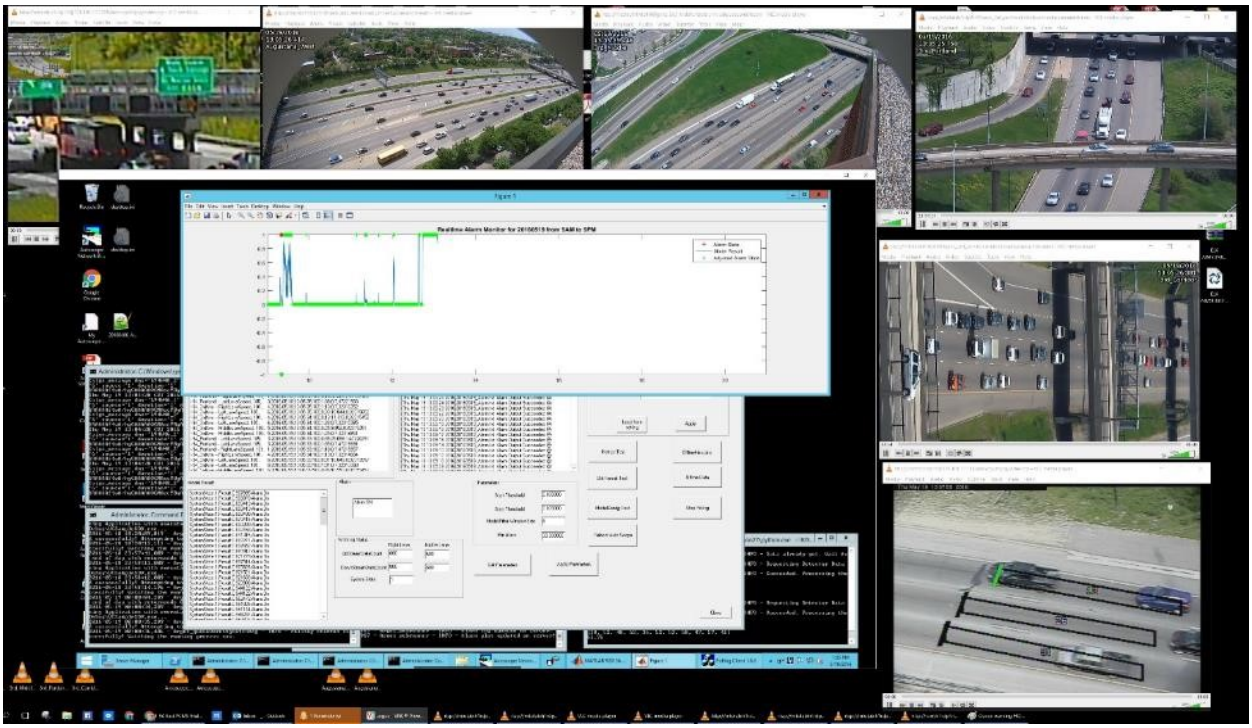

Figure 2-5 Control Interface of the Real-Time I-94 Queue Warning System

As previously mentioned, the MNQWARN system was affected by agency overrides at the time of deployment. The overrides were intended to limit possible overexposure of drivers to the warning by what was, at the time of implementation, an unproven system. They consisted of a time override and a congestion override. The time override prevented the ILCS from being turned on, regardless of the alarm status before noon or after 8 p.m. The congestion override also prevented the sign from being turned on when five consecutive 30- second average speed measurements at the loop detector near the farthest upstream sign are below 25 mph. This override was intended to reduce driver overexposure to the warning by not displaying a warning when drivers are already travelling slowly. The time override was removed in November 7th 2016, during this phase of the MNQWARN's lifespan.

2.3 EVALUATION METHODOLOGY

MNQWARN was monitored during the three phases of the field implementation. Phase 1 lasted from March 1st, 2016 to April 30th, 2016 and involved the operation of the system in silent mode, meaning the sign was not activated but alarms where recorded. During this phase, the system's ability to operate correctly and reliably were tested and minor adjustments were made in the system parameters. Phase 2 lasted from May 1st, 2016 to June 1st, 2016 and involved full system operation as well as the introduction of a heuristic test to reduce the time it took the alarm shut off at the end of the day when traffic

returned to free-flow for the day. Phase 3 lasted from June 2nd, 2016 to August 31st, 2016 and involved the full operation of the system with no further changes or fine-tuning. The system continued running through August 31st, 2018, with sporadic minor outages. The results presented in this report are those gathered between June 2016 and August 2018.

With construction on I-35 and I-94 beginning in August 2017, several changes to the geometry of the MTO Field Lab were made as discussed in (section). The rooftop stations were not affected by the construction. However, with shifts in lanes and temporary outages due to the construction, the MNQWARN system as a whole was affected by the construction. During the video reduction process, complete (6am to 8pm) days with full coverage of the downtown corridor were prioritized. This prioritization minimizes abnormalities due to construction.

As discussed in (section), several overrides were put in place by MnDOT. These overrides included restriction of time the gantry signs could operate (removed in Nov 2016); congestion, to avoid overexposing drivers to the messages; and "sign busy", where the signs were being used to display a message from MnDOT rather than MNQWARN. In addition to planned overrides, MnDOT's sign logs indicated that sometimes a connectivity or refresh issue prevented the sign from being seen by the driver, and that sometimes, MNQWARN did not raise an alarm.

2.3.1 Video Reduction Process

To determine the effectiveness of the system, video captured by MTO's rooftop station was watched by Undergraduate Research Assistance (UGRAs) from the period of April 2016 to August 2018. During the reduction process, a shift in the data being captured by the UGRAs occurred to ensure all aspects of the effectiveness of the system were being considered. The final capture process consisted of coding events observed on video, utilizing the system described in Figure 2-6 and Table 2-2.

Event Details							Sign Status		
Camera	Event Time	Event Type	Event Lane	Comments	Duplicate?	Duplicate Override	Time Under Sign	Sign Seen Code	Sign Seen Code 2
[C, P, M]	[HHMMSS]	[C, N, S, E, U]	[R, M, L, B]	[ ]	[0 or 1]	[0 or 1]	[HHMMSS]	[ ]	[ ]
P	115444	S	R		0			N2	N2.0
P	115447	N	R		0			N2	N2.0
P	122205	S	R		0			N2	N2.0
P	134120	S	R		0			C1	C1.0
P	135120	S	R		0			Y1	Y1.0
P	135754	S	R		0			C1	C1.0

Figure 2-6 Coding used to capture event data

Table 2-2 Video reduction code definitions

Column Names and Codes for Video Analysis	Definition
Camera [C, P, M]	Which camera recorded the video the student is watching: Corridor, Portland or Middle (see Figure XX for screenshots)
Event Time [HHMMSS]	Time of the event
Event Type [C,N,S,E,U]	Type of event: crash, near-crash, scared driver, emergency vehicle, or unknown.
Event Lane [R,M,L,B]	Event lane: right, middle, left, both shoulders
Comments []	General comment on the event
Duplicate [0 or 1]	This column checked times of events to ensure UGRAs were not recording duplicate events. If two events occurred within four seconds, they would be flagged for review
Duplicate Override [0 or 1]	UGRAs could enter 1 here to confirm events were not duplicated
Time Under Sign [HHMMSS]	Only used in cases of "close" sign codes; UGRAs would trace vehicles back to when they were underneath the ILCS and record the time to confirm if the ILCS sign displayed a warning
Sign Seen Code []	Automatically generated through MnDOT's sign logs, this code represented whether a driver could have seen the ILCS or not, and why.
Sign Seen Code 2 []	Only used in cases of "close" sign seen codes; automatically generated using MnDOT's sign logs when a UGRA entered the "Time Under Sign"

UGRAs watched video captured by three cameras along the field lab, located at Portland, along the Corridor, and Middle. Screenshots are shown below in Figure 2-7.

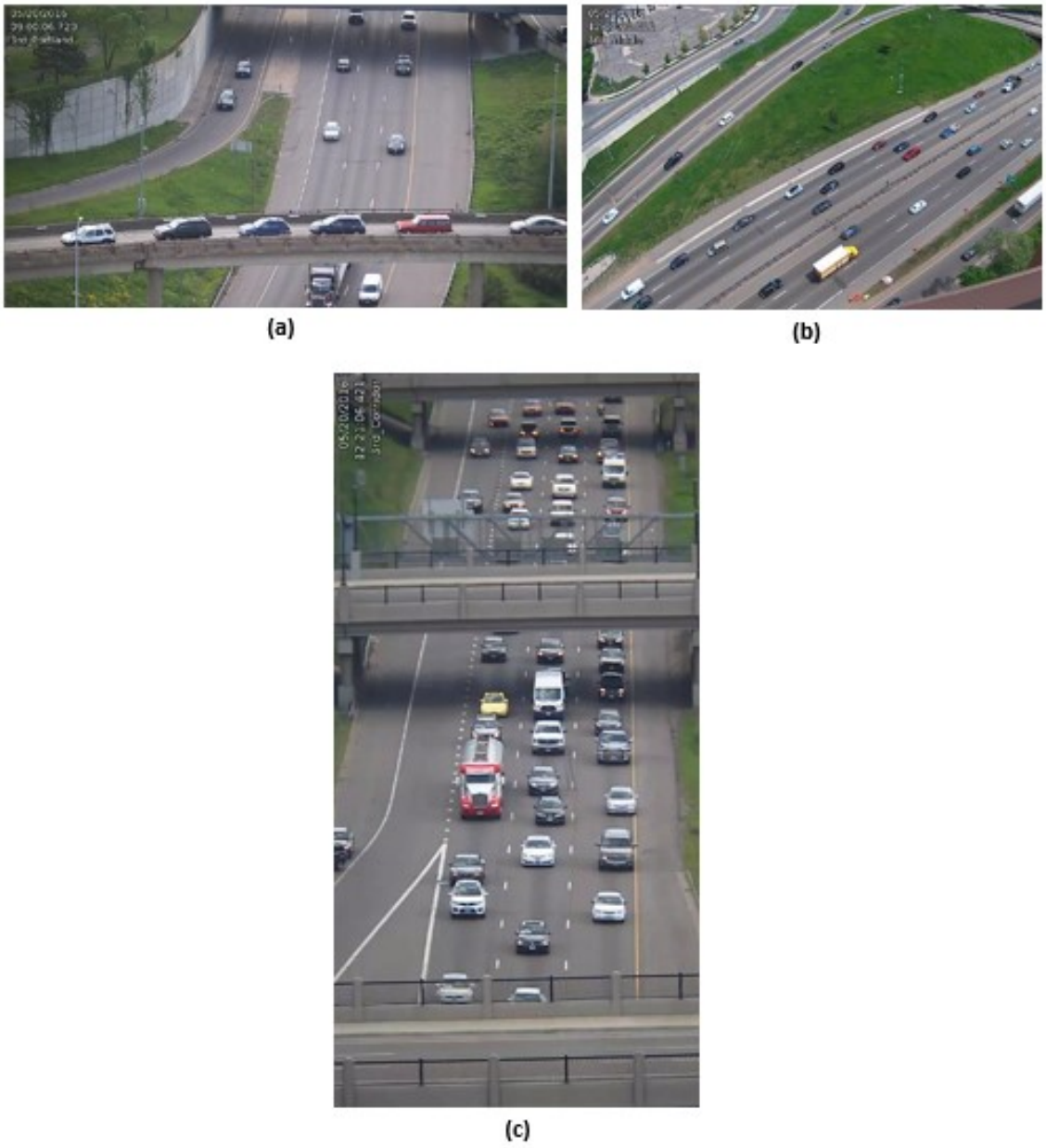

Figure 2-7 Views from MTO Field lab cameras: a) Portland, b) Middle and c) Corridor

The differences between “crash”, “near-crash”, and “scared driver” were a critical piece of UGRA training. A crash involved one or more vehicles colliding, though the angle of the MTO’s cameras sometimes made it difficult to tell the moment one occurred. UGRAs would look for vehicles pulling off to the shoulder and trace them back to the moment of collision. An example of a crash is shown in Figure 2-8.

Figure 2-8 Crash on Corridor camera (circled in red)

Near-crash was defined as a vehicle encountering a shockwave and veering out of lane into a shoulder to avoid impact. To be designated a near-crash, the vehicle leaving the lane must have not been able to come to a stop before its front bumper passed the rear bumper of the vehicle it was following; more likely than not, a rear-end collision would have occurred had the driver not swerved. An example of a near-crash is shown in Figure 2-9.

Figure 2-9 Near-crash on Portland camera (circled in red)

A scared driver was defined as a vehicle swerving out of its lane in response to a slowdown ahead; unlike a near-crash, this vehicle would stop or pull back into lane before its front bumper passed the rear bumper of the vehicle ahead of it.

Figure 2-10 Scared driver on Middle camera (circled in red)

Emergency vehicles were noted to account for any abnormalities with the algorithm when they came through could be explained, as many vehicles would be forced out of lane depending on the amount of congestion at the time they passed through. “Unknown” events were true abnormalities that couldn’t

be assigned a cause, like a vehicle swerving in and out of the shoulder seemingly attempting to get a better view of traffic ahead, or someone with vehicle trouble pulling over outside of a shockwave event.

To ensure the data captured by UGRAs was consistent and of quality, the UGRAs were split into two groups. Group 1 watched Mondays, Tuesdays and Wednesdays of each week, and Group 2 watched Wednesdays, Thursdays, and Fridays. The Wednesday overlap days were then checked by a UGRA to determine if the two groups agreed on events or not. The UGRA would then report which group had a more accurate event log, and this would be included in the final master list of events to avoid duplication. Errors, false events, and differences in event descriptions were noted and an MTO researcher would follow up with either group or specific UGRAs for additional training. This double-blind approach helped ensure the data was captured accurately and reflected the true effectiveness of the MNQWARN system.

2.4 RESULTS

This section presents results as of the time of publication. UGRAs have watched 413 complete weekdays out of 650 potential (total partial and complete) weekdays from April 2016 to August 2018.

2.4.1 Detection Rates

To assess the performance of the system, the detection rate of all conflict events between 3rd Ave and Chicago Ave during the three-month evaluation period was calculated separately for the control algorithm and for the system as a whole. The detection rate was calculated for just the crashes, near crashes, and both events combined. To find the actual number of conflict events, all the events observed during the evaluation period were tabulated and sorted based on whether the drivers involved were warned or not warned about CPCs before the event and if the drivers were not warned, the events were separated by the reason the system failed to warn them (the results are tabulated in Table 2-3 and displayed in Figure 2-11). This study uses 2013 event rates as the reference because they are the most recent results of video data that were fully analyzed by the MTO prior to this report and prior to the MNQWARN system being activated.

Table 2-3 Breakdown of system performance in right lane by component

Reason For Failure to Warn Driver	Event Type					
	Crashes		Near Crashes		All Events	
	[Count]	[% of Tot.]	[Count]	[% of Tot.]	[Count]	[% of Tot.]
Driver warned	65	29.4%	261	34.6%	326	33.4%
System buffering or inoperative	26	11.8%	42	5.6%	68	7.0%
Alarm was not raised	68	30.8%	234	31.0%	302	30.9%
MnDOT congestion override in place	28	12.7%	60	7.9%	88	9.0%
MnDOT time override in place	5	2.3%	46	6.1%	51	5.2%
65	0	0.0%	10	1.3%	10	1.0%
System delay	29	13.1%	102	13.5%	131	13.4%
Total	221		755		976	

The results are also presented here in a Sankey diagram in Figure 2-11, for ease of viewing.

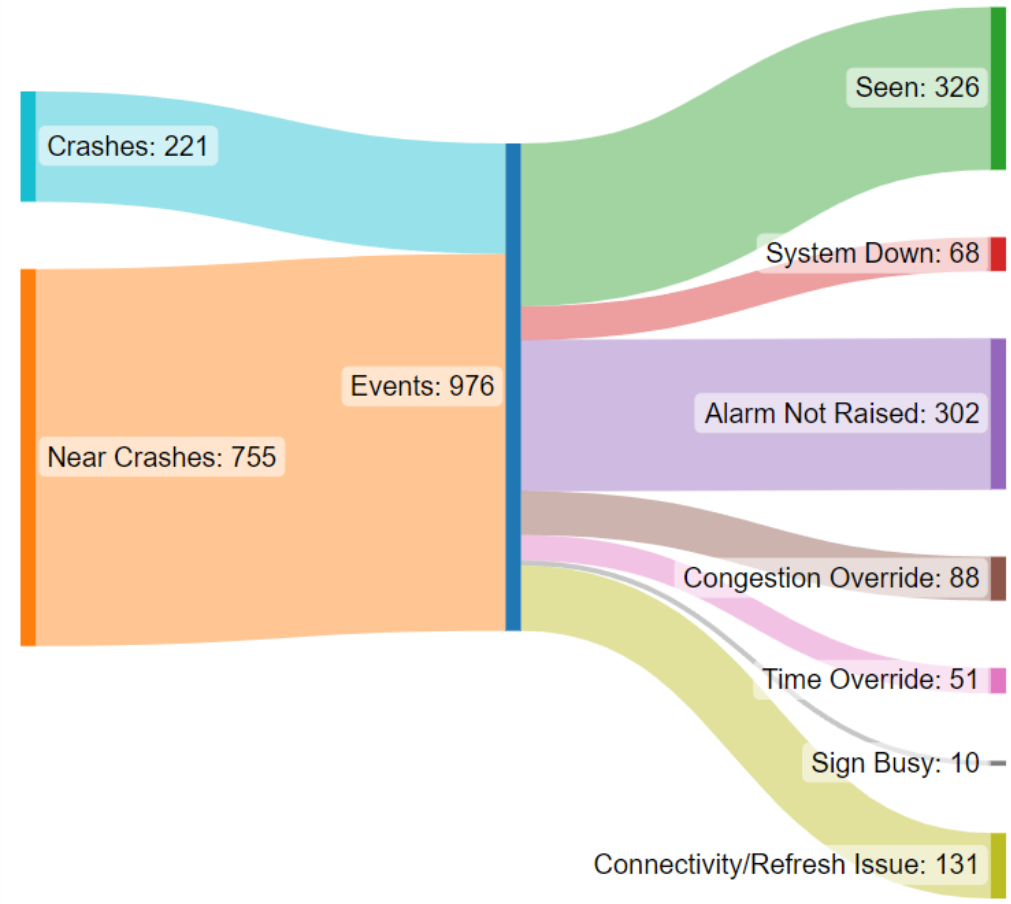

Figure 2-11 Sankey diagram showing system performance 2016-2018

As seen in Table 2-4, following a successful detection by the control algorithm, the main reason the sign was not activated is a connectivity or refresh issue. However, in around one-third of both crash and near-crash cases, the alarm was not raised by the CPC algorithm. Further investigation is required to determine why the alarm was not raised in those cases.

Using the results shown in Table 2-3, the detection rates were calculated. To assist the reader in comparing the different detection rates and to measure the effect the overrides had on system performance, the results are separated in two categories; one is based on the algorithm decision and the other is based on the whole system which includes the algorithm, the overrides, and the sign refresh rate. In addition, these results are grouped into two categories based on time period; one for the full time that surveillance data were available (9 a.m. to 8 p.m.) and the other for the system operational period of noon to 8 p.m. during which the system was fully functioning. The results are tabulated in Table 2-4 which shows the rates at which various event types were detected by the algorithm and the rates at which the system as a whole provided a warning to the drivers involved in those events for the entire day and for just the time the MnDOT time override was not imposed. As the override was only

imposed through November 2017, it did not have as much of an impact on the results as in the previous study.

Table 2-4 Detection rates during the evaluation period

Detecting Component	Event Type		
	Crashes [%]	Near Crashes [%]	Both [%]
Algorithm (9 a.m. to 8 p.m.)	65.13%	67.18%	66.74%
Whole System (9 a.m. to 8 p.m.)	33.33%	36.61%	35.90%
Algorithm (noon to 8 p.m.)	64.21%	54.28%	64.76%
Whole System (noon to 8 p.m.)	31.58%	32.23%	32.09%

Table 2-5 shows the frequencies at which events occurred in any lane between 9 a.m. and 8 p.m. on weekdays in June, July, and August of 2013 compared to weekdays over the entire study period (April 2016 to Aug 2018). These events occurred in the same length along the I-94 corridor. The system appears to have resulted in a 61% reduction in crashes and 73% reduction in near-crash events.

Table 2-5 Event frequencies per million vehicles traveled (VMT)

Observation Period	2013	2016-2018	Percent Change
Crashes	11.9	6.86	-42.32%
Near Crashes	111.8	23.88	-78.64%

Table 2-6 shows the average number of vehicles passing under the MN 65 bridge per day in 2013 and 2016. The change in the average from 2013 to 2016 is also reported in this table. It is interesting to note that the total Average Daily Traffic (ADT) decreased by roughly 15% over the course of 2016-2018.

Table 2-6 Average daily volumes during historical and current studies

Time Range	2013 Average	2016-2018 Average	Percent Difference
9 a.m. to 8 p.m.	45259.62	37492	-17.15%
Whole day	74070.05	62639	-15.43%

2.4.2 System False Alarm Rate

A prominent concern when implementing the system was minimizing overexposure of drivers to the warning sign. This concern is what prompted MnDOT to impose what, in hindsight, turned out to be somewhat excessive congestion and time overrides. Of all types of overexposures, the case of a driver seeing a warning about slow or stopped traffic but not having to slow or stop is the one that must be avoided the most. In order to reduce the false alarm rate and help alleviate potential driver overexposure, an override was built into the control algorithm to deactivate the alarm, regardless of the

model result at the time, when both MVDs observe 10 consecutive vehicles with speeds greater than 30 mph.

2.4.3 Analysis of "Alarm was not Raised" crash cases

The goal of any queue warning system is to prevent rear-end collisions on the freeway in cases where a queue or shockwave is encountered requiring the vehicles to decelerate to a stop. Naturally, since we do not control the actual vehicles yet, this is accomplished through the driver controlling the vehicle. The premise of any rear-end collision avoidance system, infrastructure or vehicle based is to communicate to the drivers the not yet encountered event in the hope that the additional time and heightened attention will allow them to handle the traffic flow state transition safely. Naturally, especially in the case of an infrastructure-based system like MN-QWARN that communicates the information through an external sign, there is no guarantee that the drivers will notice the warning, let alone change their behavior. As is the case of most prevention systems, it is very difficult if not impossible to know when they work successfully. We depend on the failures to gage the systems performance.

In the case of MN-QWARN the hypothesis is that, as long as the "Slow Traffic Ahead" sign was activated and in the line of sight of a driver that afterwards rear-ended another vehicle, the system was successful in its operation and the reason for the crash was purely driver error. On the other hand, if the sign was not activated prior to a rear-end collision, that was a failure of the system as a whole or a failure of a specific component. The results in Table 2-3 follow this directive by considering as a "success" only the "Driver Warned" cases and breaks down the "failures" in a number of root causes. From a system perspective, if the computer running the software was offline at the time of a rear-end collision event, that is a "fail". The same applies if the sign was not raised on time for the driver involved in the crash to see it before the event. As part of the new MN-QWARN implementation, system improvements have been devised and many already implemented that can potentially reduce the "fails" due to system offline and delays in the alarm condition dissemination.

Time and congestion overrides are also causes for failure since the hypothesis on these is that crashes do not happen during override times neither happen when congestion is so severe that speeds are very low. As expected, reality is never absolute, so it is possible to have shockwaves and queues form at times of the day that are not normally observed or expected and it is possible to have rear-end collisions at very slow speed conditions and small localized traffic stream speedups missed by the point detectors. The logic of the time override was that, at least initially, we could not trust the algorithm to have zero false alarms during uncongested conditions, so it was preferable to deactivate the system rather than communicate the wrong information. The false alarm would be a case where the algorithm raises the alarm, but the vehicles exposed to it never encounter a queue or are required to come to stop. Later, when trust in the system increased, the time override was removed. The logic of the congestion override is that, although crashes do happen during slow-and-go and stop-and-go conditions, displaying a warning during such obvious conditions it will reduce the validity of the warning in the eyes of the drivers and cause them to ignore the sign or perhaps all warning signs. As mentioned above, the

hypothesis is that crashes happening as very slow speeds are 100% driver error and a sign would not have made a difference.

As seen in the results, this hypothesis is mostly valid because the percent of crashes happened when the warning was not active only because of the congestion override is only ~12%. To emphasize this point, these are events where the algorithm has requested the warning activation but due to the override this request was canceled. We have not scrutinized each of these 28 crash events to determine if the warning was warranted or not. From analyzing a sample of these events, we have observed that in this particular road section, it is possible to have heavy congestion upstream of 11th Ave, where the speed driving the override is measured, and at the same time have the traffic stream between Chicago Ave and TH-65 accelerate to speeds of 35mph and higher. These localized low density, higher speed conditions are detected by the algorithm along with the propagating shockwave/queue on 3rd Ave. Therefore, there was room to fine tune the congestion override and attempt to optimize its influence and allow the warning to be displayed. Unfortunately, such a fine tuning is very site dependent and cannot be planned or implemented until the system is observed operating in the new location.

The majority of the research effort in Task 5 was spent in scrutinizing the worst case of failure, the case where a crash happened, and the algorithm had not raised the warning at all. These cases are not only the most severe of failures but also, on first view, account for 30% of the outcomes, equal to the frequency of successes (29%). Clearly, if one is looking for improvement opportunities this is the most likely place. Towards that end, we have isolated and scrutinized each of the 68 crash events where the model hadn't estimated the probability of CPC to be higher than the selected threshold. Before, discussing further the results it will be helpful to identify the scenarios where such a failure can happen.

1. Assuming that the prevailing conditions on the road are Crash Prone:
    a. The algorithm reports a very low CPC probability that never raises above the selected threshold before and after the observed crash event.
    b. The algorithm is very slow in raising the probability and the warning is raised after the event takes place.
    c. The algorithm is somewhat slow in raising the probability and the warning is raised after the vehicle involved has passed the sign but before the event takes place.
2. Assuming that the prevailing conditions on the section between 3rd Ave and Portland Ave are NOT Crash Prone but the speeds upstream at 11th Ave are higher than the congestion override threshold.
    a. The algorithm, correctly, reports a very low CPC probability but a rear-end collision takes place.

Naturally, other than the CPC probability model incorporated inside MN-QWARN there is no other factual criteria for classifying traffic conditions as crash prone or not. So, for the purposes of this analysis we established some as strict as possible albeit subjective criteria to classify conditions observed in the video as Non-Crash-Prone resulting to have any other condition as CPC by default. The criteria are simple and follow the logic of the congestion override, if the stream, on the section between 3rd Ave and Park Ave (halfway to Chicago Ave) density is very high and in extend vehicle speeds are well below

25mph continuously for the 2.5 minutes before the event, then the conditions during the crash were non-crash prone. I is difficult to visualize this conditions without a video example but the fames presented in Figure 2-12 from the three cameras covering this section can give the reader an idea. This particular event took place on the section between Park and Portland Avenues at exactly 17:43:52 on September 27th, 2016, about 10 seconds after the snapshot on the topmost video frame in the figure. So, this takes care of the event condition 2.a in the aforementioned list.

Out of the 68 events classified as "Alarm Not Raised", 28 of these took place during the described non-crash prone, heavy congestion conditions and hence can be considered that the algorithm not raising the warning was the right decision. Indeed, for most of them it is unbelievable how they happened assuming even a miniscule attention by the driver spent looking at the road.

Table 2-7 presents the performance results adjusted by reducing the "Alarm not raised" cases from 68 to 40. Similar analysis can be done for the near crashes but given that those are 234 cases the effort is not justified. In the table we see some improvement in the performance but only in the range of about 4% improvement on the "success" cases. Table 2-8 presents the relevant version of the detection rates table after the adjustment. The bottom line is that even after the adjustment, more than 20% of the events took place under CPCs and the system failed to generate a warning on time (conditions 1.a, 1.b, or 1.c).

Figure 2-12 Example of Non-Crash Prone Traffic conditions prior to crash

Table 2-7 System performance with non-Alarm raised heavy congestion crashes removed

Reason For Failure to Warn Driver	Event Type	
	Crashes	
	[Count]	[% of Tot.]
Driver warned	65	33.7%
System buffering or inoperative	26	13.5%
Alarm was not raised	40	20.7%
MnDOT congestion override in place	28	14.5%
MnDOT time override in place	5	2.6%
System delay	29	15.0
Total	193	

Table 2-8 Detection rates with non-Alarm raised heavy congestion crashes removed

Detecting Component	Event Type
	Crashes [%]
Algorithm (9 a.m. to 8 p.m.)	76.05%
Whole System (9 a.m. to 8 p.m.)	38.92%
Algorithm (noon to 8 p.m.)	75.31%
Whole System (noon to 8 p.m.)	37.04%

2.4.3.1 First Wave (FW) traffic patterns

From early observations of the algorithm performance, we have detected that it takes some time for the real-time adjusted probability to raise above the selected threshold. From long observations on this location, we know that the most common CPC pattern involves several short-lived shockwaves that dissipate before they reach the area upstream of TH-65. Given that these waves very rarely produce crashes or near-crashes, the algorithm has been trained to be less sensitive to them, building the CPC probability gradually. Regardless, there are observed cases where the upstream demand is high enough to produce what we call a “first wave”. This condition basically is a single shockwave, generated downstream of 3rd Ave and propagates rapidly all the way to Portland and upstream. This fast evolution

of CPCs does not leave much time for the algorithm to react hence the delay or complete failure in generating the warning. From the remaining 40 cases of CPC conditions, 16 (~40%) involved a "first wave" traffic pattern. In these situations, the warning has been inactive for a long period of time.

From the 16 FW cases, in 3 of them the crash took place on the section between 3rd Ave and TH-65. From the crash records, we know that such events are very rare and happen so soon after the disturbance is first detected that it is impossible to do anything about them. From these 4, two (2) involved an isolated event, not followed by additional shockwaves resulting in the warning to never being raised. For the other two, the warning was raised less than 30 seconds later. Therefore, if the event hadn't been one of the rare ones, the warning would have been activated fast enough.

From the remaining 13 FW cases, in 2 cases the warning was never raised because this fast-moving shockwave was a singular event followed either by a complete recovery (1 case) or heavy congestion (1 case). It is very little that can be done in such cases since the only solution is to raise the warning every time there is any slowdown (not preferred).

From the remaining 11 FW case, another 2 resulted for the warning being raised only a few seconds after the crash event (not including the delay in communicating with IRIS). In these cases, the distance between the two detection stations played a critical role. If the two stations were farther away, the travel time of the shockwave would have been longer and allow the warning to be initiated before the disturbance reaches the upstream station. In the original system deployment, given that the detectors were located on the rooftop of the high rise on 3rd Ave, the distance between stations was the maximum the site could accommodate. In the new deployment, we have planned for three consecutive detection stations. The first two are approximately at the same distance as in the original implementation but the third is more than twice that distance from the first. This detection layout will allow us to observe the CPC probability estimation produced simultaneously from pairs of stations with very different distances and find out if that successfully resolved this issue. No modifications to the algorithm logic are necessary.

The final 9 FW cases involved the warning being raised more than 2 minutes after the event. Although increasing the distance of the stations will affect some of these situations, 2 or more minutes is a long time period under which a strong isolated wave can travel half a mile or more upstream. We will explore lower thresholds, but it may be that such cases remain unresolved.

2.4.3.2 Non-FW traffic patterns

Excluding from the original 40 cases the 16 FW cases, we have 24 remaining cases where the warning was not raised at the right time and the event was not the result of the very first shockwave. From these 24, in 5 cases the warning was never raised, before or after the event (at a range of 5-7 minutes). In 2 of these cases there is a potential environmental condition involved. In one case the downstream detection area was in deep shadow from the 3rd Ave Bridge while the surroundings were covered with snow. This most likely resulted in a very dark video feed rendering the vehicles almost invisible to the Autoscope. The second case involves a day with very strong winds that caused the masts the Autoscopes

were mounted on the roof top to shake. Under those conditions the Autoscope does not produce speed measurements because it senses that the error will be large. The remaining 3 cases of “never warning” do not include any detectable reasons why the probability never raised above the selected threshold.

From the remaining 19 cases, in 10 of them the warning was active a minute or less earlier and had recently been deactivated. These cases involved very long slow-moving shockwaves resulting in the algorithm to get confused between high probability due to the disturbance and low probability due to the long size of the wave being confused for established congestion. In half of these 10 cases the warning was raised less than 30 seconds later. Only for 3 out of the 10 the warning was raised again more than 2 minutes later. Therefore, given this system response, increasing the distance between stations should also help since it will reduce the cases where the same wave occupies both stations almost simultaneously resulting for the warning to not being deactivated or raised before it is too late. Again, no further modifications to the algorithm are needed for this to be implemented.

For the remaining 9 cases where the traffic pattern did not involve a first wave, in 4 of them the alarm was raised less than 30 seconds later, therefore increasing the station distance will help. For the final 5 one (1) involved low light with rain. Such conditions create reflections from the headlights that confuse the Autoscope. We cannot say that this was the reason, but the data are not reliable to make further conclusions. From the remaining 4 cases 3 involved fluctuations between heavy congestion and recovery resulting in slow raises of the probability and more than 2 minutes delay in raising the warning.

The final case is a real mystery since based on the numerical data the warning should have been raised but for some reason that remains unexplained it remained inactive. It is not worth scrutinizing it further since it could be a computer glitch.

2.4.4 System Limitations

Due to the fact that the system is still in the prototype phase, several aspects of it are less than ideal and result in uncertainties of varying degrees. The limitations and uncertainties include the non-ideal configurations of the MVDs and warning sign, the limitations of the hardware, the fact that some of the equipment was shared with MnDOT, and the fact that the model result is currently computed for only the right lane. In the interest of cost and time, the MVDs were installed on a high-rise near the road rather than on a gantry or bridge directly over the road. The warning messages were displayed on the relatively small MnDOT changeable message board rather than a purpose-made display with potentially different characteristics (location, size, color, etc.). The limitations of the hardware also presented a source of uncertainty in that the speed data from the MnDOT single loop detector was only a 30-second average and was not completely accurate. Issues with power outages and lack of sufficient data storage at the rooftop station resulted in missing video data. Because control of the sign and the camera monitoring was shared with MnDOT, the sign was occasionally used to display incident management messages from MnDOT rather than the queue warning messages. Because the capability of the system to function as intended and the effect that it would have on drivers were unknown at the time of installation, it was only applied to one of the three lanes. As a result, it is unclear what effect this partial deployment had on driver's actions.

2.4.5 Conclusion

With a statistically significant amount of data from the two-year operational period analyzed, the system appears not only to have continued to reduce crashes from the original 22% reduction, but also to have a greater effect on crashes and near crashes. Crashes were reduced by 56% and near crashes were reduced by 69%.

CHAPTER 3: REDEPLOYMENT OF MN-QWARN (HIAWATHA AVE)

As discussed in the introduction, the second goal of the project was to test the transferability of the MN-QWARN system. Although, any freeway section that experiences congestion and has a relatively high frequency of rear-end collisions would suffice, the desire to take advantage of the extensive data collection and surveillance infrastructure of the MTO I94- Field Lab paired with the expectation of severe congestion upstream of the original test section due to the four yearlong reconstruction project prompted the project to target the area over Hiawatha Ave as the second system evaluation site.

The rooftop stations were not affected by construction on I-35 and I-94, but some changes were made throughout the Field Lab as construction affected the downtown corridor. In addition, concurrent to the previous project that developed and implemented MN-QWARN, a separate project funded by USDOT through the RSI, upgraded the I-94 Field Lab to include CAV Testbed functionality. The main addition involved the introduction of sensing infrastructure at the roadway level, either deployed on MnDOT ITS infrastructure elements (gantries, NIT Poles) or on MnDOT ROW in the form of solar powered, wirelessly communicating stations.

Figure 3-1 Original Field Lab site showing radar sites (red dots), radar coverage (outlined in red), rooftop stations (yellow dots) and camera coverage (outlined in green).

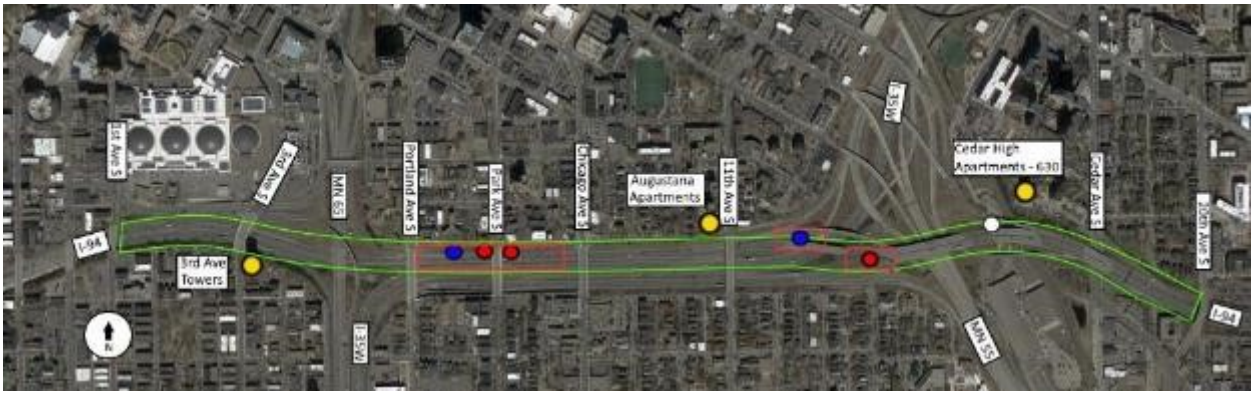

Figure 3-2 New Field Lab site showing radar sites (red dots), Wavetronix sites (blue dots), radar coverage (red outlines), rooftop stations (yellow dots), and a future MnDOT station (white dot).

The RSI sponsored project allowed for continuing operation of the CAV Testbed part of the Field Lab and also included provision for the inevitable removal and relocation of some of the stations due to the construction on I-94 that began in August of 2017. The goal of relocating stations was to change the area of coverage, without losing any capabilities in regard to the CAV Testbed functionality. With cooperation from the project contractors, MTO was able to keep stations running right up until they would be in the way of the excavators. Figure 3-1 shows the original Field Lab and areas of camera and radar coverage. Figure 3-2 shows the Field Lab after stations were retrieved and relocated.

As shown in Figure 3-2, both the 3rd Ave station and Portland Ave stations were removed because of the construction. Using parts from those stations with some refurbishment and rebuilding, new stations were deployed east of the 11th Ave overpass and on the I-94 median just east of the I-35 junction. Specifically, the 11th Ave station is using the same wooden pole and solar panels originally deployed on Portland Ave while the median station employs one of the MTO owned solar powered work zone trailers previously acquired for a different MnDOT project. Additionally, at the end of the 2019 construction season, MnDOT deployed a new NIT pole on the north side of I-94, over Hiawatha Ave.

3.1 UPGRADES AND MAINTENANCE OF EXISTING MTO INFRASTRUCURE

For the purposes of this project, a lot of effort was spent in upgrading and repairing parts of the I-94 Field Lab that had fallen in disrepair due to lack of funding given they didn't have a direct relevance to an active project. For example, the rooftop station on Augustana and Cedar Ave buildings had several functionalities non-operational either on purpose, to reduce the system load, or simply because malfunctioning components were not replaced/repaired. In the new project, since the physical location where the MN-QWARN system will be operational moved to the east end of the Field Lab, these stations are on the center of the video and data flow. An example of the work accomplished can be seen in Figure 3-3 presenting photos taken during the several field visits by MTO personnel.

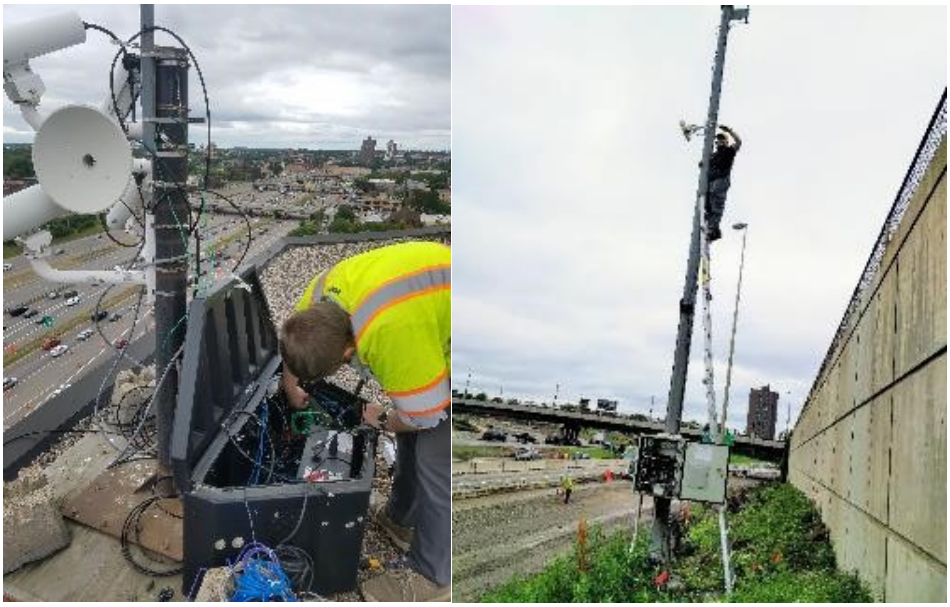

Figure 3-3 Field hardware repair and maintenance efforts

Figure 3-4 Augustana and Cedar Rooftops Monitoring Feeds

The traffic monitoring cameras on Augustana and Cedar rooftops were repaired and repositioned to collect video for the purposes of this project. Examples of the new feeds can be seen in Figure 3-4.

3.1.1 New Traffic Detection and Monitoring Stations

As already mentioned, the implementation of the MN-QWARN system on a new road section, requires the deployment of new detectors. Two new MTO traffic detection and monitoring stations were deployed and a specially installed MnDOT NIT pole for use in this project was instrumented and integrated into the MTO I-94 Field Lab system. These stations, described by their approximate location on the road, are the 11th Ave Solar station, the Median station, and the Hiawatha NIT pole station.

3.1.1.1 11th Ave Solar Station

The 11th Ave Solar station consists of a solar pole moved from Portland Ave due to construction on I-94. While a contracting company moved the pole itself, MTO staff rented a bucket truck and re-assembled the station on site. Figure 3-5 shows the pole after being assembled, with bucket truck still in view. The figure also shows a closer view of the pole's SMS radars, camera, Wavetronix, and solar panels. (This shows the westward facing SMS radar. There was an identical radar facing east on the opposite side of the pole, not shown.). Later in the project, these two radars were relocated to the Hiawatha NIT pole station.

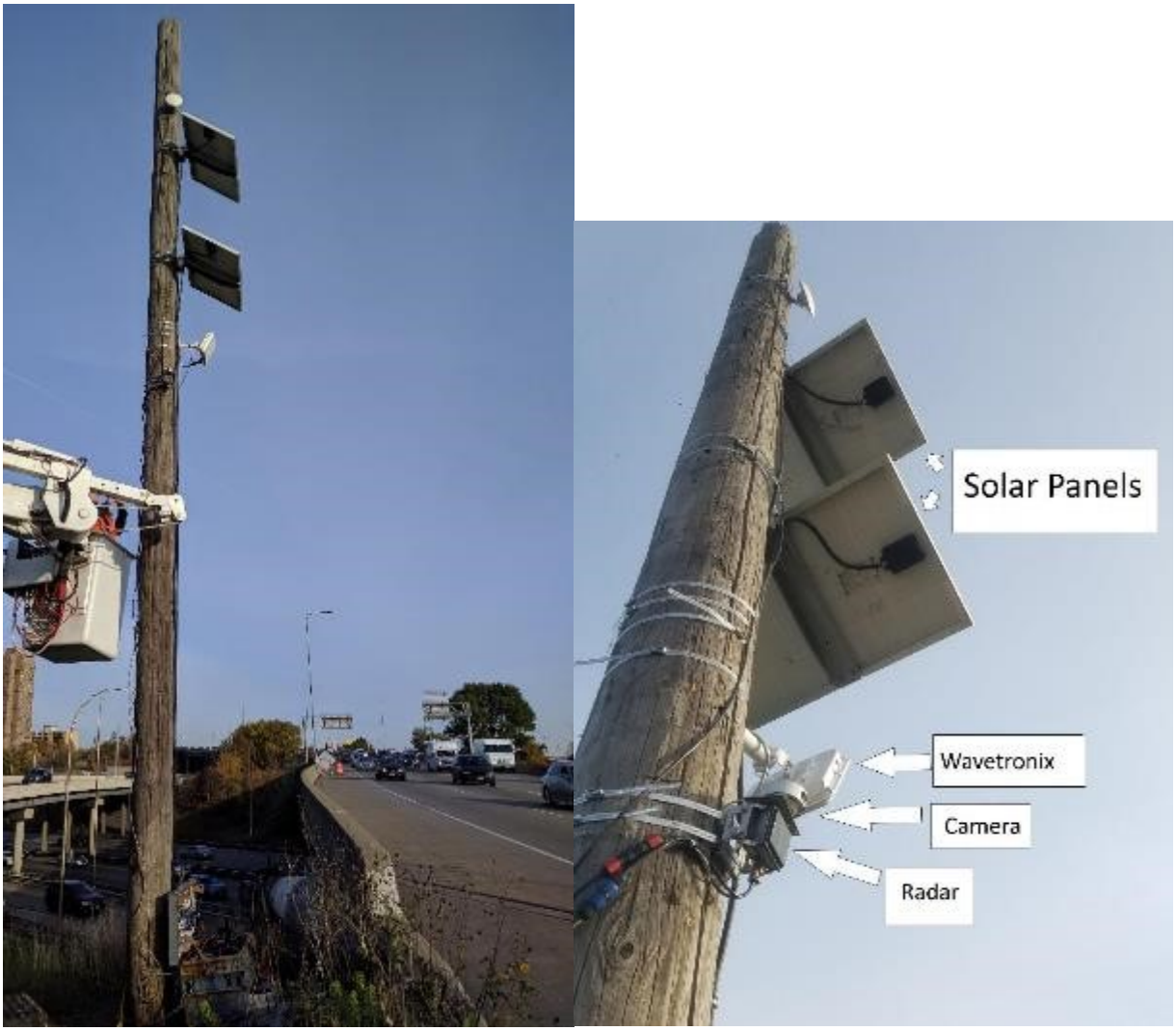

Figure 3-5 Hiawatha station being assembled.

The instrumentation and power control devices for this unit had to be redesigned in order to eliminate power overloads caused by the addition of new sensors and cameras as compared to the Portland Ave deployment. The major hurdle that had to be overcome was the use of the Wavetronix radar. Although simple in its integration as compared to other MTO sensors, the power requirements are very high and incompatible to our dependence on solar power for the station operation. Although the 11th Ave station has several sensors and cameras, to proceed with the project needs all components except the Wavetronix were deactivated. Even with this scale down, we had to deploy additional enclosures with batteries to maintain operation during the winter. Snowfall and freezing temperatures reduce considerably the power harvesting and storage of the solar system.

The station is also equipped with two cameras looking east and west as shown in Figure 3-6. Video from before the cameras were deactivated is used in the shockwave analysis in this location that will help in

the implementation of the new MN-QWARN system.

Figure 3-6 View from Hiawatha station, looking east (a) and west (b) (bucket arm from assembly in view).

3.1.1.2 Median Station

The Median station was located approximately 700 feet east of the 11th Ave station. As seen in Figure 3-7 this station used a work zone solar trailer as the supporting structure. The trailer, owned by MTO, has been retrofitted to carry the MTO custom set of sensors, power control and network equipment. Similar to the 11th Ave station, the Median station is solar powered and in extend has the same advantages and disadvantages in respect to the use of a Wavetronix sensor. For this reason, additional batteries have been deployed and sensors, like the SMS radar and the cameras, that are not critical for the operation of MN-QWARN have been deactivated.

Figure 3-7 Deployment of the TH 52 trailer.

3.1.1.3 Hiawatha NIT Pole station

Given the roadway layout, from the beginning of the project it was emphasized that a station as close to the crest of the vertical and horizontal curve on the roadway after the Cedar Ave exit was required. Alternatives were explored on how to deploy such a station, and for a period of time early in the project a second trailer, similar to the Median Station was considered. The deployment of such a trailer would have been extremely challenging because of the slope of the ground outside the road barrier as can be seen on left picture in Figure 3-8. Thankfully, the RTMC offered to deploy a permanent NIT Pole on that location and allow the project team to add on it additional sensors and radios. The pole, deployed fall of 2019 can be seen on the right photo. Because of delays in ordering the sensors and other pieces of equipment, it was not possible to complete the activation of this station till mid-2020.

The pole has constant power but it is using wireless radios to connect to the MTO. As a test for MnDOT, a Houston Radar Speedlane radar detector has been installed in this location. The project developed drivers for this device similar to the ones developed for the Wavetronix that stream to the MTO database an identical stream of data. Given the abundance of power in this location the station not only operates 24/7 but also includes a surveillance camera and two SMS downlane radar sensors. Since November 2020 this station is used as the Upstream station for the system.

Figure 3-8 Hiawatha MnDOT NIT Pole location and road view.

3.2 CAV TESTBED SYSTEM ARCHITECTURE ENHANCEMENT

Figure 3-9 shows the CAV Testbed data collection system architecture as it was delivered spring of 2019. That system was developed to handle the enormous data flow generated by the seven SMS radar sensors deployed that capture vehicle trajectories at 20Hz rate.

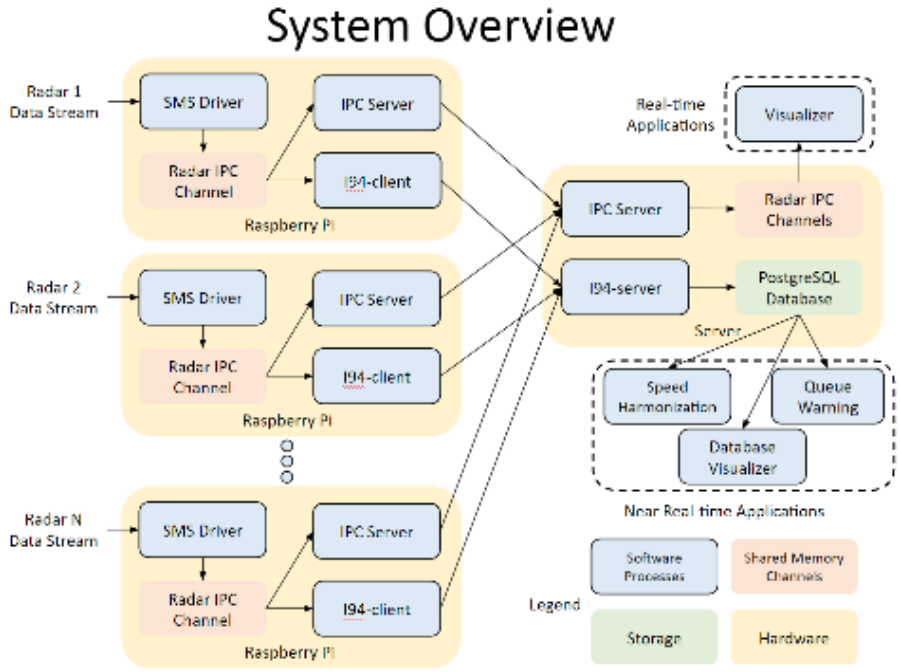

Figure 3-9 Data collection system architecture

This architecture involved custom developed software running on stations in the field forming direct information pipelines to processes running at the MTO lab. This architecture guaranteed synchronization over multiple sensors, data flow preservation in cases of network interruptions, and

more importantly complete control of all system parts remotely since the CAV Testbed sensors were on MnDOT ROW and difficult to access. For example, the station deployed on the Park Ave gantry requires the use of bucket truck parked on the median of I-94 to access it. So, it made sense to expand the CAV Testbed system to cover the needs of MN-QWARN. This resulted in the development of new sensor drivers (software running in the field) and their counterparts at the MTO lab. The new upgraded architecture can be seen in Figure 3-9. Apart from the introduction of a new sensor in the system and its data stream integrated in the MTO database server, the new MN-QWARN application does not communicate directly with the sensors, as it was the case with the Autoscopes, but it is requesting data from the database server. This way the new MN-QWARN is also more sensor agnostic.

3.3 SYSTEM CHANGES TO ADAPT TO THE NEW DEPLOYMENT LOCATION

The new implementation of the MN-QWARN algorithm utilizes a changeable message sign at the far upstream end of the corridor where there is also a Minnesota Department of Transportation (MNDOT) vehicle speed detector reporting 30 second average vehicle speed data. In addition, there are three point vehicle speed detectors at 1250 ft, 2025 ft, and 2665 ft along the corridor which report individual vehicle speed measurements. Figure 3-10 shows the study area including the intersection with I-35W. Also marked on the figures are black lines where each of the three individual vehicle detectors is located, a red line marking the queue warning sign and 30 second average vehicle speed detector, and two blue lines marking the critical zone. This is the location that is assumed to be the most dangerous and is demonstrated to contain the most crashes (see Section 5.4).

Figure 3-10 Aerial view of I-94 Corridor studied.

Initially, this system was intended to warn vehicles that are around 800-1200 feet along the corridor when they encounter shockwaves. This location was assumed to be the most dangerous along the corridor since vehicles are moving downhill a curve in the road limits visibility. However, there was no way to confirm this assumption prior to 2017 due to a lack of details in the crash reporting system. A more recent analysis (see Section 5.4) suggests that many of the crashes (both in 2019 before implementation and after implementation in 20201) happen further downstream on the straight section between Hiawatha and I-35W. For this reason, the bounds of the critical zone (the area where we want to warn drivers of dangerous conditions) were extended to 800-1400 ft. The study area has 4 lanes until the point where the dedicated exit lane onto I-35W diverges, and the MN-QWARN system is

implemented for both the far right and far left lanes as described below in Section 3.3.1 . This system uses the warnings: “Slow Traffic Ahead Left Lanes”, “Slow Traffic Ahead Right Lanes” or “Slow Traffic Ahead All Lanes” on a single sign.

The two sides of the road experience fundamental differences in the traffic flow at this location. For the right side implementation, the right lane generally does not have a high demand coming from upstream. Drivers know about the high volume on-ramp at 11th Street and have a good view of the oncoming traffic due to the hill. This allows them to move into the middle and left lanes ahead of time and prevent the propagation of this congestion into the critical zone. For this reason, the shockwaves progressing along this lane generally move more slowly. On the left side, patterns change due to the left-hand exit onto I-35W. The left lane is very high volume since all of the vehicles exiting are forced into the left lane. However, there are fewer lane changes on the left side since everyone is going to the same place. The differences in geometry and traffic pattern make this location an important contrast to the original development of the algorithm and will demonstrate the versatility of the implementation.

It is also important to note that the right and left lanes experience fundamentally different congestion propagation. The congestion on the left side comes primarily from I-35W and the congestion on the right side come from I-94. Some examples of how congestion propagates are shown in Figure 3-11. In Figure 3-11a on November 3rd, 2020, the left lane becomes very congested early in the day due to high traffic volumes on I-35W. Figure 3-11b and Figure 3-11c show that some of this congestion influences the middle and right lanes, but there are no strong shockwaves during this period. Later in the day, however, traffic on I-94 gets worse, and shockwaves arise independently, which later affect the middle lane and to a lesser extent the left lane.

Figure 3-11d, Figure 3-11e, and Figure 3-11f depict another common scenario. On July 8th, 2021, I-94 became congested early in the day and remained congested for much of the period. In this scenario, there are a few stronger shockwaves along the right lane, but most of the congestion in the middle and left lanes is propagating from cautious drivers passing slower moving vehicles to their right. This prolonged congestion on I-94 continues back past the lane split for the exit onto I-35W, which in turn prevents long queue from building up at the exit as capacity doubles when the new lane is added.

In this location, congestion regularly forms and propagates from both the right and left sides of the road. For this reason the regular pattern of congestion starting in the right lane, then the middle, then the left, does not always hold. Instead, there are many cases of congestion propagating farthest in the middle lane as vehicles merge to avoid the slower traffic on the right and the left sides. These characteristics have important implications for the function of the algorithm.

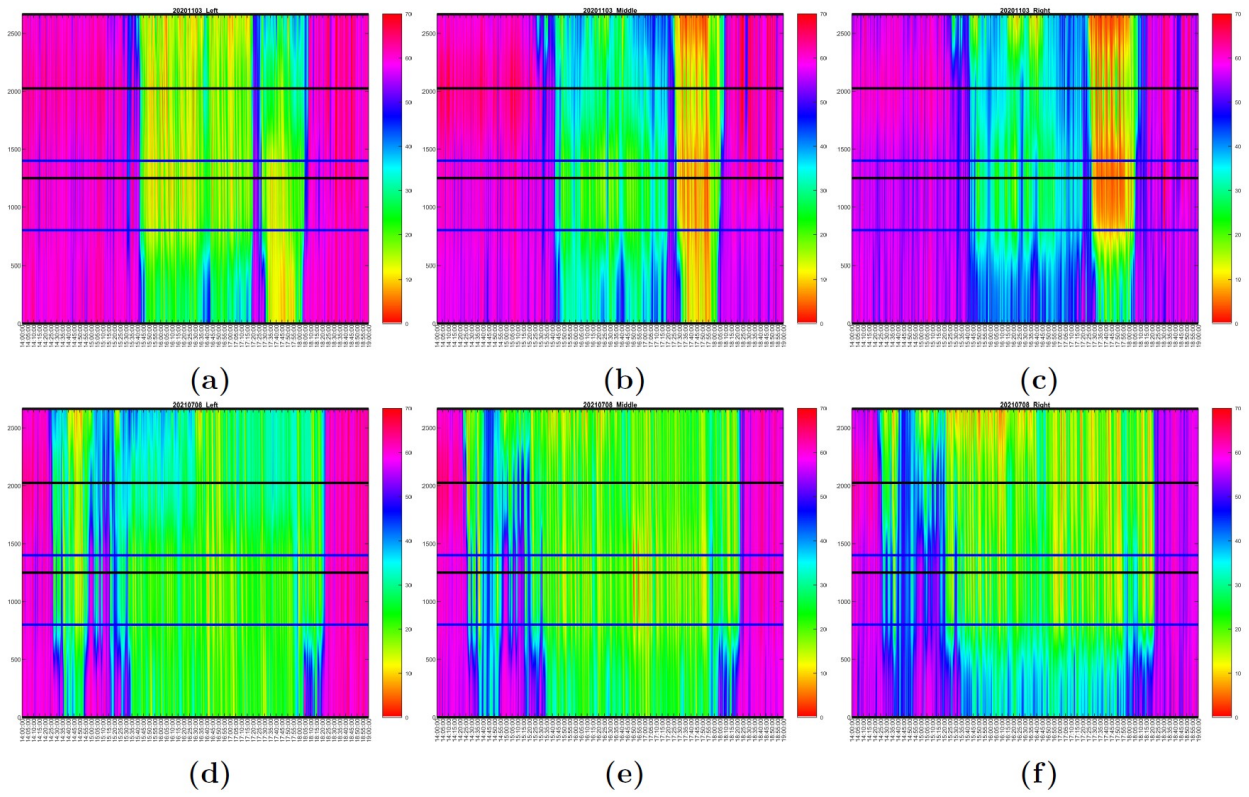

Figure 3-11 Heatmaps of vehicle speeds between 2:00 pm and 7:00 pm on November 3rd 2020 (a, b, c) and July 8th 2021 (d, e, f) depicting different stages of traffic propagation. (Black lines - detectors, Blue lines - critical zone boundaries.)

3.3.1 Updated MN-QWARN System

Any queue warning system attempts to detect dangerous traffic conditions along a roadway and alert drivers to prevent them. The assumption is that drivers tend to experience CPCs whenever they experience slow-and-go traffic. Generally, crashes occur at the ends of queues where drivers are forced to decelerate quickly. However, based on the methodology of Hourdos et al. (55), the MN-QWARN system instead relies on the assumption that only some of these slow-and-go conditions are dangerous. Instead of warning drivers of any slow traffic ahead, the MN-QWARN algorithm targets quickly moving shockwaves which typically encompass only a small number of vehicles. These shockwaves are often isolated and can be especially dangerous for distracted drivers.

The fundamental idea behind the system is that drivers are often in most danger of rear end crashes when they are distracted by an attempt to change lanes. In particular, a driver moving out of a lane that moves at low speeds into a lane with higher speeds will experience the most difficulty, and will spend the most time looking away from the road ahead. This will make them susceptible to crashes due to unexpected shockwaves in front of them. These waves move the fastest when there is low speed traffic downstream and traffic that is both high speed and high density upstream. Ideally, when all of these conditions are present, the alarm will be raised since drivers will be in the most serious danger.

MN-QWARN system collects real-time individual vehicle measurements and processes them to remove noise. These measurements come from two lanes a “target lane” (the right lane for the right side model and the exit/left lane for the left side model) and a “secondary lane” (the lane adjacent to the target lane that most directly affects the traffic flow on the target lane). The filtered data then passes to the crash-probability model to assess the likelihood of a crash. Based on this crash probability, the algorithm determines if a warning message should be generated by comparing the crash probability with preset thresholds and real-time traffic conditions.

The metrics entering the model include temporal metrics such as average speed and coefficients of variation of speed and time headway. In addition, spatial metrics are used which are derived from assumed vehicle trajectories moving at constant speeds. These metrics include density, acceleration noise, mean velocity gradient, quality of flow index, traffic pressure, and kinetic energy. Finally, some heuristic metrics are included such as the upstream/downstream speed difference the target/secondary lane speed difference, and he maximum/minimum speed difference.

To find the actual crash probability, and additional extension in space and time is included since it may make time for traffic to deteriorate after an initial trigger. To account for this, a moving window is used encompassing a set number of vehicles and shifted a set time step in the past. Given this window, the traffic metrics mentioned above are calculated for this group of vehicles. These variations on the described metrics were determined based on a fitted logistic regression model at the initial implementation location on I-94. These metrics remained the same when the system was moved to the new implementation further upstream.

The crash probability is continuous variable and needs to be converted to a decision about when to raise and lower the alarm. To do this a two threshold approach is used (one for raising and the other for lowering the alarm). There is also a minimum alarm length of 1 minute since individual vehicle data is inherently noisy and can change very quickly. In addition, a dynamic window of average crash probability is used instead of the raw crash probability to reduce the impacts of outliers in the data.

Several overrides are included by policymakers as part of the deployment on the preexisting MnDOT sign. The time override prevents the sign from being turned on, regardless of the alarm status before noon or after 8 p.m. The congestion override also prevents the sign from being turned on when five consecutive 30-second average speed measurements at the loop detector upstream of the sign are below the MnDOT-imposed threshold of 25 mph. This override is intended to reduce driver overexposure to the warning by not displaying a warning when drivers are already travelling slowly. Finally, initial activation can vary from a few seconds to one minute, depending on the synchronization between the independent queue-warning system and the traffic operations system that controls the signs. This delay amplifies short gaps in the alarm activation and is dictated by the refresh rate of the sign.

The application of the MN-QWARN algorithm resides on a secure server at the Minnesota Traffic Observatory. It is integrated with MnDOT’s Regional Traffic Management Center’s Intelligent Road Information System. A live feed of the model result, detector data, sign status, and cameras used for

event detection is available during the system's operation, and data are stored in a database for future analysis.

There are three primary location specific characteristics that the original MN-QWARN system took advantage of. First, that section of I-94 had very high demand on the right lane because of the upstream entrances at University and I-35W South. Along with this high demand, the middle lane often had significantly higher speeds when crashes occurred. Finally, at the entrance from 3rd Street there were often shockwaves on the right lane and many lane changes as vehicles tried to move over to avoid the congestion. Based on these three factors, the system was built on the assumption that most rear-end crashes were caused by drivers that were distracted looking over their shoulder to change lanes (from a low speed lane to a high speed lane) when fast moving shockwaves came through unexpectedly. The algorithm was designed and calibrated primarily for these conditions and was not modified when it was implemented at the new location. For more details on the original implementation, the metrics, the thresholds, or the hardware, refer to (57).

The new implementation of the MN-QWARN algorithm has several differences from the original. The original implementation was on a 3 lane section of road, while the newer one has 4 lanes. In addition, the old version utilized a lane specific warning for the right lane only using two changeable message boards, while this new system uses the warnings: "Slow Traffic Ahead Left Lanes," "Slow Traffic Ahead Right Lanes," or "Slow Traffic Ahead All Lanes" on a single sign. This system is running the algorithm simultaneously for the right and left target lanes and giving specific warnings for each. Finally, the distance between detectors was modified slightly from 700 feet in the original system to 1415 ft in the new implementation and the distance between the first detector and the sign was changed from 1.7 miles to only 2665 ft.

There are also some more subtle differences in detection. The old implementation and the right side model of the new implementation use data from the right (target lane) and middle (secondary lane). However, the left side model does not have lane continuity since there is a lane addition. Downstream, the exit lane is used as the target lane and the left lane is used as the secondary lane. However, before the exit lane to I-35W begins, the left lane of I-94 is the target lane and the middle lane is the secondary lane. As a general rule, the system will raise the alarm when there is low speed traffic downstream, and traffic upstream is both high speed and high density. The lack of lane continuity could cause these conditions to occur more often on the left lane, even though much of that upstream traffic exits onto I-35W and the shockwave does not propagate. Though this traffic pattern is often less dangerous than the pattern at the original implementation, it is recognized similarly by the algorithm and causes similar behavior of the crash probability. This makes the left side model an important contrast to the original deployment since it appears similar to the system but is based on different traffic patterns and there is no lane continuity.

As discussed in 3.3 , the right side model is also different than the original implementation. Since upstream demand is low and the middle lane is often moving slower than the right in the critical zone, the crash probability is often very low. Instead of increasing early in the day and staying high throughout congestion, the crash probability has very narrow peaks. This behavior is shown in Figure 3 which shows

the crash probability for the original deployment, as well as the models for the right and left sides of the new deployment. This could either mean exposure to the sign is lower and unnecessary vehicles are not being warned, or it could mean the algorithm is insufficiently sensitive to the dangers of these traffic conditions. Regardless, the phenomenon is very different than anything seen at the previous location, so it is important to see whether the algorithm translates to this new scenario.

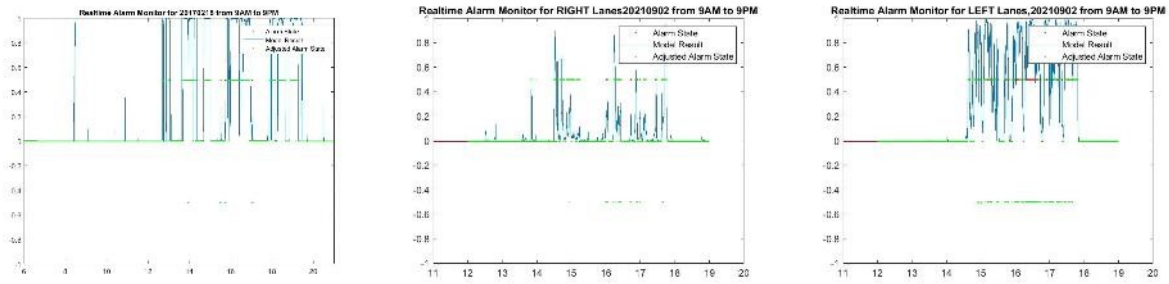

(a) **(b)** **(c)**

Figure 3-12 System output from the original implementation (3a), the right side model (3b) and left side model (3c) of the new implementation.

When deployed at the new location, several parts of the system were calibrated. The distance between detectors was altered between 1415 ft and 640 ft, and it was determined that the larger separation between detectors (and having a detector closer to the critical zone) was more beneficial. In addition, the thresholds were calibrated separately for the left and right models. The right model used 0.03 for both the raising and lowering threshold, and the left side used 0.4 for both. Other than these, the rest of the parameters of the model were left the same as the original implementation.

Finally, the location of the second deployment has far fewer crashes than the original implementation and evaluation, making the methodology used in by Hourdos et al. 2021 (57) difficult to replicate. There are not enough crashes or near crashes along this stretch of road to draw strong conclusions without waiting for several years. However, there are still consistently crashes along this corridor and it is still important to find a way to prevent them. For this reason, a new methodology for finding a ground truth of dangerous conditions is necessary.

CHAPTER 4: EVALUATION METHODS

One of the most common tools for evaluating the roadway conditions is to use the trajectories of vehicles. With this in mind, this methodology constructs the trajectory of a hypothetical vehicle moving along the roadway. Along with the trajectory itself, we keep track of the vehicles speed and acceleration at each point. Based on characteristics of these trajectories, the effects of implemented ATM systems and TSMO strategies can be evaluated.

Figure 4 depicts the process taken to arrive at these trajectories. First, the generalized adaptive smoothing method (GASM) discussed in Treiber and Helbing (125) and Treiber et al. (126) is used to interpolate average vehicle speeds in space and time to find the speed at every point along the roadway. With this information, a contour plot of vehicle speeds (speedmap) can be constructed. The data in this study was had some problems (discussed in Section 4.1), so it had to be cleaned before it could be used as an input into GASM.

Based on the speedmap, vehicle trajectories can be constructed using kinematics (Section 4.4). However, to increase the accuracy, the acceleration potential (the potential of the traffic stream to accelerate) is used as an estimate of the vehicle acceleration as described in Section 4.5 . Once that trajectory is created, the speed vs. time graph can be smoothed and the real acceleration can be found. However, a new trajectory needs to be created utilizing the smoothed speed and the acceleration calculated. This step aligns the vehicle location, speed, and acceleration at each point in time.

Finally, once each trajectory is created, and the speed and acceleration of each vehicle is known, the characteristics of each vehicle can be analyzed. Several metrics for analyzing vehicle trajectories can be developed such as their maximum acceleration, and the average acceleration between their maximum and minimum speeds. Other metrics could include an evaluation of the environmental impacts by examining the speed and acceleration of each trajectory, or examinations of changes in travel times and extent of congestion throughout the day.

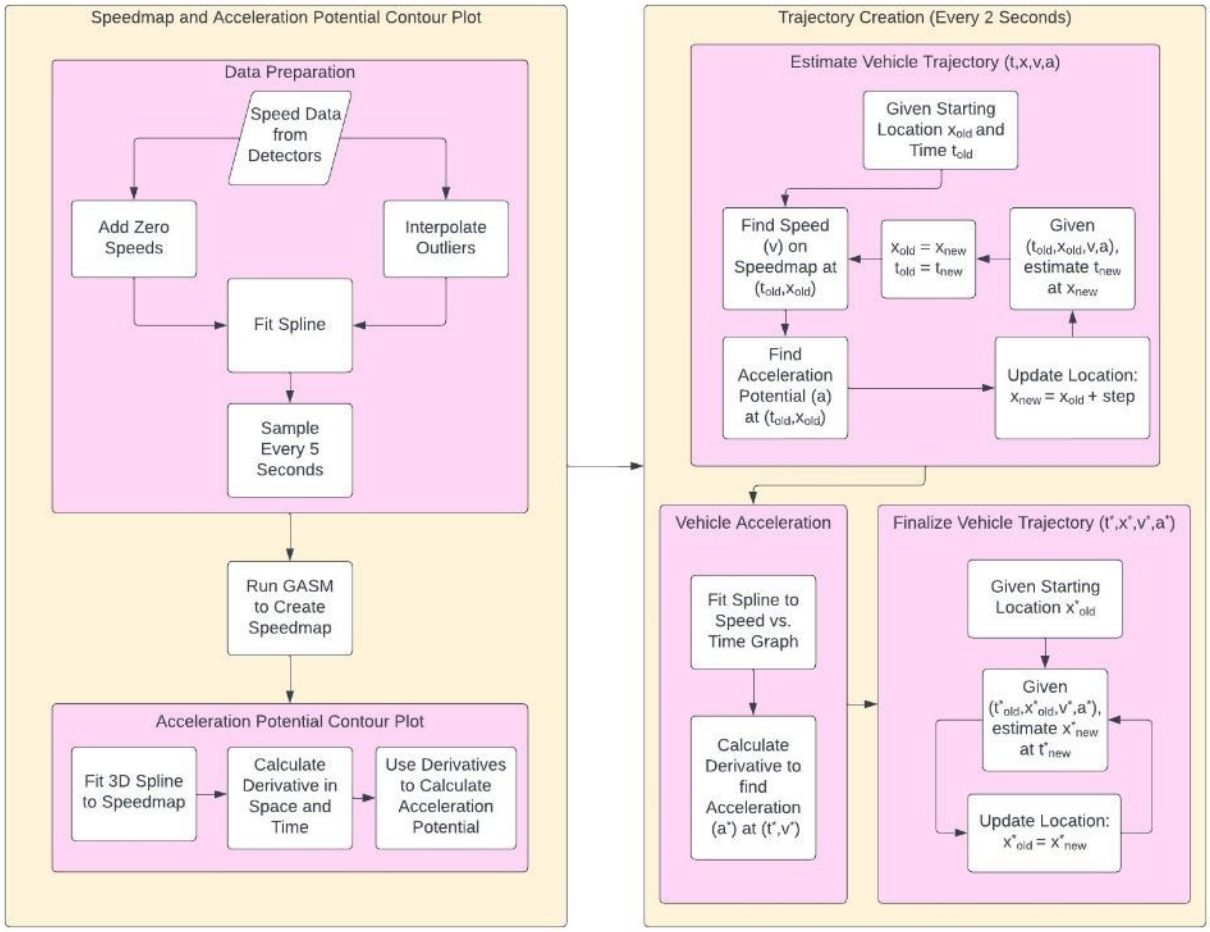

Figure 4-1 Flowchart depicting the process of developing hypothetical vehicle trajectories.

4.1 DATA PREPARATION

The methodology presented here is scalable, and can be applied to any road section. However, for the purposes of this report, we examine the 2665 ft segment of roadway on I-94 in Minneapolis, MN where the queue warning system is deployed. The primary data source used in this study is taken from four detectors. Detector 1 is a Minnesota Department of Transportation detector reporting average speeds every 30 seconds (x = 0 ft). Downstream at x = 1250 ft, Detector 2 is a SpeedLane detector, reporting individual vehicle speed measurements. Finally, Detectors 3 and 4 (x = 2025 ft and x = 2665 ft) are Wavetronix radar detectors reporting individual vehicle speed measurements. A diagram of these detectors along with the lane configuration is included in Figure 4-2

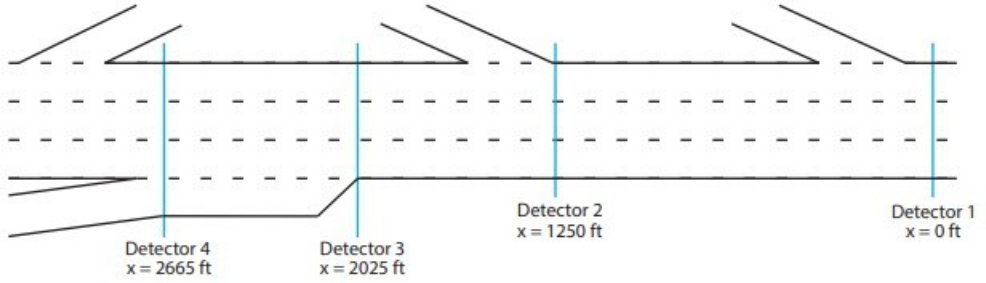

Figure 4-2 Study Area - I94 near downtown Minneapolis, MN.

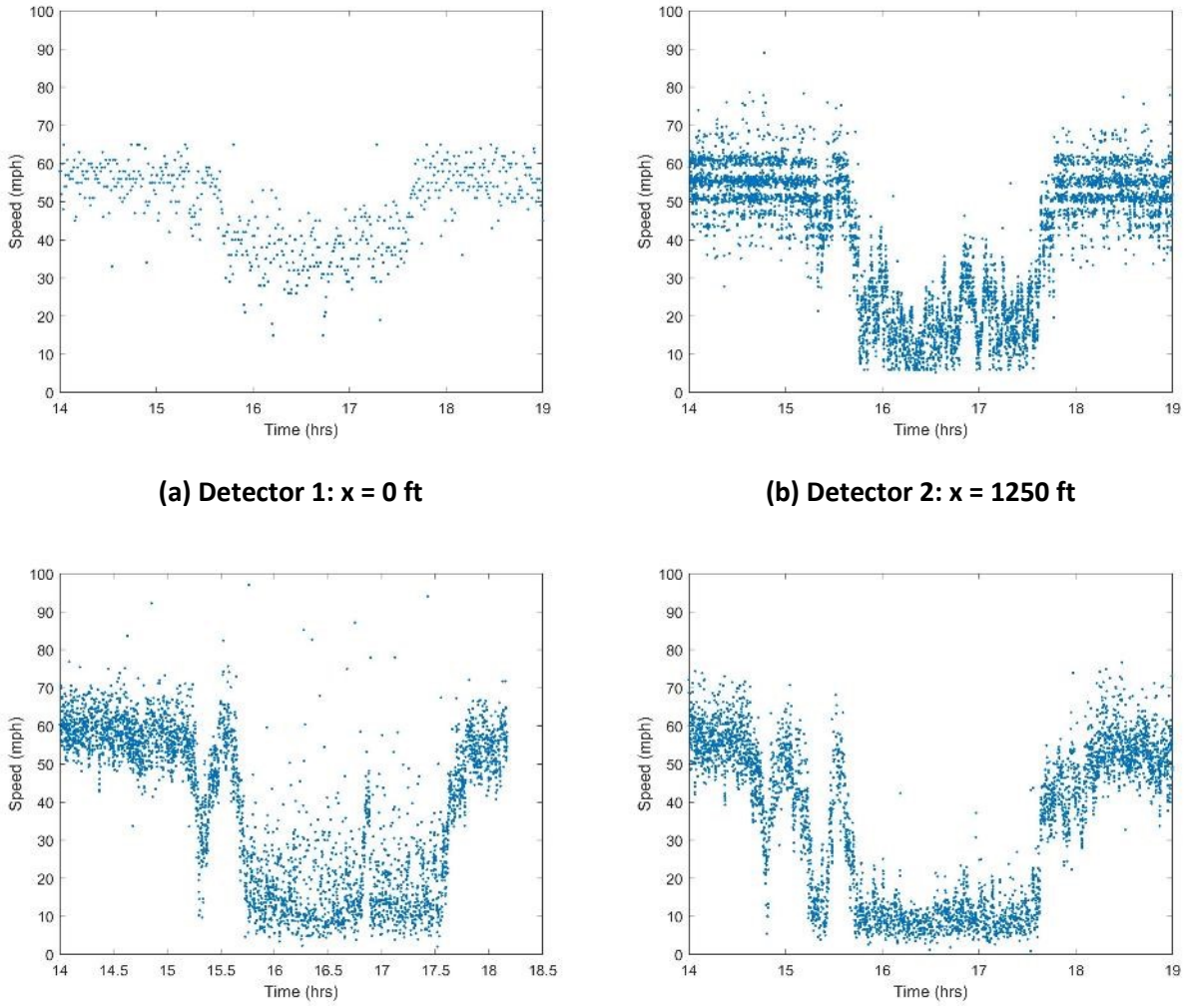

(a) Detector 1: x = 0 ft

(b) Detector 2: x = 1250 ft

(c) Detector 3: x = 2025 ft

(d) Detector 4: x = 2665 ft

Figure 4-3 Vehicle speed measurements from each of the four detectors between 2:00 pm and 7:00 pm on October 19th, 2020 (right lane).

Figure 4-3 shows the raw data from these sensors. There are some immediate differences noted between these detectors. Figure 4-3a shows that the 30 second average speed data has far fewer outliers than the other data. However, this data does not show nearly the same resolution in terms of the sharp speed changes that the other three data sources show. This is unfortunate since the goal is to detect these sharp changes in speed. Figure 4-3b depicts individual speed measurements taken by the Detector 2. The large bands of data show that the sensor has done some processing of the data already before reporting it. In addition, there are no data points moving at speeds less than 6 mph. Finally, Figure 4-3c and Figure 4-3d show the data from the two Wavetronix sensors at the downstream end of the study area. These sensors do not display as obvious changes to the data as the previous two. In addition, there are some data points below 5 mph (though not many). However, there are many of outliers in this data. This is especially true in the far lane of traffic from the detectors where there is more interference from the other two lanes.

In addition to the large number of outliers, another problem with this dataset is that it is not possible to have a speed of zero. This is because radar data cannot detect stationary vehicles, only slow-moving ones. In addition, it is rare for vehicles to stop exactly in front of the detector. Instead, they are usually detected when they are slowing down prior to stopping or accelerating after they have already stopped. For this reason, vehicles are most often detected at speeds only as low as 5-10 mph. Figure 4-4 shows data on a single day which contains both of these problems. The inset on the left shows a series of points less than 20 mph with one outlier greater than 40 mph. The headway between the two adjacent vehicles traveling at a speed difference greater than 30 mph is only 2.5 seconds. On the right, the inset shows a series of vehicles moving slower than 5 mph. At around time 17.2 there is a headway of 34.5 seconds. This very large gap suggests that vehicles stopped between these two points. Examination of the video at both these locations indicates that both of these problems should be corrected.

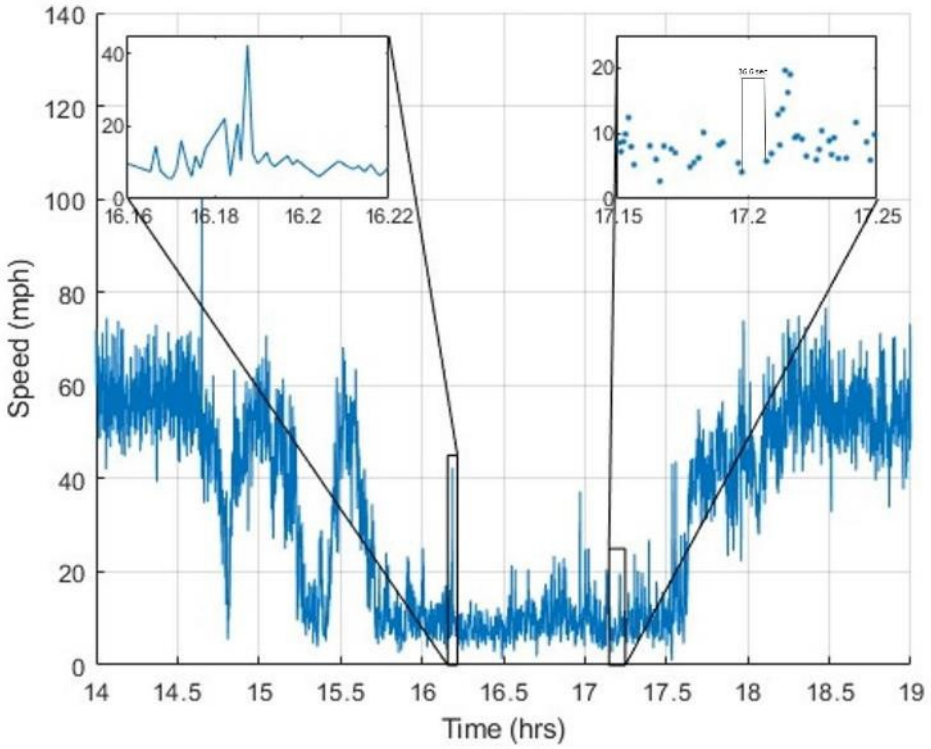

Figure 4-4 Individual Vehicle Speed Measurements

The first step to alleviating these problems is to correct outliers. This is done using a moving mean of 20 data points and a threshold of 2.5 standard deviations from the mean. Outlier points are replaced with a linear interpolation between the two neighboring points. However, the goal of this study is to detect vehicles that were forced to decelerate quickly. These vehicles are often moving slower than other vehicles around them. In addition, most large outliers are vehicles moving at high speeds, not lower speeds. For this reason only outlier above the mean are removed.

The next step is to insert low values into the data. In doing so, it is important to keep in mind how this data will be used. Only the speed measurements are necessary to construct the speedmaps, not flow or density. This means that we can add data points at key locations to deepen the valleys in the speedmap without negatively impacting the results. This step was not necessary in the study done by Treiber et al. (126) because the GASM method was originally designed using 30 second averaged speed data and stops lasting over 30 seconds are very rare. However, with individual vehicle speed measurements it is important to determine where exactly the queues form. In order to add instances of zero speed to the data, we need to make some assumptions about driver behavior. The first assumption is that vehicles traveling at speeds less than 15 mph when they cross the detector could potentially be slowing to a stop or accelerating from a stop. In addition, vehicles traveling at such slow speeds tend to travel in closely packed groups with small headways. For this reason, large time headways (greater than 5 seconds) at low speeds suggest that vehicles may have stopped between detections. We insert a speed of zero between two vehicles if they are both traveling less than 15 mph and the time headway between them

is greater than 5 seconds. As these parameters were determined empirically, the presence of these queues was verified with video to confirm vehicles were stopping.

Finally, a time series was created by using a spline is fit to the raw data. This spline is sampled every 5 seconds which also reduces some of the most extreme perturbations in the data. This is a slightly higher resolution than the headway of vehicles, so some data is lost. However, there is a tradeoff between resolution and computational efficiency.

4.2 SPEEDMAP CREATION

Based on sparse data (in this example data from 4 point detectors), the speeds of vehicles can be interpolated in time and space. This is accomplished using the generalized adaptive smoothing method (GASM) discussed in Treiber and Helbing (125) and Treiber et al. (126). The input data is speed (v_{ij}), at the locations of each detector (x_i) and times when speed is known (t_j).

The goal is to find the speed $V(x,t)$ at all locations along the corridor $x \in [x_{min},x_{max}]$ and all times $t \in [t_{min},t_{max}]$. To do this, two filters $Z_{cong}(x,t)$ and $Z_{free}(x,t)$ are created, which correspond to the expected propagation of speeds in congested and free flowing traffic. Equations (3) and (4) define these two filters. These filters are combined using a weight function to find the final velocity at every location.

$$V(x,t) = w(x,t)Z_{cong}(x,t) + [1 - w(x,t)]Z_{free}(x,t \tag{1}$$

$$w(x,t) = \frac{1}{2}\left[1 + \tanh\left(\frac{V_{thr} - \min[Z_{cong}(x,t), Z_{free}(x,t)]}{\delta V}\right)\right] \tag{2}$$

$$Z_{cong}(x,t) = \frac{\sum_i \sum_j \phi(x_i - x, t_j - t + \frac{(x-x_i)}{c_{cong}})v_{ij}}{\sum_i \sum_j \phi(x_i - x, t_j - t + \frac{(x-x_i)}{c_{cong}})} \tag{3}$$

$$Z_{free}(x,t) = \frac{\sum_i \sum_j \phi(x_i - x, t_j - t + \frac{(x-x_i)}{c_{free}})v_{ij}}{\sum_i \sum_j \phi(x_i - x, t_j - t + \frac{(x-x_i)}{c_{free}})} \tag{4}$$

$$\phi(x,t) = \exp\left[-\left(\frac{|x|}{\sigma} + \frac{|t|}{\tau}\right)\right] \tag{5}$$

Where:

- v_{ij} - The speed data from the sensors.
- x_i - Locations in space of the sensors.
- t_j - Times of data points collected at the sensors.

- $V(x,t)$ - The interpolated speed at every point in space and time.
- $w(x,t)$ - The weight function between the free flow and congested speed.
- $Z_{free}(x,t)$ - Filtered speed for free flow traffic.
- $Z_{cong}(x,t)$ - Filtered speed for congested traffic.
- V_{thr} - Transition speed from free flow to congested flow.
- δV - Width of the transition region between congested flow and free flow.
- $\varphi(x,t)$ - Smoothing kernel of anisotropic filter
- c_{cong} - Congested wave speed.
- c_{free} - Free flow wave speed.
- σ - Range of spatial smoothing.
- τ - Range of temporal smoothing.

The values of c_{cong} and c_{free} are set based on known traffic flow patterns. In free flow traffic, perturbations in the flow of traffic travel downstream based on the movements of individual vehicles. Thus c_{free} is set close to the speed of vehicles in free flow. In congested traffic, shockwaves travel backwards, against the flow of traffic. In this case, c_{cong} is set to a negative value which is approximately the speed of those shockwaves.

This method is more effective than simple spatial interpolation to find what is happening between detectors, since it takes into account predicted paths of any disturbances. The effects of the spatiotemporal interpolation can be seen in Figure 4-6. However, there are still some problems. Figure 4-6 shows lines of real data along where each detector collects it. Even at these locations, we see variations between the real data and the smoothed version. This method takes out some of the most extreme variations in the data. In addition, since our detectors are fixed and measure speeds as vehicles cross them, they do not measure stopped vehicles. This means the speeds listed here tend to be an overestimate. This needs be taken into account later on as these speeds are utilized in practice.

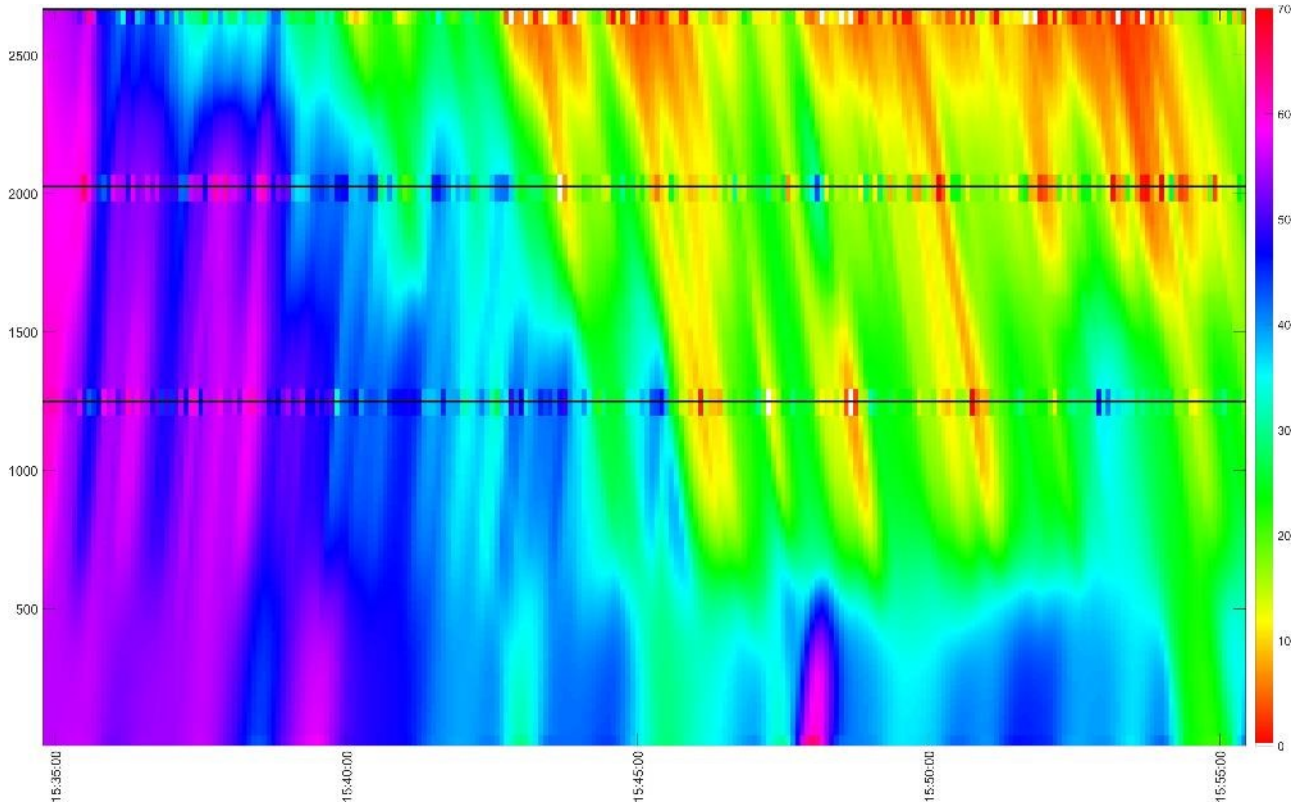

Figure 4-5 Spatiotemporal smoothing with real data plotted along detectors on October 19th, 2021 (20 minute window at the start of congestion).

4.3 CALIBRATING THE GASM MODEL

The GASM model relies on 6 parameters: congested wave speed (c_{cong}), free flow speed (c_{free}), two parameters for transition speed (δV and V_{thr}), and two smoothing parameters in space (σ) and time (τ). These parameters need to be optimized for each new section of roadway since they correspond to assumed parameters on the Fundamental Diagram. First, the values of σ and τ were optimized to remove discontinuities in the speedmap. Then, a root mean square error (RMSE) minimization process on predicted vehicle speeds was used to optimize the other 4 parameters. To perform this optimization, the speeds are predicted at detector 3 (the middle of the three individual speed detectors) using the GASM method, but the data at that detectors is not included with the input data. Instead, this data is used as the ground truth and the RMSE is found when comparing predicted values. The objective of this optimization problem is to minimize the RMSE at this detector.

The optimization program was run using data from 9 separate shockwaves across 7 different days. Of those cases, 6 came from the right lane and 3 came from the middle lane. Before the RMSE was minimized, the two smoothing parameters in space (σ) and time (τ) were optimized. Treiber et al. (126) used values of $\boldsymbol{\tau = \frac{\Delta t}{2}}$ and $\boldsymbol{\sigma = \frac{\Delta x}{2}}$. However, distances between detectors and time between data points were much higher in their study. When lower values were used, irregularities were created. To avoid this phenomenon, each value was set to an arbitrarily small value and increased incrementally

until the discontinuities were removed. This method determined the smallest sigma and tau values (the least smoothing) while still interpolating to reasonable values during the GASM process. The final values used in this study are σ = 264 feet and τ = 6 seconds. As in Treiber et al. (126), the optimal σ value is slightly less than half the distance between detectors. However, a much larger value of τ was found to be optimal. A value of 2.5 seconds (half of the 5 second time between data points) for tau created significant distortions in the speedmaps and only at values of 6 seconds did those disappear.

The input data into GASM is noisy and the RMSE minimization problem is non-convex, making it challenging to find a global optimum solution. This problem is compounded by very high computation times for different input parameters over an entire day. For this reason, small portions of the day were chosen for the optimization process to increase the speed and reduce the noise. For the purposes of this study portions of the day with transitions between congestion and free flow traffic were chosen to try to optimize the prediction at this transition when conditions are typically more dangerous for drivers. A pattern search algorithm was used to calculate the objective at a mesh of points. The mesh was expanded and contracted around the lowest known objective until the optimal solution was found (Audet and Dennis, 2002) (12). For the optimization process only (and not subsequent to actually create the final speedmaps) the data was smoothed to reduce noise and speed up the optimization. First a 1 second spline was fit to the raw data and sampled every 1 second. To clean up this noise, a moving average with a window of 15 seconds and step size of 1 second was applied to the evenly spaced 1 second data. This data was then sampled only every 15 seconds.

Minimizing the RMSE of vehicle speeds, several patterns emerged. The values of the free flow speed c_{free} remain consistently at 35 mph, with a few cases where it dropped to 12 mph. This value is lower than we would typically expect, but is understandable since vehicles tend to slow down as density increases and many are traveling at 35-40 mph even before many shockwaves occur. The optimized congested wave speed c_{cong} was between 11 and 18 mph. This is in the range we would generally expect to see for freeway traffic. Based on this information we set c_{free} = 35 mph and c_{cong} = −17 mph, the most commonly occurring values.

The relationship between the transition speed V_{thr}, the width of the transition region δV , and the weight function $w(x,t)$ is described in Equation 2. To better illustrate this relationship, Figure 4-6 depicts how the weight changes with speed and various values of V_{thr} and δV . V_{thr} represents a translation of the weight between the two smoothing kernels, and δV is related to the slope of that transition. Taking this information into account, the width of the transition region must be less than the the speed difference between c_{free} and c_{cong}: $\delta V < c_{free} + |c_{cong}|$. Similarly, the transition speed itself must fall between these two values: $c_{cong} < V_{thr} < c_{free}$. Based on the optimization results it appears that the choice of these parameters does not have a large effect on the RMSE. This is consistent with the findings of Treiber et al., (126). The optimized values used for the final speedmaps are: V_{thr} = 30 mph and δV = 7 mph.

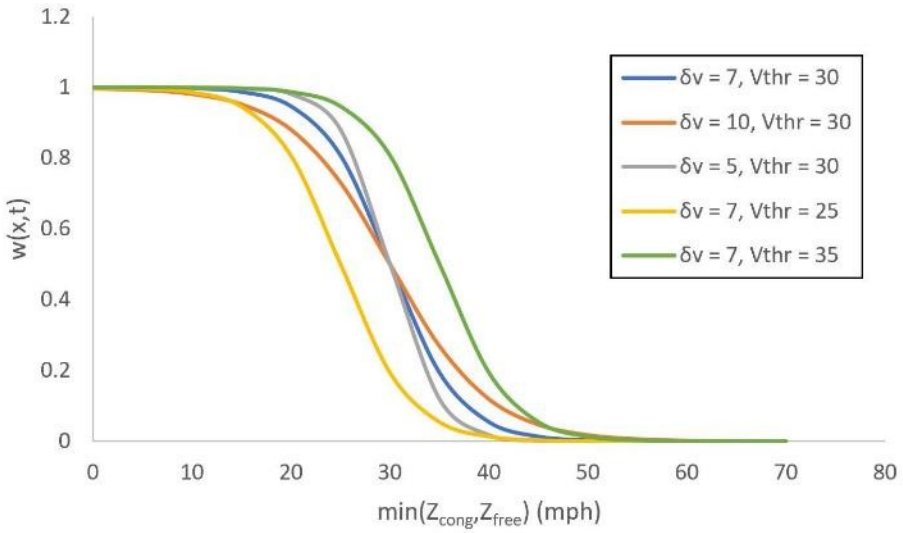

Figure 4-6 Changes to the weight w(x,t) with different values of transition speed Vthr and transition region δV .

4.4 FINDING HYPOTHETICAL VEHICLE TRAJECTORIES

One way to evaluate the path of a single vehicle is to reconstruct its trajectory. This is simple once the speedmap has been constructed because this tells us how fast the vehicle would be moving at each point in space and time. We also assume that the acceleration at each point is known (an approximation is described in Section 4.5).

The known speeds and accelerations are used to find hypothetical vehicle trajectories. In this instance we do not match up these trajectories with the individual measurements at each of the detectors. Instead, we create a hypothetical trajectory every two seconds that represent that path a vehicles would have followed if it had actually been there. This gives us realistic velocity, acceleration, and positions for individual vehicles, but doesn't tell us anything meaningful about time and space headways between any two vehicles. For this reason, only measures of vehicle movements are applicable to these trajectories individually, not flow or density over several adjacent trajectories.

In creating the hypothetical trajectories, it is also important to consider how error occurs. Most importantly, error in vehicle position accumulates as the trajectory moves farther from the point at which it was created. This error is combated in three ways. The first is a product of the speedmap itself. This speedmap was made as fine as possible so the vehicle speed could be updated often. The second approach is to include the predicted acceleration term. Finally, the trajectories are created from a point in the middle of the speedmap and propagated both upstream and downstream to minimize the accumulated error in displacement at each end of the study area.

We create a hypothetical vehicle at the midpoint of the study area every 2 seconds and set its velocity and acceleration to that calculated on the speedmaps. We can then move the vehicle an arbitrarily small distance Δx along the corridor and update its speed, acceleration, and the time. The speed and acceleration will always be given by the speedmap as a function of location and time ($v(x,t)$, and $a(x,t)$), and the time can be updated based on kinematics. This is done by using the known speed and

acceleration at the initial location to estimate the final velocity. Then, that velocity can be used to calculate the time the vehicle will arrive at the next location.

$$v_f = \sqrt{2 \times a \times \Delta x + v_i^2} \tag{6}$$

$$t_f = t_i + \frac{2 \times \Delta x}{(v_f + v_i)} \tag{7}$$

Where:

- Δx - The difference in space between starting location x_i and ending location x_f.
- v_i - Known velocity at location x_i.
- v_f - Estimated velocity at location x_j.
- a - Constant acceleration between locations x_i and x_f.
- t_i - Time at location x_i.
- t_f - Time at location x_j.

This procedure is followed until each vehicle reaches the end of the study area. However, the speedmap created only provides the speed of each vehicle. More refinement needs to be done to find an estimate for the acceleration at each point. Figure 4-7 shows a time-space diagram overlaid on top of the speedmap for a small section of the day.

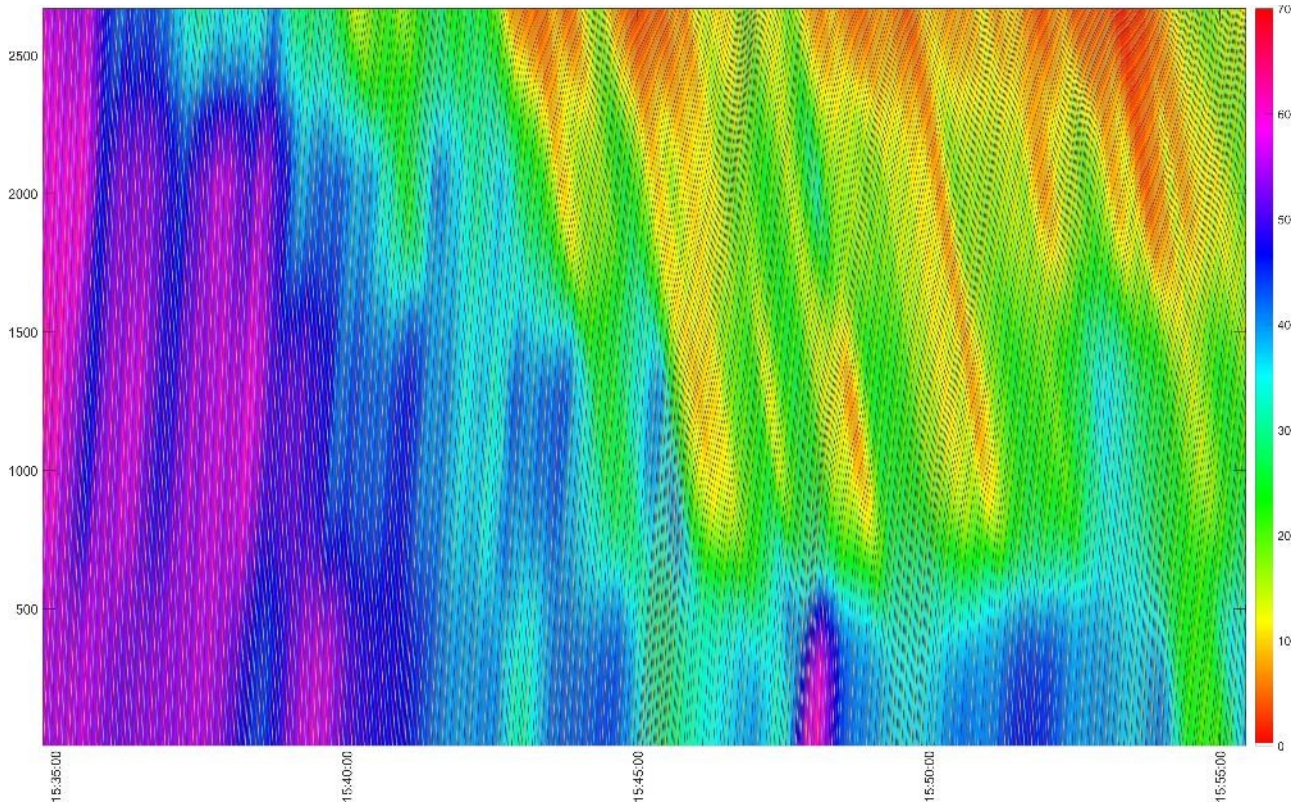

Figure 4-7 Time-space diagram overlaid on speedmap on October 19th, 2021 (20 minute window at the start of congestion).

4.5 FINDING ACCELERATION POTENTIAL

Once the speedmap has been created, it can be further refined and a potential surface can be created. This is done by fitting a three dimensional spline surface to the data. The data points can then be interpolated between to get higher resolution vehicle speed data. This is helpful in creating smoother trajectories.

In addition to interpolating the velocities to additional points, the spline surface provides a set of equations that define the data. The derivative can be found in time and space denoting a change in speed. The derivative of the speed with respect to time is the change in speeds in time at a single point along the highway. Similarly the change in speed with respect to space is the change in speed along the length of the highway at a constant time. We denote these two potentials as P_x and P_t respectively and define them as:

$$P_x(x,t) = \frac{\partial V(x,t)}{\partial x} \tag{8}$$

$$P_t(x,t) = \frac{\partial V(x,t)}{\partial t} \tag{9}$$

Based on these two partial derivatives of the speed map, the gradient is defined as:

$$\nabla V(x,t) = [P_t(x,t), P_x(x,t)] \tag{10}$$

The magnitude $||\nabla V(x,t)||$ and direction **v** of this map can then be found:

$$||\nabla V(x,t)|| = \sqrt{P_t(x,t)^2 + P_x(x,t)^2} \tag{11}$$

$$\boldsymbol{\theta} = \operatorname{atan2}\left[\frac{P_t(x,t)}{P_x(x,t)}\right] \tag{12}$$

Where atan2 is defined as:

$$\operatorname{atan2}(y,x) = \begin{cases} \arctan\frac{y}{x}, & \text{if } x > 0. \\ \arctan\frac{y}{x} + \pi, & \text{if } x < 0 \text{ and } y \geq 0. \\ \arctan\frac{y}{x} - \pi, & \text{if } x < 0 \text{ and } y < 0. \\ +\frac{\pi}{2}, & \text{if } x = 0 \text{ and } y > 0. \\ -\frac{\pi}{2}, & \text{if } x = 0 \text{ and } y < 0. \\ \text{undefined}, & \text{if } x = 0 \text{ and } y = 0. \end{cases} \tag{13}$$

Finally, we need an approximation of the acceleration of a vehicle at each point. The acceleration of a vehicle is $\frac{\partial V}{\partial t}$. However, this derivative with respect to time needs to be taken along the trajectory of the vehicle moving in both space and time. We cannot calculate this value exactly since we do not know the trajectory of the vehicle and we only have potential speed changes with respect to space and time alone. However, we use the signed magnitude of the gradient as an approximation:

$$a \approx ||\nabla V(x,t)|| \times \cos\vartheta \tag{14}$$

Figure 4-8 shows a contour plot of the acceleration potential at every point in space and time along the roadway. Near the bottom of the figure, the acceleration potential is more often closer to zero. This is due to the more smooth data from the 30 second detector. Around the other detectors, the data is much more chaotic. This is in part due to the differentiation of the data, which exaggerates any perturbations. However, there are some promising trends in the crisscrossing slopes of the free flow and congested wave speed. These slopes match the types of accelerations we would expect. At higher speeds (uncongested) the trajectories follow these lines of acceleration, either not changing speed often or accelerating smoothly. At lower speeds (congested) the vehicles instead change speed often and more sharply as they cross these lines of acceleration propagating backwards.

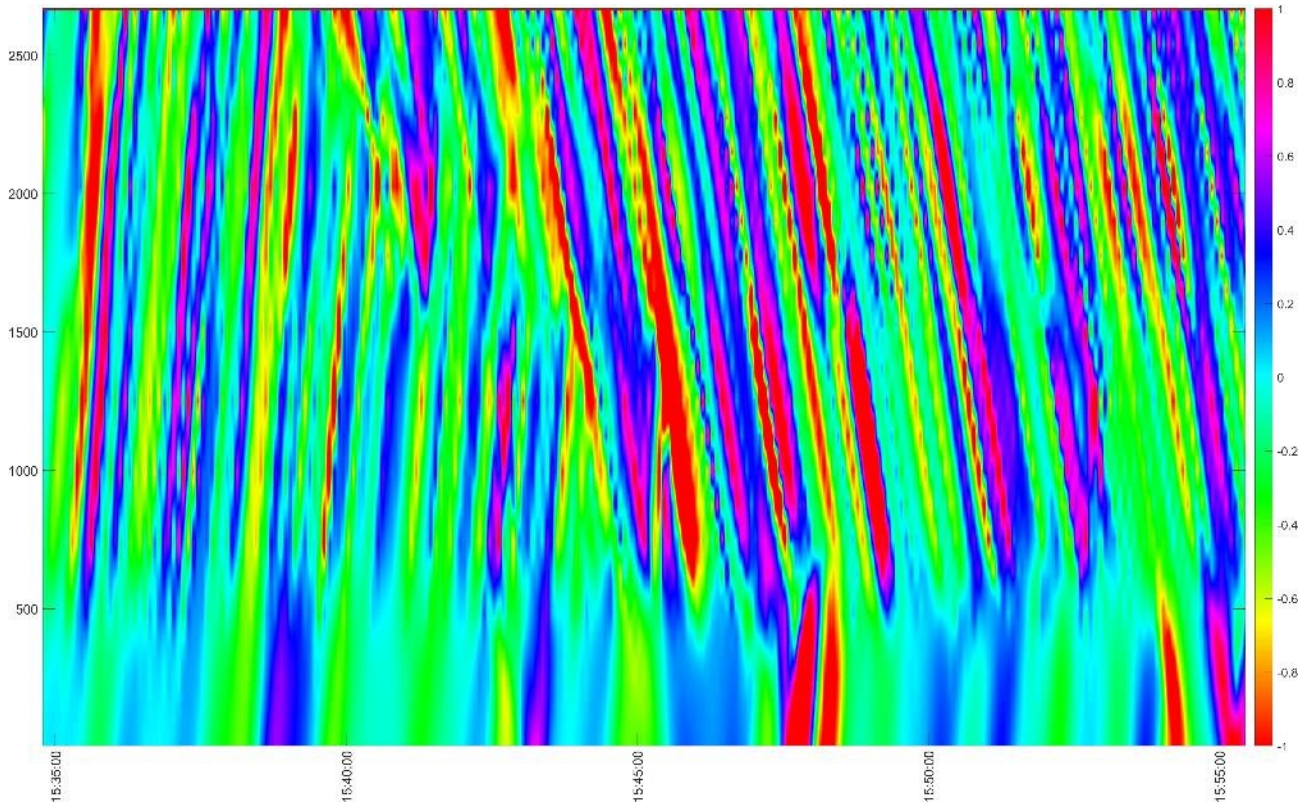

Figure 4-8 Contour plot of acceleration potential on October 19th, 2021 (20 minute window at the start of congestion).

This approximated acceleration can be used along with the velocities of the vehicles to create each hypothetical trajectory.

4.6 CALCULATE VEHICLE ACCELERATIONS

Using the procedure outlined in Section 4.4 , four quantities are known about each point along each trajectory: vehicle location at each time, speed, and acceleration potential. We can use this information to calculate the actual acceleration of each vehicle at each point along the roadway instead of the acceleration potential.

Typically, trajectories are recorded as points in time and space. These can be differentiated with respect to time to find the velocity, and differentiated again to find the acceleration. However, in this scenario, we know the speed already and this quantity has less introduced error than the calculated points of the trajectory since errors in vehicle position accumulate along the path of the vehicle. For this reason, these trajectories are analyzed as known speeds versus time points.

The trajectories coming from the speedmaps appear very smooth in space. However, there are discontinuities in the speed since it can only be sampled with the same resolution as the speedmap. For this reason, a spline is fit to each trajectory. A smoothing spline is fit to minimize the following objective:

$$p\sum_i (y_i - s(x_i))^2 + (1-p)\int \left(\frac{d^2 s}{dx^2}\right)^2 dx \tag{15}$$

The parameter p is fit visually to ensure the fitted function follows the data as closely as possible without oscillating through each point. *p* is set to 0.9185. This parameter needs to be high enough that it does not introduce curves into the straightest trajectories, but low enough that it follows the shape of all trajectories well. An example of the fitted curve is shown in Figure 4-9.

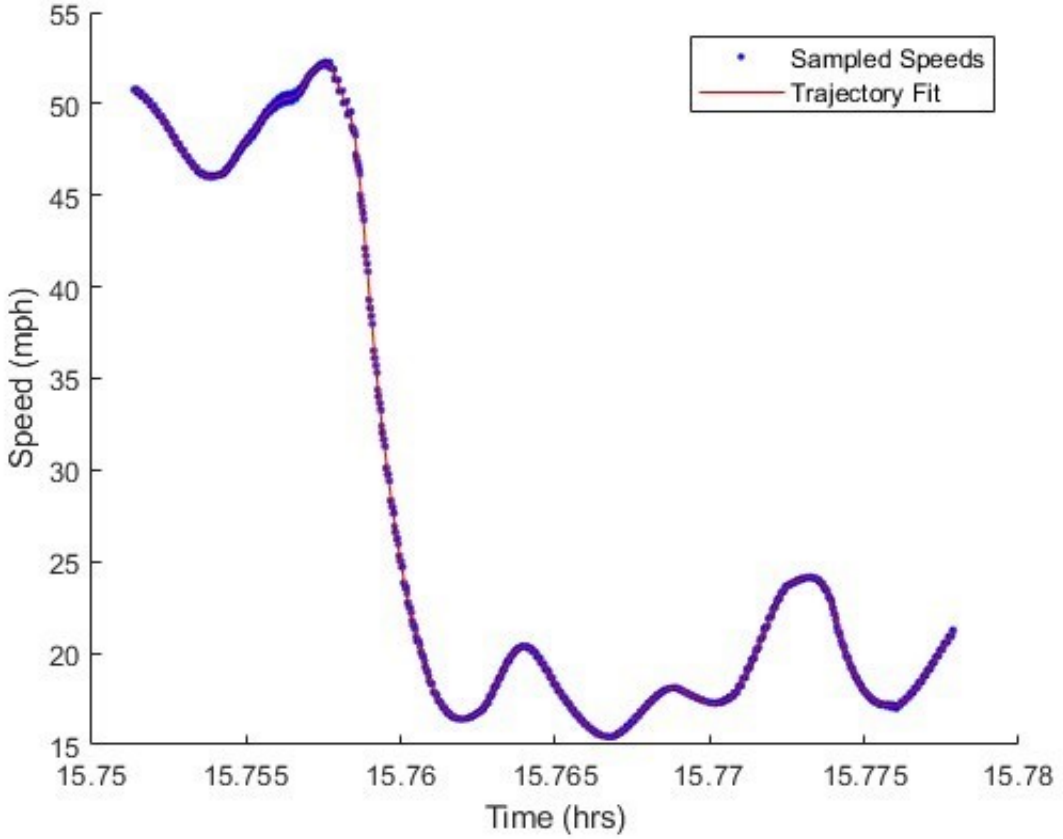

Figure 4-9 Speed versus location for a hypothetical trajectory smoothing spline fit to the data.

The spline is fit to the speed vs. time graph of the vehicle trajectory. The equations of this spline allow for easy calculation of the instantaneous acceleration (*a*) at every point by taking the derivative of the velocity (*v*) with respect to time (*t*):

$$a = \frac{dv}{dt} \tag{16}$$

Finally, with these new acceleration and speed values, the trajectory can be recalculated.

This time, the sampled time points from the last iteration are left constant, and a new location is calculated. The change in the trajectory is very minimal, but this is an important step to keep all of the points aligned.

4.7 SENSITIVITY TO NUMBER OF DETECTORS

It is important to know the impacts of removing one of the detectors, as this provides us with valuable information for future use of this methodology when knowing how many detectors to install. In addition, throughout the study period of the case study below, there were periods when the detectors were not functional. This analysis is helpful in determining whether there is still usable data from days when that occurred.

This analysis used data from three separate weeks in late 2020 and in 2021. These 15 days were run with data from all 4 detectors, and then again with each one of the four detectors eliminated. This process shows us some valuable trends in the changes to the speedmaps, as well as in changes to the trajectories created. Of the days examined, March 16th, 2020 had the largest differences when detectors were removed since the congestion comes to an end between detectors in several locations. This causes problems when one detector is removed since the algorithm cannot tell how far the congestion propagates between data points. This figure can be compared to Figure 4-10 below. This figure contains a speedmap of the same day with each of the detectors removed. In addition, it depicts the absolute percent difference between original speedmap and the modified version.

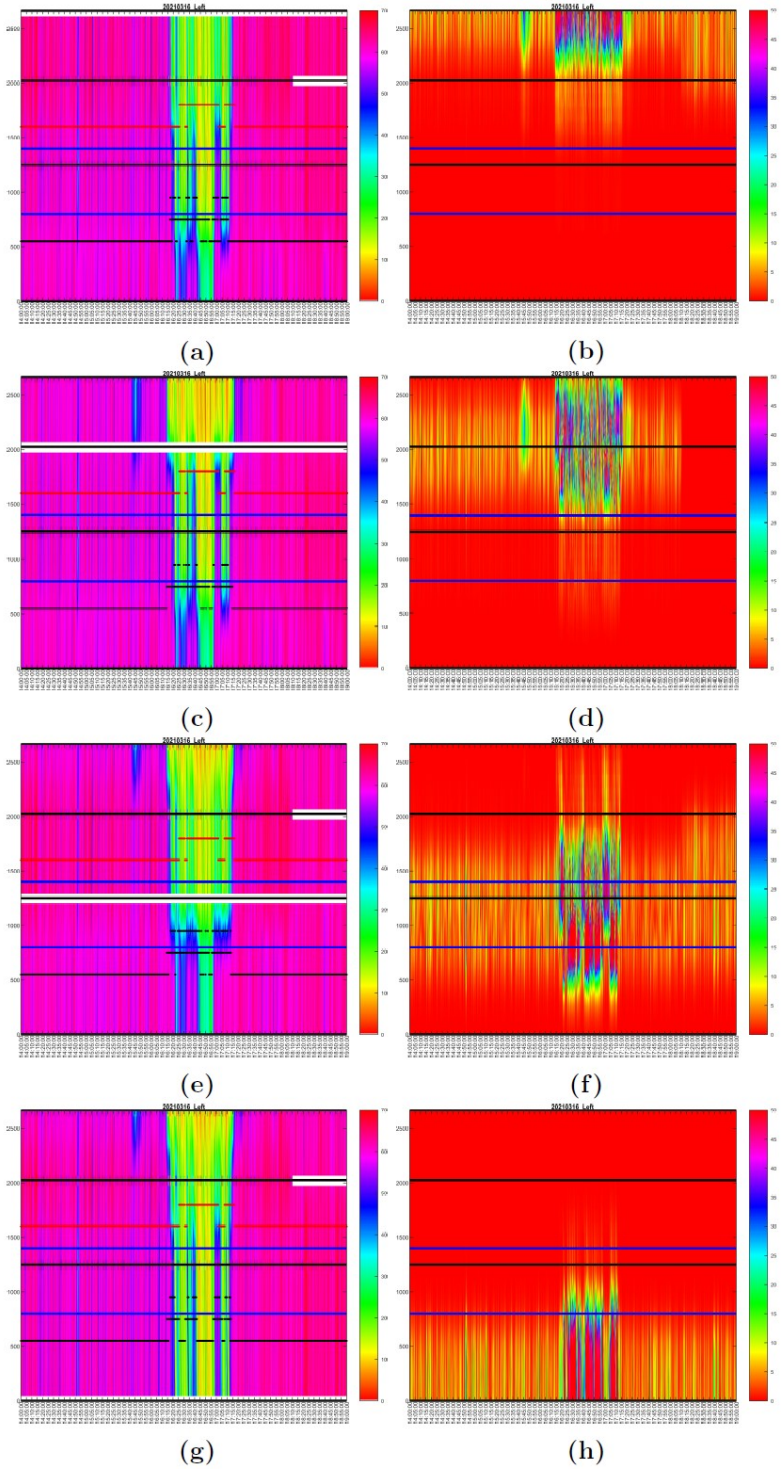

Figure 4-10 Speedmaps of vehicle speeds between 2:00 pm and 7:00 pm on March 16th 2020 (a, c, e, g) and percent difference when compared with the complete speedmap (b, d, f, h).

The biggest differences in percent difference are where there is most congestion. One reason for this is that these numbers are smaller, so percent differences increase faster. However, the speeds in the congested reason are also more difficult to predict since the shockwaves are more pronounced and move backwards. This causes large discrepancies to form when there are gaps between detectors. However, these errors persist only between detectors. These deviations disappear quickly once there is data from another detector since the GASM method is a numerical heuristic that does not rely on the flow and density of traffic. Thus, once new speed values are provided, the estimation is quickly corrected.

As described in the following sections, to evaluate the performance the Queue Warning system has on warning drivers about CPCs, deceleration rates of hypothetical vehicles are calculated in a region called the critical zone (shown on the figures as between the two blue lines). For this reason, small discrepancies are inconsequential outside that zone. The black dots on the Figure 4-10b, Figure 4-10c, Figure 4-10e, and Figure 4-10g represent the trajectories with maximum decelerations. It is clear from the above figures that the largest discrepancies come from the speedmaps where the detectors are on either side of the critical zone, located at at x = 0 and at x = 1250 ft.

When comparing the number of vehicles in the high deceleration category between the 15 days studied, there is a significant difference depending on which detector is removed. If the detectors at x = 2025 or x = 2665 ft are removed, there is less than a 10% decrease in the number of high decelerations. On the other hand if the detector at x = 0 ft is removed, there is a 41% decrease in the number of high decelerations and in the detector at at x = 1250 ft is removed there is a increase of almost 300%. This suggests that (for the purposes of the case study below) the detectors furthest upstream are much more important as they bound the critical zone.

4.8 DETERMINE WHICH TRAJECTORIES ARE DANGEROUS

Based on these trajectories, we can determine if there are any dangerous behaviors occurring. To do this, we rely on two assumptions. First, we assume that these reconstructed hypothetical trajectories represent behavior similar to that of real vehicles. Second, we use the deceleration of a vehicle (the negative of the acceleration) as a surrogate safety measure.

There are three cases that are important to distinguish. Some trajectories are not dangerous because their speeds are always high or always low. The goal of this category is to limit overexposure to the system by limiting warnings to vehicles about slow or stopped traffic which do not have to slow or stop. Though less of a concern than vehicles that never slow down, this category also encompasses vehicles that are already stopped underneath the sign and continue to move slowly throughout the corridor. These vehicles are never in significant danger since they are already aware of the congestion. In addition, even if these vehicles are involved in a crash, the low speeds mitigate the overall danger.

At the other end of the spectrum, the goal of the system is to warn distracted drivers in the critical zone (where visibility is the lowest). These drivers are identified by their high deceleration rates which suggest that they may be in danger. These are typically vehicles that encounter quickly moving shockwaves when the driver is distracted and is forced to decelerate rapidly. These hypothetical

trajectories show that the vehicle has a deceleration rate in the critical zone. These trajectories are categorized as dangerous.

Finally, there is an in-between of hypothetical trajectories where a warning is allowed but not needed. These vehicles decelerate and stop somewhere in the study area, but not in the critical zone. Though these warnings do not fit into the category of overexposure, they are not the real goal of the system.

In the process of rating the trajectories, we make several assumptions. First, we assume that a speed of less than 20 mph on our speed heatmap is the equivalent of stopping. Again, this is because the speed sensors do not actually sense stopped vehicles. Generally they sense them either as they are slowing down or speeding up just before or after a stop, so we do not actually get speeds of 0 mph. Even though values of zero speed have been inserted at some locations, the five second spline removed many of these. These insertions served to lower the speeds overall, but true values of zero are rare. This problem is exacerbated by the smoothing which tends to cause very low speeds to increase slightly, and cannot predict shockwaves intensifying between sensors.

The second assumption that we make is that a maximum deceleration (negative of acceleration) greater than $3 ft/sec^2$ is the typical deceleration of inattentive drivers hindered by poor visibility. This is the chosen threshold for a dangerous deceleration in the critical zone for a driver to need to be warned. In addition, we require that the average deceleration between the minimum and maximum speed of the vehicle is $1.3 ft/sec^2$. We find this by finding the local maximum and minimum speeds on either side of the maximum deceleration. Then the average acceleration $\bar{a}$ is:

$$\bar{d} = \frac{v_{max} - v_{min}}{t_{max} - t_{min}} \tag{17}$$

Where:

- $\bar{a}$ - Average acceleration of the vehicle.
- v_{max} - Previous local maximum speed of the vehicle.
- v_{min} - Next local minimum speed of the vehicle.
- t_{max} - Time of previous local maximum speed of the vehicle.
- t_{min} - Time of next local minimum speed of the vehicle.

Finally, we define a region called the critical region, where visibility is the lowest. We assume that if drivers are before or after this region, visibility is good enough that even inattentive drivers will recognize shockwaves approaching. Only in the critical region do we consider shockwaves to be particularly dangerous and worth warning drivers about.

CHAPTER 5: RESULTS AND DISCUSSION

The results described below utilize data from 371 days from October 2020 through June 2022. The selected days have at least 3 out of 4 detectors functioning and Detectors 3 and 4 are functioning in all selected days. The study period is from 2:00 pm to 7:00 pm each week day, which is the same as the operating time of the MN-QWARN system.

When discussing the performance of the MN-QWARN system we refer to either the algorithm or the system. When discussing the algorithm we refer to the 0 or 1 output coming from applying thresholds to the raw crash probability. This does include the 1 minute minimum alarm time, but does not include the speed override required by MNDOT. When discussing the system as a whole, we utilize logs of the actual messages displayed on the sign. This evaluation includes the speed override, communication delays, and instances when the sign was busy, etc.

To reiterate, three lanes are examined in this evaluation. The right and left lanes are the target lanes used by the system, and the lanes where crash probability is predicted. However, we also include the middle lane (used as the secondary lane for both models). To evaluate this lane we consider the alarm to be raised if either the right or left side models raises the alarm.

5.1 HYPOTHETICAL VEHICLE BASED RESULTS

To rate the performance of the MN-QWARN algorithm, we define 4 major categories of events based on the ratings of each hypothetical vehicle. The first category (G) is the most common: when drivers do not need to be warned and when they are not warned. The second category is when the driver was warned when they needed to be warned (Y). Both of these cases are examples of successful operation of the algorithm. The third case is a failure of the system when the alarm is not raised, but a warning was needed (N). This category corresponds to a missed alarm. Finally, the last category (M), is when drivers were warned and did not need to be. These four general categories can be described in a truth table. The ground truth determining whether the driver should or should not be warned is created using the methodology rating the trajectories, and these decisions are compared to the decisions made by the MN-QWARN algorithm.

Table 5-1 MN-QWARN Truth Table

	Ground Truth	
	0	1
0	G	N
1	M	Y

In addition to the algorithm, the system as a whole can be evaluated. This is a similar process, but takes into account several other factors including delay in relating information to the sign, connectivity issues, or other messages displayed on the sign. When rating the algorithm alone, we assume that the driver sees any message instantly. However, there are communication delays and the message is only changed every 30 seconds even though the crash probability is calculated every 2 seconds. In this case the

categories G, N, M, and Y are defined the same way but the ground truth is compared to a record of the message displayed on the changeable message sign itself instead of the algorithm result.

Several statistics to demonstrate the performance of the sign. The first category is the detection rate. This is the number of times a message is displayed when the ground truth determined that a warning is needed divided by the total number of times a message should have been displayed regardless of the outcome of the algorithm:

$$DetectionRate = \frac{Y}{Y + N} \tag{18}$$

The false alarm rate is the number of times the alarm is raised when the ground truth determines that it should not be, divided by the total number of times the alarm is raised regardless of the ground truth. In order to calculate this statistic, the M category must be further split into three separate cases. M1 denotes when the driver was warned but should not have been because vehicles were going slowly under the sign and continued to move slowly throughout the study area (less than 20 mph). M2 is when the driver was warned when it decelerated to a stop in the study area, but not at a high enough rate to be dangerous. Finally, M3 is when a vehicle's speed never dropped below 30 mph in the study area. This is the most important case to avoid since it erodes driver trust in the sign. To simplify the equations below, we define $M = M1 + M2 + M3$.

It is also important to consider the impact of the sign on driver behavior. The M2 category designates vehicles that came to a stop more slowly when they were warned. Some of these cases could have lead to high deceleration rates if drivers were not warned, but the warning alerts drivers to the shockwave approaching and allow them time to decelerate more slowly. For this reason (and because they did encounter congestion and stop), warning these drivers should not be considered a failure. The other two cases (M1 and M3) are unlikely to change due to the alarm since reaction time is not the driving factor in their behavior.

$$FalseAlarmRate = \frac{M3}{Y + M} \tag{19}$$

A modified version of the false alarm rate includes the vehicles that were going slow everywhere. This is also a problem since these drivers are already aware of congestion and do not need a warning. However, this type of error is possible to correct with a speed override which shuts off the alarm when speeds drop below a threshold. This makes these errors less of a concern than the false alarm rate defined above. We still do not include case M2 (vehicles which still had to stop eventually but may have decelerated more slowly after seeing the sign) since these vehicles are not the main focus of the algorithm, but are also not failures of the system since they do encounter congestion. The modified false alarm rate is defined as:

$$ModifiedFalseAlarmRate = \frac{M1 + M3}{Y + M} \tag{20}$$

Finally we define the good detection rate and the false detection rate. The good decision rate is rate of ”correct” decisions that agree with the ground truth, and the false decision rate is all those decisions that are ”incorrect” and disagree with the ground truth. In both cases the denominator of the equation is all total decisions made by the algorithm. As above, we only consider cases of M3 as incorrect decisions, though we also include the modified good and false rates where M1 is also included as incorrect.

$$GoodRate = \frac{G + Y + M1 + M2}{G + Y + M + N} \tag{21}$$

$$FalseRate = \frac{N + M3}{G + Y + M + N} \tag{22}$$

$$ModifiedGoodRate = \frac{G + Y + M1}{G + Y + M + N} \tag{23}$$

$$ModifiedFalseRate = \frac{N + M1 + M3}{G + Y + M + N} \tag{24}$$

Table 5-2 shows the results when the Algorithm is evaluated and Table 5-3 shows what happens when the system as a whole is evaluated. The left side model has a much higher detection rate than the right side model. In addition, it has a lower false alarm rate, but a higher modified false alarm rate. This suggests that the left side model is often raising the alarm when conditions are too congested while the right side model is raising it when there is insufficient congestion to form dangerous shockwaves. On both sides we see a very high good rate. As expected, the middle lane has a lower good rate and higher false rate since neither of the models is explicitly targeting conditions on that lane.

Table 5-2 Algorithm Results

Result	Left	Middle	Right
Detection Rate	63%	63%	25%
False Alarm Rate	23%	32%	37%
Modified False Alarm Rate	47%	52%	40%
Good Rate	93%	89%	94%
False Rate	7%	11%	6%
Modified Good Rate	85%	82%	93%
Modified False Rate	15%	18%	7%

Table 5-3 System Results

Result	Left	Middle	Right
Detection Rate	54%	54%	22%
False Alarm Rate	26%	36%	40%
Modified False Alarm Rate	45%	51%	42%
Good Rate	94%	90%	92%
False Rate	6%	10%	8%
Modified Good Rate	90%	86%	92%
Modified False Rate	10%	14%	8%

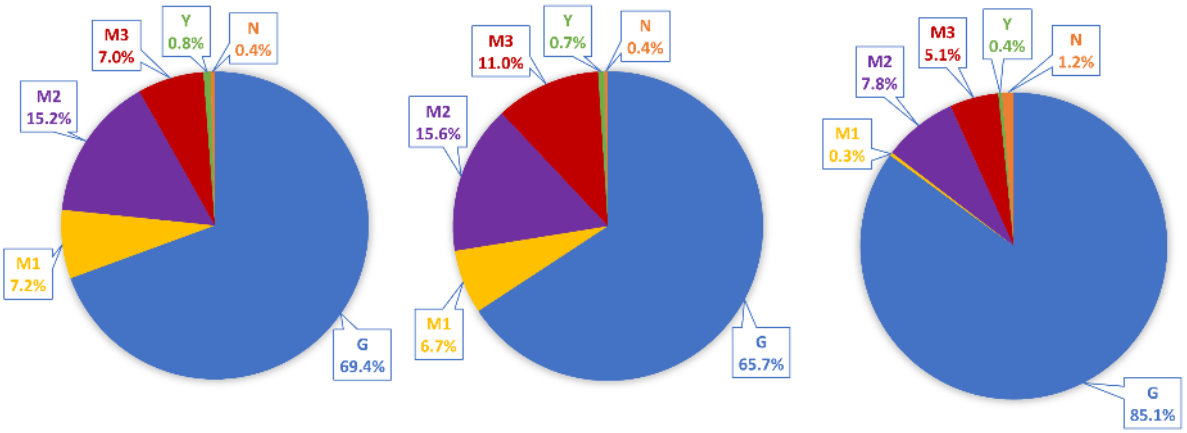

(a) Algorithm Left (b) Algorithm Middle (c) Algorithm Right

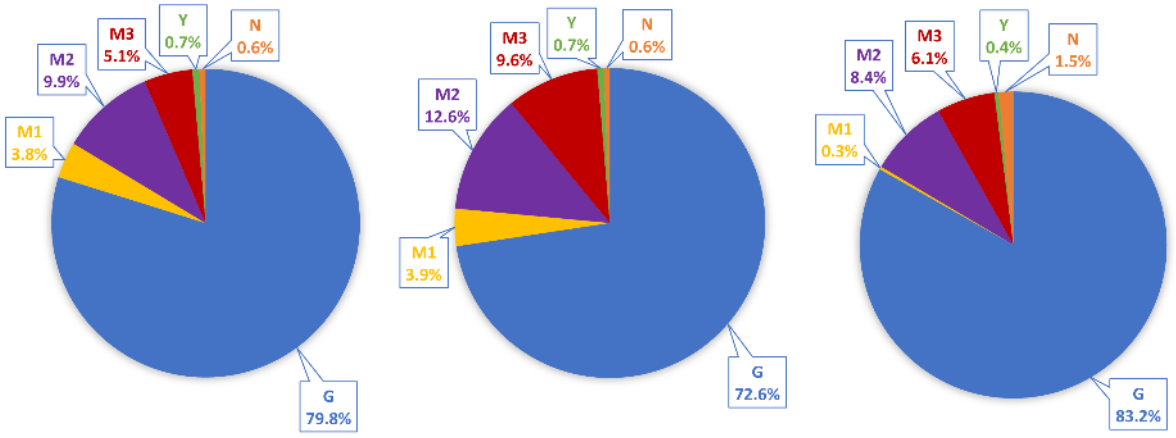

(d) System Left (e) System Middle (f) System Right

Figure 5-1 Categorization of the hypothetical trajectories based on results of the Algorithm and System for all lanes.

The detection rate goes down for the system in comparison with the algorithm. In addition, the false alarm rate increases. This is likely due to the alarm being raised and lowered too late due to communication delays. This is a problem noted at the previous location also since in both cases the sign only updates every 30 seconds while the algorithm makes a decision every 2 seconds (Hourdos et al., 2021).

Figure 5-1 shows the categorization of each hypothetical trajectory. It is notable that for the right lane, the M1 category is very small. This suggests that the speed override is more effective for this lane than the other two. False alarms, M3, account for only 5 − 7% of the total time. However, there is still a lot of time when the alarm is on when it does not need to be (all M categories). Though this is not necessarily a bad thing if these alarms fall into the M2 case, it suggests that more calibration could be helpful in narrowing down the alarm to the most important cases.

5.2 EVENT BASED RESULTS

The evaluation metrics based on the hypothetical trajectories are helpful but are often on too fine a time scale for a sign that is only updated every 30 seconds and an algorithm intended to warn groups of vehicles, not individual drivers. For this reason, it is important to group these trajectories into "events" made up of several dangerous trajectories. This is done using a heuristic process to determine the most important time periods each day for the sign to be on.

To do this, we view the set of vehicles that need to be warned as a binary time series with equally spaced points at which conditions are dangerous. In many cases there are long strings of vehicles which need to be warned, within which only one or two vehicles do not. In this case, these small pockets of vehicles that do not need to be warned are less important than the vehicles on either side that are important to warn. In contrast, there are some instances when only a few vehicles need to be warned within a large group that should not. If this grouping is sufficiently small, it may be safe to ignore it. In making these assumptions, it is important to remember that these are hypothetical vehicles, and real vehicles would never enter the study area at a constant rate of 1 vehicle every 2 seconds.

Based on the logic above, 2 rules are created. First, gaps between sets of vehicles that need to be warned are filled in if they span less than 10 seconds. Second, entire groups spanning less than 30 seconds can be removed since the sign is only updated every 30 seconds. The groups created define 'events' as time periods when the alarm should have been raised. This process is shown in Figure 5-2. 5270 events occurred when the system was operational.

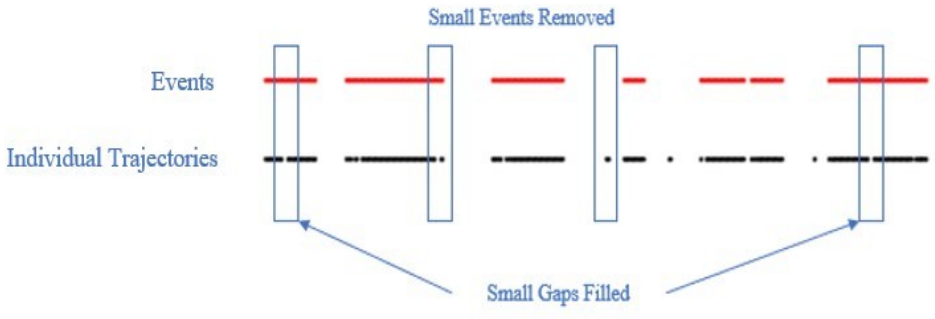

Figure 5-2 Creation of events from individual trajectories.

Once groups have been created, they can be categorized based on their relationship with alarms. A Missed group means the alarm did not come on within 5 minutes before or after the group. Missed - Early Alarm means the alarm would not have been seen by any drivers in the group but was on and ended within 5 minutes of the beginning of the group. Similarly, a Missed - Late Alarm means the alarm came on within 5 minutes of the end of the group. Hit - Off Early means part of the group saw the alarm but it went off before some vehicles at the end of the group saw it. Hit - On Late means the end of the group saw the alarm, but not the beginning. Hit - Short Alarm means the alarm came on late and went off early, and Hit - Long Alarm means the alarm come on early and went off late. These events are categorized in Figure 5-3.

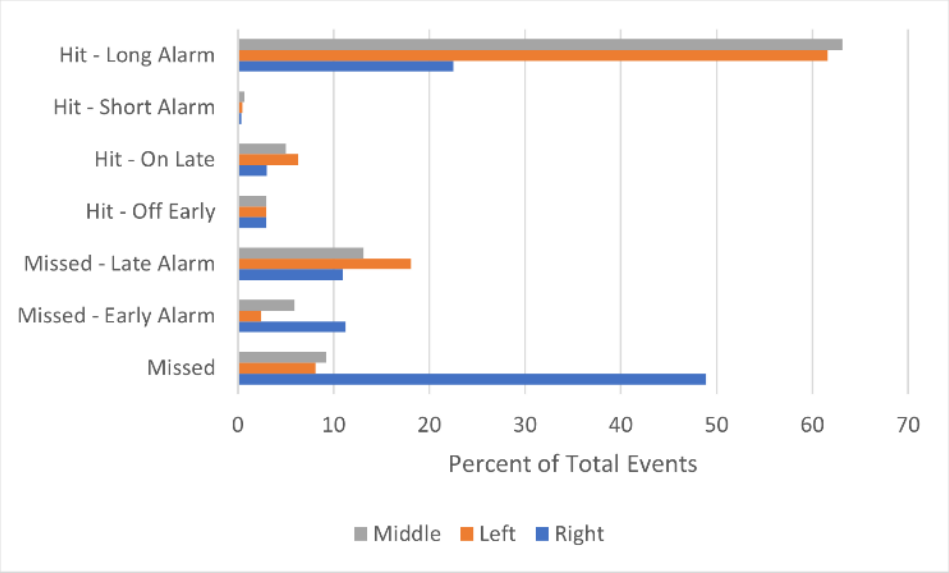

Figure 5-3 Categorization of all 5270 events in the 371 day study period

Figure 5-3 shows some interesting trends in the data and some important differences between the performance of the right and left side models. Over 60% of the events for both the middle and left lanes fit into the long alarm category. The left lane has only 8% of events missed completely and an additional 16% either missed early or late. The middle lane has similar trends. On the other hand, the right lane

misses almost half of the events completely, and an additional 23% were missed either early or late within 5 minutes.

These trends make sense based on the original design of the model. As discussed in Section 3.3 , the left side model operates much more closely to design and philosophy of the original system. It also makes sense in a practical sense, the left side model raises the alarm for a much larger portion of the day than the right side model, so is much more likely to have it raised when something dangerous happens.

Combining the information in this section with 5.1 , it appears that the right side model is not sensitive enough, while the left side model may be too sensitive. This suggests that the algorithm may need to be refit for future implementations to achieve better performance.

To dig deeper into these categories, two time periods are defined. Over-warning is when the alarm is raised and there is no event occurring. In contrast, under-warning is when the alarm is not raised during an event. By summing up all these errors made by the system, we can find the percent of the time when drivers are over and under-warned. However, to evaluate the system fairly, the effect of the 1-minute extension needs to be considered. Anytime the alarm is raised, it is required to stay on for at least 1 minute. To account for this, the over-warning category can be relaxed to only begin after an alarm has been up for one minute if it was raised while an event was occurring. These numbers are reported as percentages of time calculated as the total over or under-warning time divided by the total time the system was in operation. The results are listed in Table 5-4.

Table 5-4 Percent of time Over and Under-Warning

Result	Left	Middle	Right
Under-Warning	0.34%	0.28%	0.69%
Over-Warning	24%	26%	10%
Modified Over-Warning	21%	24%	8%

These results suggest that the sign is on too often (especially the left side model). It is rarer that the sign is under-warning drivers, though this is skewed lower by the very small number of drivers that need to be warned in the first place. The right-side model under-warns drivers twice as often.

Finally, the errors in start and end time of each alarm can be examined. The start of each event is compared to the start time of the nearest alarm. This discounts some events that were missed entirely or began part way through a much longer alarm (as shown in Figure 5-4). However, this method is effective in examining how well the system predicts the passing of a shockwave through the critical zone. A similar procedure can be used to examine when the alarm is dropped by comparing the end of the alarm to the end of the nearest event.

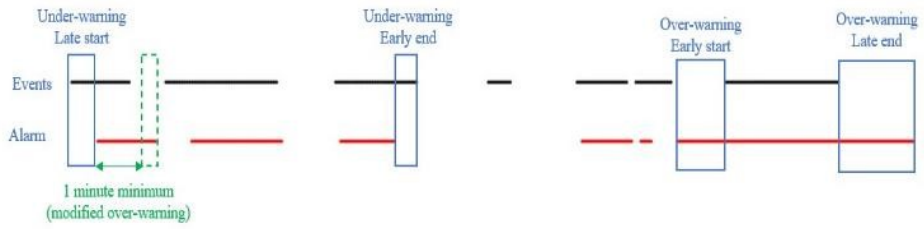

Figure 5-4 Comparison of events with the alarm

In Figure 5-5, a negative time difference corresponds to an alarm coming on (or ending) early, and a positive time difference corresponds to a late (or long) alarm.

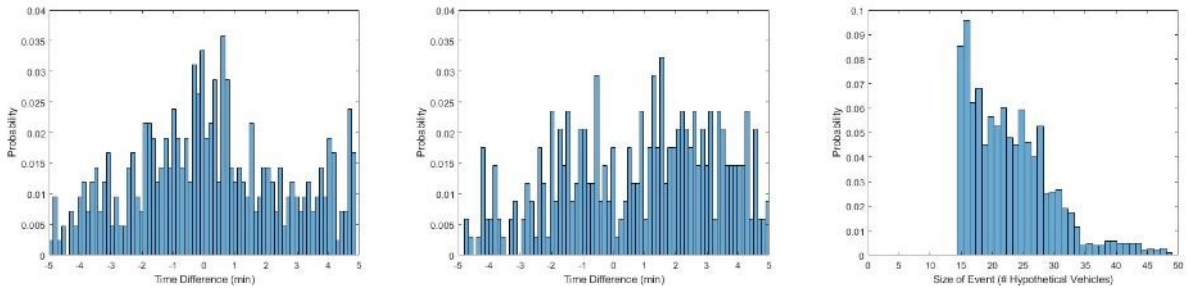

(a) Left Start **(b) Left End** **(c) Left Event Size**

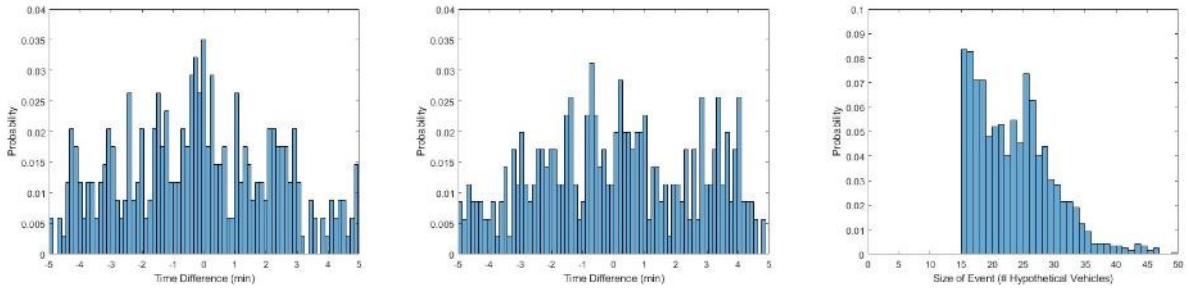

(d) Right Start **(e) Right End** **(f) Right Event Size**

Figure 5-5 Time difference between the start of alarm and start of event (a and d) and the end of alarm and end of event (b and e), and number of vehicles contained in each event (c and f).

For all three lanes, the start of the alarm peaks more towards the center of the graph (time difference of 0) then the end of the alarm/event. In particularly both graphs Figure 5-5a and Figure 5-5d peak between 0 and -1 minutes (raising the alarm 1 minute early). This is ideal since it is generally better to warn a few extra vehicles at the beginning of an event than it is to miss any part of the event. These figures show that the MN-QWARN algorithm is better at precisely predicting the beginning of an event than it is at predicting the end (this is especially true for the left lane). For the left lane, the end of the alarm also tends to be late, suggesting we keep the alarm on too long.

5.3 EFFECTS OF THE SIGN ON DRIVER BEHAVIOR

In addition to evaluating the ability of the sign to successfully warn drivers of dangerous conditions ahead, it is also important to determine whether there are larger changes to the traffic flow based on driver reactions to the sign. These could come in the form of lane changes as drivers move out of congested lanes. This could reduce congestion by reducing pressure from upstream, or could create more turbulence from excessive lane changes. Drivers could also slow down early and more smoothly in anticipation of shockwaves, which could slow the approaching waves. It is important to evaluate these larger impacts of the sign on traffic patterns.

The first step in evaluating these effects is to group the study period into days when the sign is off and when it is on. This is done using the GEH statistic. Though not statistically significant, this is a statistic commonly used in traffic forecasting and modeling which takes traffic volume as an input (Horowitz et al., 2014; Hourdos et al., 2015). Generally, this statistic is used with hourly volumes, and a GEH of 5.0 is considered a strong correlation. In some cases, values between 5.0 and 10.0 are also considered acceptable, though these values are excluded here.

$$GEH_{ij} = \frac{\sum_{t=1}^{N_t} \sum_{x=1}^{N_x} \sqrt{\frac{2(V_{t,x,i} - V_{t,x,j})^2}{V_{t,x,i} + V_{t,x,j}}}}{N_t \times N_x} \quad (25)$$

Where:

- GEH_{ij} - Value of the GEH statistic for before date i and after date j (0.0-5.0 considered acceptable)
- V_t,x,i – 5-minute traffic volume t from detector x on before date i.
- V_t,x,j – 5-minute traffic volume t from detector x on before after j.
- N_t - number of 5-minute traffic volumes t.
- N_x - number of detectors x.

In this formulation, a 5-minute traffic volume is used instead of a 1-hour volume. In addition, this analysis is done for the 5-hour study period from 2:00 pm to 7:00 pm, so $N_t = 60$. There are 4 detectors ($N_x = 4$) used for each of the 4 I-94 mainline lanes at Huron Ave. These are detectors 2681, 2682, 2683, and 2684 in 2019 and most of 2020. In 2021 and 2022 these detectors were replaced with detectors 8848, 8849, 8850, and 8851. This is the same process followed by Hourdos et al. (59).

Once a comparable set of dates is found, the average and standard deviation of vehicle travel times can be plotted on days when the system is on and off for comparison. These travel times are found by subtracting the time the vehicle enters the study area from the time it leaves the study area. Large differences in average or standard deviation of travel time with and without messages on the sign suggest that there are impacts on driver behavior.

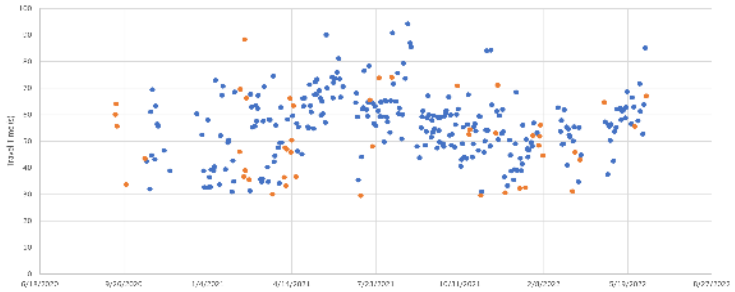

(a) Left Average

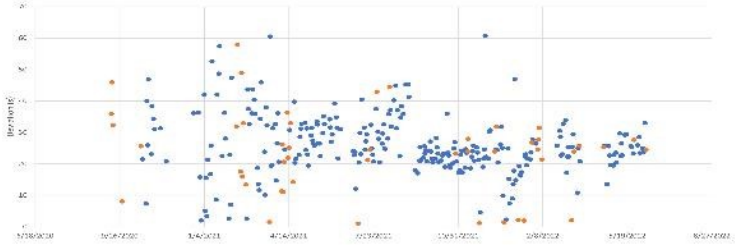

(b) Left Standard Deviation

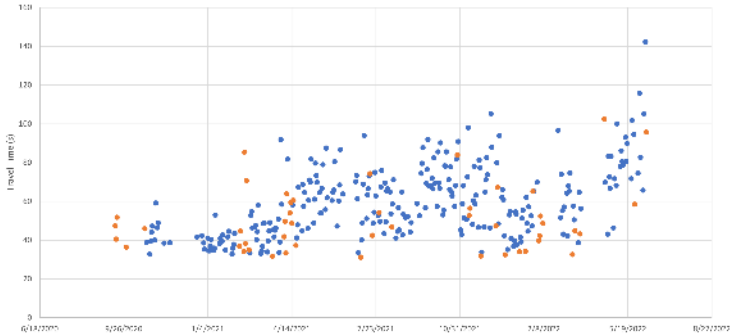

(c) Right Average

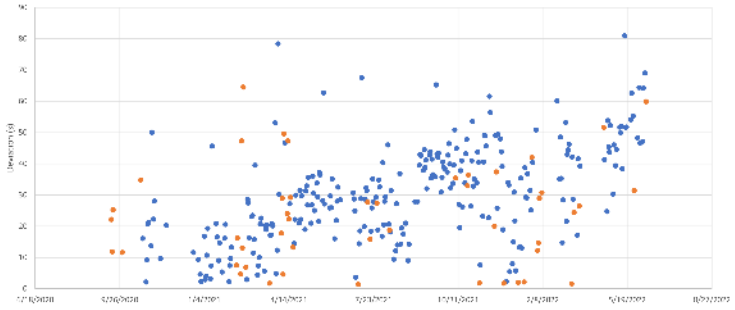

(d) Right Standard Deviation

Figure 5-6 Average and standard deviation of vehicle travel times split by system on (blue) and system off (orange).

Figure 5-6 shows increasing average travel times throughout the study period. In addition, travel times for this lane have a higher standard deviation towards the end of the period than at the beginning in contrast to the left lane which has smaller and more consistent standard deviations. However, these figures are not sufficient to show a major change in overall traffic patterns when the sign is working compared to when it is not.

5.4 CRASH ANALYSIS

Chapter 2 presented the evaluation of the original deployment of MN-QWARN, which had a critical zone, downstream of Portland Ave. As noted, that road section, prior to the reconstruction of the junction with I-35W NB, had been an extremely dangerous one, resulting on average in one crash every two days and four times as many near-crashes. Although it is fortunate that no other road section in MN even comes close to such crash activity, the fact that such a large number of crashes took place in such a small section of roadway made evaluation by simple observation possible.

In the second deployment of the system, result of which were presented earlier in this chapter, it became very quickly in the project, that although the construction downstream on I-94 and I-35W (pre-covid) did increase congestion and frequency of flow breakdown, crashes did not generate in numbers that made possible a similar evaluation methodology with the original deployment period. This as well as the enhanced nature of the evaluation based on hypothetical vehicle trajectories prompted the project team in putting the majority of the effort in the methods described in the earlier chapters.

Regardless, during the period prior to system activation and later, the segment of I-94 WB between the Cedar Ave exit to the 11th Ave overpass did experience some normal crash activity. Although the frequency of crashes combined with the short time interval, for a safety study, of this project does not allow concrete results to be drawn regarding the success of MN-QWARN in reducing crashes in general, nevertheless information exists and is summarized in the following sections.

5.4.1 MnCMAT2 Data retrieval

The Minnesota Crash Mapping Analysis Tool (MnCMAT2) is the latest tool developed by MnDOT to archive and allow access to crash records in the state of Minnesota. The MnCMAT2 software enables the user to analyze crashes based on a large number of crash attributes, including county, city, township, measure, intersection, and date ranges. The tool also enables the user to produce charts or maps to graphically view crash data and crash locations. Charts can be created by various crash attributes, including crashes by county, month, day of the week, crash severity, manner of collision, surface conditions, and type of roadway. The software can produce a color map with plotted crashes and a series of charts or reports based on selected crash attributes. MnCMAT2 contains a rolling 10-year dataset plus current year crash data as reported to Department of Public Safety.

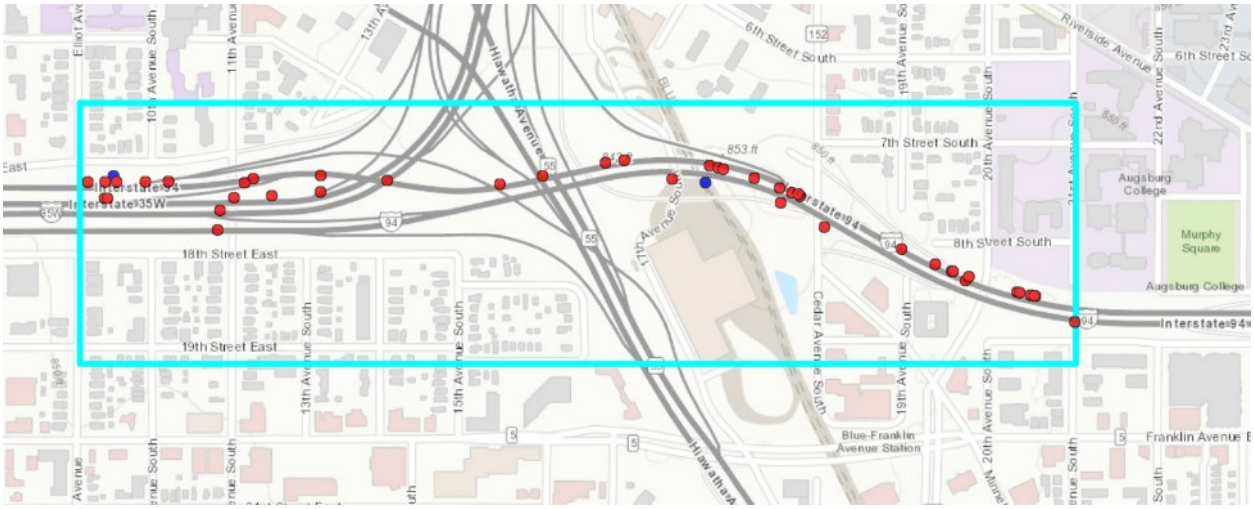

Figure 5-7 MnCMAT2 example output from selected geographical boundary.

The project team utilized MnCMAT2 in retrieving crash records for the project site for 2019 (pre activation) and 2021-22 (post-covid with system activated.) Figure 5-7 shows the boundary of the selected region of I-94 WB. A larger area was selected in order to avoid errors in the coding of the crash location. Frequently, following minor crashes, vehicles move downstream of the Cedar-Hiawatha section (minimal shoulder) before they stop and are responded to by the State Patrol. For all the crashes described in this section, the research team inspected the crash record narrative in order to verify the actual location of the collision.

In addition to the geographic boundary, a number of other filters were introduced in order to focus more the investigation. These filters are the following:

- Day of the Week: Given that MN-QWARN operated only during weekdays, the extracted crash records only cover Monday to Friday.
- Time of day: MN-QWARN was active between the hours of 2pm and 8pm. To avoid missing any information crash records were extracted for a slightly larger time period of noon to 10pm.
- Divided Roadway Direction: West
- Route System: Interstate Trunk Highway – ISTH

In total in the entire area shown in the previous figure and for the time constraints discussed above, in 2019 there were 39 crashes, in 2020 there were 27, in 2021 there were 47, and in 2022 at the time of this writing (9/19/2022) 30 crashes have occurred. The trends follow what has been generally observed in the entire network, with crashes reducing during 2020 since congestion was a minimal, while returning in much greater numbers in 2021 and it seems like 2022 continues this trend. For the purposes of the MN-QWARN evaluation we narrowed down the roadway section of interest. Table 5-5 shows the different sections we divided the aforementioned area and the 2019 and 2021 crash numbers that took place.

Table 5-5 MnCMAT2 Crash Records for 2019 and 2021

	I-35W exit	Hiawatha Ave	7th St exit	Cedar Ave	20th Ave	Total
2019	2	10	5	5	6	**28**
2021	3	9	0	10	3	**25**

The MN-QWARN implementation was planned based on the assumption that the location where the most crashes are likely to happen is the horizontal and vertical curve just downstream of the 7th St exit. As can be seen in the table, this assumption is not supported by the data since a significant amount of crashes happen further downstream above Hiawatha Ave. This section is much less curved and downhill offering no sight distance issues so this fact is somewhat peculiar. MN-QWARN was timed to produce warnings just before the back of the queue reaches the critical zone described earlier so in some ways it was by design not able to produce warnings targeting queue ends over Hiawatha. Overall, in 2021, the year the system was in full operation, in the aforementioned section 3 fewer crashes occurred. More interesting is the observation that on the critical zone in 2019 5 crashes took place while none happened in 2021. For all fairness, it is also interesting to mention that for the section just upstream of the VMS to just downstream of the Cedar Ave the number of crashes doubled in 2021 to 10 from the 5 observed in 2019. It is difficult to say if MN-QWARN had something to do with either favorable or unfavorable trend changes.

Drilling a little further on the 2021 crash records from the total 25 crashes, excluding single vehicle crashes and crashes that happen upstream of the VMS, 19 crashes remain. For these 19 crashes the following observations can be made:

- During 5 of the crashes the system was non-operational
- 4 crashes were not relevant to queue since they took place during free flow conditions (drunk driving, illegal lane change, etc.)
- 3 crashes took place while the alarm was active, and warning was displayed
- 2 crashes took place while the system deemed that no alarm was necessary
- 2 crashes took place under the VMS
- 2 crashes took place while the alarm was overridden because of congestion.

Given the small numbers of crashes and the limited observation period, all discussions in this section are offered as anecdotal evidence and should not be totally trusted.

CHAPTER 6: CONCLUSIONS

This report presented both the evaluation results of the MN-QWARN queue warning system at the original location where it was developed as well as its second deployment on a further upstream section of the same freeway (I-94). The second evaluation of the MN-QWARN queue warning system was different from the first in two important ways. First, the MN-QWARN system was implemented at a new location with minimal calibration. Only the thresholds were modified for the new location. This was important since the original system was designed to detect a very specific type of CPC at the original location and was calibrated for traffic there. Because the new location experiences very different patterns of congestion, the versatility of the model can now be illustrated.

The second major difference was In the methodology of the evaluation. In the first study, researchers watched thousands of hours of video and coded events as “crash" or “near-crash." However, at the new location, there were too few crashes for this type of evaluation. Instead, a more data-driven approach was used in this study. The benefit of this approach was that it allowed for a more consistent evaluation of the entire period when the sign was on and provided information about false alarms as well as the detection rate. However, it relied on the empirical set of assumptions regarding dangerous driver behavior described earlier. These assumptions were made based on observations of the roadway from video data, but another set of thresholds could create different results. Regardless, this methodology provided a consistent estimate of the level of danger that traffic conditions pose to drivers on the roadway and provided detailed information on the efficacy of the queue warning algorithm.

This study used data collected from 371 days from 2:00 pm through 7:00 pm during the operational hours of the MN-QWARN system. The evaluation found that the right-side model had a detection rate of 25% and a false alarm rate of 36%. The left side model had a detection rate of 64% and a false alarm rate of 23%. We also noted high over-warning rates on both lanes. This over-warning rate came primarily from alarms ending too late since the algorithm predicted the beginning of each even more reliably than the end.

Empirical evidence from video data suggests that the left-side model raises the alarm much faster than the right and leaves it on for longer. This phenomenon explains the higher detection and false alarm rates. Video data shows very slow-moving shockwaves on the left encompassing more vehicles, causing the alarm to be raised. However, the event sizes show that the number of vehicles needing to be warned in each shockwave is similar for the right and left lanes (though the left side has more total events). This suggests that only small portions of these slow-moving waves are actually dangerous for drivers, and the model may need to be refined to detect only these portions.

The results of this study are promising but suggest there is still room for improvement. These results show that the MN-QWARN algorithm can be more easily transferred to a new location that closely matches the traffic patterns of the original location (such as the left-side model). However, detection rates are low and false alarm rates are high on the right side of the road, and there is still room for improvement on the left-side model. The methodology used in this study provides a ground truth that can more easily be used to refit the model than previous work. This ground truth provides information

regarding when the alarm should be raised as well as when it should not be on. In addition, this numerical method provides a higher density of data so refitting the model will not take years to fully calibrate. Future work should examine how much improvement can be gained by refitting the model at this location to see if this is a valuable procedure to include at future implementations.

REFERENCES

1. Abdel-Aty, M. A., & Pemmanaboina, R. (2006). Calibrating a real-time traffic crash-prediction model using archived weather and ITS traffic data. *IEEE Transactions on Intelligent Transportation Systems, 7*(2), 167–174.
2. Abdel-Aty, M., & Gayah, V. (2010). Real-Time Crash Risk Reduction on Freeways Using Coordinated and Uncoordinated Ramp Metering Approaches. *Journal of Transportation Engineering, 136*(5), 410–423.
3. Abdel-Aty, M., Cunningham, R. J., Gayah, V. V., & Hsia, L. (2008). Dynamic Variable Speed Limit Strategies for Real-Time Crash Risk Reduction on Freeways. *Transportation Research Record, 2078*(1), 108–116.
4. Abdel-Aty, M., Dhindsa, A., & Gayah, V. (2007). Considering various ALINEA ramp metering strategies for crash risk mitigation on freeways under congested regime. *Transportation Research Part C: Emerging Technologies, 15*(2), 113–134.
5. Abdel-Aty, M., Dilmore, J., & Dhindsa, A. (2006). Evaluation of variable speed limits for real-time freeway safety improvement. *Accident Analysis & Prevention, 38*(2), 335–345.
6. Abdel-Aty, M., Haleem, K., Cunningham, R., & Gayah, V. (2009). Application of Variable Speed Limits and Ramp Metering to Improve Safety and Efficiency of Freeways. 2nd International Symposium on Freeway and Tollway Operations, Hawaii, USA.
7. Abdel-Aty, M., Uddin, N., Pande, A., Abdalla, M. F., & Hsia, L. (2004). Predicting Freeway Crashes from Loop Detector Data by Matched Case-Control Logistic Regression. *Transportation Research Record, 1897*(1), 88–95.
8. Ahn, S., Bertini, R. L., Auffray, B., Ross, J. H., & Eshel, O. (2007). Evaluating Benefits of Systemwide Adaptive Ramp-Metering Strategy in Portland, Oregon. *Transportation Research Record, 2012*(1), 47–56.
9. Akcelik, R. (1998). *A queue model for HCM 2000*, ARRB Transportation Research Ltd., Vermont South, Australia.
10. Ariza, A. (2011). Validation of Road Safety Surrogate Measures as a Predictor of Crash Frequency Rates on a Large-Scale Microsimulation Network (PhD thesis), University of Toronto, Ontario, Canada.
11. American Road & Transportation Builders Association. (2015) Innovative End-of Queue Warning System Reduces Crashes Up to 45%. Paper presented at the ARTBA Work Zone Safety Consortium. Texas, USA
12. Audet, C., & Dennis, J. E. (2002). Analysis of Generalized Pattern Searches. *SIAM Journal on Optimization, 13*(3), 889–903.
13. Balke, K., Charara, H., & Parker, R. (2005). *Development of a traffic signal performance measurement system (TSPMS)*, Texas Transportation Institute, The Texas A&M University System College Station, Texas.
14. Bashir, S., & Zlatkovic, M. (2021). Assessment of Queue Warning Application on Signalized Intersections for Connected Freight Vehicles. *Transportation Research Record, 2675*(10), 1211–1221.

15. Bertini, R.L., Boice, S., & Bogenberger, K. (2006). Dynamics of Variable Speed Limit System Surrounding Bottleneck on German Autobahn. *Transportation Research Record, 1978*, 149-159.

16. Caliendo, C., Guida, M., & Parisi, A. (2007). A crash-prediction model for multilane roads. *Accident Analysis and Prevention, 39*(4), 657–670. doi: 10.1016/ j.aap. 2006.10.012

17. Cassidy, M. J., & Rudjanakanoknad, J. (2005). Increasing the capacity of an isolated merge by metering its on-ramp. *Transportation Research Part B: Methodological, 39*(10), 896– 913.

18. Catling, I. (1977). A time dependent approach to junction delays. *Traffic Engineering and Control, 18*(11), 520-526.

19. Chambers, A. L. (2016). Benefits of Advanced Traffic Management Solutions: Before and After Crash Analysis for Deployment of a Variable Advisory Speed Limit System (PhD thesis), California Polytechnic State University, San Luis Obispo, California.

20. Chan, C. (2012). Monitoring and Improving Roadway Surface Conditions for Safe Driving Environment and Sustainable Infrastructure, University of California Berkeley – PATH, Richmond Field Station, Richmond, CA.

21. Chang, T., & Lin, J. (2000). Optimal signal timing for an oversaturated intersection. *Transportation Research Part B: Methodological, 34*(6), 471-491.

22. Chatterjee, I., & Davis, G. A. (2016). Analysis of Rear-End Events on Congested Freeways by Using Video-Recorded Shock Waves. *Transportation Research Record, 2583*(1), 110-118. doi:10.3141/2583-14

23. Chatterjee, K., Hounsell, N.B., Firmin, P.E., & Bonsall, P.W. (2002). Driver response to variable message sign information in London. *Transportation Research Part C: Emerging Technologies, 10*(2), 149-169.

24. Chen, R., Levin, M., Hourdos, J., & Duhn, M. (2021). *Generating Traffic Information from Connected Vehicle V2V Basic Safety Messages* (Technical Report MN 2021-08), Minnesota Department of Transportation, St. Paul, MN.

25. Chen, Z., Qin, X., Zhong, R., Liu, P., & Cheng, Y. (2018). Predicting Imminent Crash Risk with Simulated Traffic from Distant Sensors. *Transportation Research Record, 2672*(38), 12–21. https://doi.org/10.1177/0361198118791379f

26. Cheng, Y., Qin, X., Jin, J., & Ran, B. 2012, An Exploratory Shockwave Approach to Estimating Queue Length Using Probe Trajectories. *Journal of Intelligent Transportation Systems, 16*(1) 12-23.

27. Chugh, J. S., & Caird, J. K. (1999). In-Vehicle Train Warnings (ITW): The Effect of Reliability and Failure Type on Driver Perception Response Time and Trust. *Proceedings of the Human Factors and Ergonomics Society Annual Meeting, 43*(18), 1012–1016.

28. Cleavenger, D. K., & Upchurch, J. (1999). Effect of Freeway Ramp Metering on Accidents: The Arizona Experience. ITE Journal*, 69*(8).

29. Comert, G., & Cetin, M. (2009) Queue length estimation from probe vehicle location and the impacts of sample size. *European Journal of Operational Research, 197*(1), 196-202.

30. Cronje, W.B. (1983a). Analysis of existing formulas for delay, overflow, and stops. *Transportation Research Record, 905*, 89-93.

31. Cronje, W.B. (1983b). Derivation of equations for queue length, stops, and delay for fixed-cycle traffic signals. *Transportation Research Record, 905,* 93-95.

32. Delta Highway Queue Warning System Evaluation (2016). Final Technical Memorandum. Retrieved from http://www.kittelson.com/projects/intelligent-transportation-systems-its-statewide-evaluations.

33. Department of Public Safety. (2017). Minnesota Traffic Crashes in 2017, Minnesota Department of Public Safety. Retrieved from dps.mn.gov/divisions/ots/reports-statistics/Documents/Minnesota%20Traffic%20Crashes%20in%202017.pdf.

34. Duhn, M., Parikh, G., & Hourdos, J. (2019). I-94 *Connected Vehicles Testbed Operations and Maintenance,* Center for Transportation Studies, University of Minnesota. Retrieved from the University of Minnesota Digital Conservancy, http://hdl.handle.net/11299/203633.

35. Dutta, N., Fontaine, M., Boetang, R., & Campbell, M. (2018). *Evaluation of the Impact of the I-66 Active Traffic Management System: Phase II. Virginia Transportation Research Council. Charlottesville, Virginia*

36. Elefteriadou, L., Roess, R.P., & McShane, W.R. (1995). Probabilistic Nature of Breakdown at Freeway Merge Junctions. *Transportation Research Record, 1484*, 80-89.

37. Farrag, S. G., Outay, F., Yasar, A. U.-H., & El-Hansali, M. Y. (2020). Evaluating Active Traffic Management (ATM) Strategies under Non-Recurring Congestion: Simulation-Based with Benefit Cost Analysis Case Study. *Sustainability, 12*(15), 6027.

38. FHWA, 2020 *Active Traffic Management: Active Transportation and Demand Management. USDOT, Washington DC*

39. FHWA, 2020. *What is Transportation Systems Management and Operations (TSMO)? Organizing and Planning for Operations*. *USDOT, Washington DC*.

40. Gazis, D.C. (1964). Optimum Control of a System of Oversaturated Intersections. *Operations Research, 12*(6), 815-831.

41. Gazis, D.C. (1974). *Traffic science.* New York: Wiley-Interscience.

42. Ghanim, M. S., & Shaaban, K. (2019). A Case Study for Surrogate Safety Assessment Model in Predicting Real-Life Conflicts. *Arabian Journal for Science and Engineering, 44*(5), 4225–4231.

43. Ghosh-Dastidar, S., & Adeli, H. (2006). Neural Network-Wavelet Microsimulation Model for Delay and Queue Length Estimation at Freeway Work Zones. *Journal of Transportation Engineering, 132*(4), 331-341.

44. Golob, T. F., & Recker, W. W. (2003). Relationships Among Urban Freeway Accidents, Traffic Flow, Weather, and Lighting Conditions. *Journal of Transportation Engineering, 129*(August), 342–353. doi:10.1061/(ASCE)0733-947X (2003)129:4(342)

45. Green, D.H. (1967). Control of Oversaturated Intersections. *Operations Research, 18*(2), 161-173.

46. H´ebert, A., Gu´edon, T., Glatard, T., & Jaumard, B. (2019). *High-Resolution Road Vehicle Collision Prediction for the City of Montreal.* IEEE International Conference on Big Data (Big Data)

47. Han, Y., Meng, Y., Zheng, J., & Liu, H. (2019). *An Urban Freeway Ramp Metering Control System based on Trajectory Data* (Number: 19-05650). Transportation Research Board, Washington, D.C.

48. Harder, K., & Bloomfield, J. (2012, August). *Investigating the Effectiveness of Intelligent Lane Control Signals on Driver Behavior,* Center for Design in Health, College of Design, University of Minnesota, Minneapolis, MN.

49. Hassan, H.M., Abdel-Aty, M., Choi, K., & Algadhi, S.A. (2012). Driver Behavior and Preferences for Changeable Message Signs and Variable Speed Limits in Reduced Visibility Conditions. *Journal of Intelligent Transportation Systems, 16*(3), 132-146.

50. Haule, H. J., Ali, M. S., Alluri, P., & Sando, T. (2021). Evaluating the effect of ramp metering on freeway safety using real-time traffic data. *Accident Analysis & Prevention, 157*, 106181.

51. Hiribarren, G., & Herrera, J.C. (2014). Real time traffic states estimation on arterials based on trajectory data. *Transportation Research Part B: Methodological, 69,* 19-30.

52. Horowitz, A., Creasey, T., Pendyala, R., & Chen, M., National Cooperative Highway Research Program, Transportation Research Board, & National Academies of Sciences, Engineering, and Medicine. (2014). *Analytical Travel Forecasting Approaches for Project-Level Planning and Design*, Transportation Research Board, Washington, D.C.

53. Hourdakis, J. & Michalopoulos, P.G. (2002). Evaluation of Ramp Control Effectiveness in Two Twin Cities Freeways. *Transportation Research Record, 1811*(1), 21–29.

54. Hourdos, J. & Zitzow, S. (2014). *Investigation of the Impact of the I-94 ATM System on the Safety of the I-94 Commons High Crash Area*, Minnesota Department of Transportation. Retrieved from http://hdl.handle.net/11299/164689.

55. Hourdos, J. N. (2005). Crash Prone Traffic Flow Dynamics: Identification and Real-Time Detection (Ph.D. dissertation), University of Minnesota, Minneapolis, MN.

56. Hourdos, J. N., Garg, V., Michalopoulos, P. G., & Davis, G. A. (2006). Real-Time Detection of Crash-Prone Conditions at Freeway High-Crash Locations. *Transportation Research Record, 1968*(1), 83–91.

57. Hourdos, J., Duhn, M., Liu, Z., & Parikh, G. (2021). *Evaluation of the Minnesota Queue Warning System, MN-QWARN* (Number: TRBAM-21-04057). Transportation Research Board, Washington, D.C.

58. Hourdos, J., Garg, V., Michalopoulos, P., & Davis, G. (2006). Real-Time Detection of Crash-Prone Conditions at Freeway High-Crash Locations. *Transportation Research Record, 1968*(1), 83–91. doi: 10.3141/1968-10

59. Hourdos, J., Geroliminis, N., Zitzow, S., & Limniati, Y. S. (2015). *Field Implementation, Testing, and Refinement of Density Based Coordinated Ramp Control Strategy* (Technical Report MN/RC 2015-37), Minnesota Department of Transportation, St. Paul, MN.

60. Hourdos, J., Liu, Z., Dirks, P., Liu, H. X., Huang, S., Sun, W., & Xiao, L. (2017). *Development of a Queue Warning System Utilizing ATM Infrastructure System Development and Field-Testing. Minnesota Department of Transportation.* Retrieved from http://hdl.handle.net/11299/189539.

61. Hourdos, J., Parikh, G., Dirks, P., Lehrke, D., & Lukashin, P. (2019). *Evaluation of the Smart Work Zone Speed Notification System* (Technical Report MN/RC 2019-21), Minnesota Department of Transportation, St. Paul, MN.

62. Hourdos, J., Xin, W. & Michalopoulos, P.G. (2008b, December), *Development of Real-Time Traffic Adaptive Crash Reduction Measures for the Westbound I-94/35W Commons Section*, Intelligent

Transportation Systems Institute, Center for Transportation Studies, University of Minnesota, Minneapolis, MN.

63. Hourdos, J., & Zitzow, S. (2014). *Investigation of the Impact of the I-94 ATM System on the Safety of the I-94 Commons High Crash Area*, Minnesota Department of Transportation. Retrieved from http://hdl.handle.net/11299/164689.

64. Hourdos, J., Parikh, G., Dirks, P., & Lehrke, D. (2019). *Implementation of a V2I Highway Safety System and Connected Vehicle Testbed*, Center for Transportation Studies, University of Minnesota. Retrieved from http://hdl.handle.net/11299/202580.

65. I-66 Active Traffic Management System. (n.d.) Retrieved from http://www.virginiadot.org/vtrc/main/online_reports/pdf/19-r7.pdf

66. Innovative End-of-Queue Warning System Reduces Crashes Up to 45%. (2015).Technical report, ARTBA Work Zone Safety Consortium.

67. Jacobson, E. L., & Landsman, J. (1994). Case Studies of U.S. Freeway to Freeway Ramp and Mainline Metering and Suggested Policies for Washington State. *Transportation Research Record, (1446)*.

68. Jiang, Y. (2001). A model for estimating traffic delays and vehicle queues at freeway work zones. *Journal of the Transportation Research Forum, 40*(4), 65-81.

69. Karim, A., & Adeli, H. (2003). Radial Basis Function Neural Network for Work Zone Capacity and Queue Estimation. *Journal of Transportation Engineering, 129*(5), 494-503.

70. Karim, H. K. (2015). *Exploratory Analysis of Ramp Metering on Efficiency, and Safety of Freeways Using Microsimulation*, University of Kansas, Kansas City, KS.

71. Khan, A. (2007). Intelligent infrastructure-based queue-end warning system for avoiding rear impacts. *IET Intell. Transp. Syst., 1*(2), 138.

72. Khazraeian, S., Hadi, M., & Xiao, Y. (2017). Safety Impacts of Queue Warning in a Connected Vehicle Environment. *Transportation Research Record, 2621*(1), 31–37.

73. Kopelias, P., Papadimitriou, F., Papandreou, K., & Prevedouros, P. (2007). Urban Freeway Crash Analysis: Geometric, Operational, and Weather Effects on Crash Number and Severity. *Transportation Research Record, 2015*(1), 123–131.

74. Lee, C, & Abdel-Aty, M. (2008). Testing Effects of Warning Messages and Variable Speed Limits on Driver Behavior Using Driving Simulator. *Transportation Research Record, 2069*(1), 55-64.

75. Lee, C., Hellinga, B., & Saccomanno, F. (2003). Real-Time Crash Prediction Model for Application to Crash Prevention in Freeway Traffic. *Transportation Research Record, 1840,* 67–77. doi:10.3141/1840-08

76. Lee, C., Hellinga, B., & Ozbay, K. (2006). Quantifying effects of ramp metering on freeway safety. *Accident Analysis & Prevention, 38*(2), 279–288.

77. Lee, S. M., Shokri, A. A., & Al-Mansour, A. I. (2019). Evaluation of the Applicability of the Ramp Metering to a Freeway Using Microsimulation: A Case Study in Riyadh, Saudi Arabia*. Applied Sciences, 9*(20), 4406.

78. Lehto, M. R., Papastavrou, J. D., Ranney, T. A., & Simmons, L. A. (2000). An experimental comparison of conservative versus optimal collision avoidance warning system thresholds. *Safety Science, 36*(3), 185–209.

79. Levinson, D., & Zhang, L. (2006). Ramp meters on trial: Evidence from the Twin Cities metering holiday. *Transportation Research Part A: Policy and Practice, 40*(10), 810–828.

80. Li, P., & Abdel-Aty, M. (2022). Real-Time Crash Likelihood Prediction Using Temporal Attention–Based Deep Learning and Trajectory Fusion. *Journal of Transportation Engineering, Part A: Systems, 148*(7), 04022043.

81. Lighthill, M.J., & Whitham, G.B. (1955). On Kinematic Waves. II. A Theory of Traffic Flow on Long Crowded Roads. *Proceedings of the Royal Society of London A: Mathematical, Physical and Engineering Sciences, 229*(1178), 317-345.

82. Lin, L., Wang, Q., & Sadek, A.W. (2015). A novel variable selection method based on frequent pattern tree for real-time traffic accident risk prediction. *Transportation Research Part C: Emerging Technologies, 55*, 444–459.

83. Liu, C., & Wang, Z. (2013). Ramp Metering Influence on Freeway Operational Safety near On-ramp Exits. *International Journal of Transportation Science and Technology, 2*(2), 87–94.

84. Liu, H.X., & Ma, W. (2009). A virtual vehicle probe model for time-dependent travel time estimation on signalized arterials. *Transportation Research Part C: Emerging Technologies, 17*(1), 11-26.

85. Liu, H.X., Wu, X., Ma, W., & Hu, H. (2009). Real-time queue length estimation for congested signalized intersections. *Transportation Research Part C: Emerging Technologies, 17*(4), 412-427.

86. Ma, W., He, Z., Wang, L., Abdel-Aty, M., & Yu, C. (2021). Active traffic management strategies for expressways based on crash risk prediction of moving vehicle groups. *Accident Analysis & Prevention, 163*, 106421.

87. MacCarley, C.A. (2005a). Methods and Metrics for Evaluation of an Automated Real-Time Driver Warning System. *Transportation Research Record, 1937,* 87-95.

88. MacCarley, C.A. (2005b). Instrumentation and Evaluation of District 10 Caltrans Automated Warning System (CAWS): Evaluation of Traffic Safety Influence Based on Historical Collision data.

89. Maerivoet, S., & De Moor, B. (2005). Traffic Flow Theory, Transportation Research Board, Washington, D.C..

90. Michalopoulos, P., & Stephanopoulos, G. (1981). An application of shock wave theory to traffic signal control. *Transportation Research Part B: Methodological, 15*(1), 35-51.

91. Michalopoulos, P.G., & Stephanopoulos, G. (1977a). Oversaturated signal systems with queue length constraints—I: Single intersection. *Transportation Research, 11*(6), 413-421.

92. Michalopoulos, P.G., Stephanopoulos, G. (1977b). Oversaturated signal systems with queue length constraints—II: Systems of intersections. *Transportation Research, 11*(6), 423-428.

93. Mirchandani, P.B., & Zou, N. (2007). Queuing Models for Analysis of Traffic Adaptive Signal Control*. Intelligent Transportation Systems, IEEE Transactions, 8*(1), 50-59.

94. Mohamed, S. A., Mohamed, K., & Al-Harthi, H. A. (2017). Investigating Factors Affecting the Occurrence and Severity of Rear-End Crashes. *Transportation Research Procedia, 25,* 2098–2107.

95. Montella, A., Colantuoni, L., & Lamberti, R. (2008). Crash Prediction Models for Rural Motorways. *Transportation Research Record, 2083,* 180–189. doi:10.3141/2083-21

96. Mudgal, A., & Hourdos, J. (2017). *Impact of Variable Speed Limits on Freeway Rear-End Collisions* (Number: 17-05229)., Transportation Research Board, Washington, D.C.

97. Naderan, A., & Shahi, J. (2010). Aggregate crash prediction models: Introducing crash generation concept. *Accident Analysis and Prevention, 42*(1), 339–346. doi: 10.1016/ j.aap. 2009.08.020

98. National Research Council. (2010). *Highway Safety Manual* (1st edition). American Association of State Highway and Transportation Officials, Washington, D.C.

99. Newell, G.F. (1965). Approximation Methods for Queues with Application to the Fixed-Cycle traffic Light. *SIAM Review,* 7(2), 223-240.

100. Nezamuddin, N., Jiang, N., Ma, J., Zhang, T., & Waller, S. T. (2011a). *Active Traffic Management Strategies: Implications for Freeway Operations and Traffic Safety* (Number: 11-3091)., Transportation Research Board, Washington, D.C.

101. Nezamuddin, N., Jiang, N., Zhang, T., Waller, S. T., & Sun, D. (2011b). *Traffic Operations and Safety Benefits of Active Traffic Strategies on TxDOT Freeways* (Number: FHWA/TX-12/0-6576-1).

102. NHTSA. (2018, October). U.S. DOT Announces 2017 Roadway Fatalities Down. Retrieved from www.nhtsa.gov/press-releases/us-dot-announces-2017-roadway-fatalities-down.

103. Office of Transportation System Management. (2018). Benefit-Cost Analysis for Transportation Projects, Minnesota Department of Transportation. Retrieved from www.dot.state.mn.us/planning/program/appendix_a.html.

104. Organization for Economic Co-operation and Development. (2003). *Road Safety: Impact of New Technologies*, Organization for Economic Co-Operation and Development, , Transportation Research Board, Washington, D.C..

105. Papastavrou, J. D., & Lehto, M. R. (1996). Improving the effectiveness of warnings by increasing the appropriateness of their information content: Some hypotheses about human compliance. *Safety Science, 21*(3), 175–189.

106. PARASURAMAN, R., HANCOCK, P. A., & OLOFINBOBA, O. (1997). Alarm effectiveness in driver-centered collision-warning systems. *Ergonomics, 40*(3), 390–399.

107. Pei, X., Wong, S. C., & Sze, N. N. (2011). A joint-probability approach to crash prediction models. *Accident Analysis and Prevention, 43*(3), 1160–1166. doi: 10.1016/ j.aap. 2010.12.026

108. Pesti, G., Wiles, P., Cheu, R., Songchitruska, P., Shelton, J., & Cooner, S. (2007). *Traffic Control Strategies for Congested Freeways and Work Zones*, Texas Department of Transportation, Austin, TX.

109. Piotrowicz, G., & Robinson, J. (1995). *Ramp Metering Status in North America, 1995 Update* (Technical Report DOT-T-95-17). USDOT Washington DC.

110. Pu, L., & Joshi, R. (2008). *Surrogate safety assessment model (SSAM): Software user manual* (Technical Report FHWA-HRT-08-050), Federal Highway Administration, Washington, D.C.

111. Qiu, L., & Nixon, W. A. (2008). Effects of Adverse Weather on Traffic Crashes: Systematic Review and Meta-Analysis. *Transportation Research Record, 2055*(1), 139–146.

112. Fakharian Qom, S., Hadi, M., Xiao, Y., & Al-Deek, H. (2017). Queue Length Estimation for Freeway Facilities: Based on Combination of Point Traffic Detector and Automatic Vehicle

Identification Data. Transportation Research Record, 2616(1), 19–26. https://doi.org/10.3141/2616-03.

113. Ren, H., Song, Y., Wang, J., Hu, Y., & Lei, J. (2017). A Deep Learning Approach to the Citywide Traffic Accident Risk Prediction. 21st International Conference on Intelligent Transportation Systems (ITSC) (pp. 3346-3351). IEEE

114. Richards, P.I. (1956). Shock Waves on the Highway. *Operations Research, 4*(1), 42-51.

115. Rindels, M., Zitzow, S., & Hourdos, J. (2016). *Evaluation of the Effectiveness of ATM Messages Used During Incidents*, Minnesota Department of Transportation. Retrieved from http://hdl.handle.net/11299/178993.

116. Robertson, D.I. (1969). *TRANSY: A traffic network study tool.* Road Research Laboratory, Crowthorne, UK.

117. Rouphail, N.M., Courage, K.G., & Strong, D.W. (2006). New Calculation Method for Existing and Extended Highway Capacity Manual Delay Estimation Procedures. Paper presented at the Transportation Research Board 85th Annual Meeting, Washington, D.C.

118. Roy, A., Hossain, M., & Muromachi, Y. (2018). Enhancing the Prediction Performance of Real-Time Crash Prediction Models: A Cell Transmission-Dynamic Bayesian Network Approach. *Transportation Research Record, 2672*(38), 58–68. https://doi.org/10.1177/0361198118797802

119. Sharma, A., Bullock, D.M., & Bonneson, J.A. (2007). Input–Output and Hybrid Techniques for Real-Time Prediction of Delay and Maximum Queue Length at Signalized Intersections. *Transportation Research Record, 2035*, 69-80.

120. Sheu, J., Chou, Y., & Shen, L. (2001). A stochastic estimation approach to real-time prediction of incident effects on freeway traffic congestion. *Transportation Research Part B: Methodological, 35*(6), 575-592.

121. Skabardonis, A., & Geroliminis, N. (2008). Real-time Monitoring and Control on Signalized Arterials. *Journal of Intelligent Transportation Systems, 12*(2), 64-74.

122. Stanitsas, P., Hourdos, J., & Zitzow, S. (2014). *Evaluation of the Effect of MnPASS Lane Design on Mobility and Safety* (Technical Report MN/RC 2014-23), Minnesota Department of Transportation, St. Paul, MN.

123. Sun, C., Edara, P., & Zhu, Z. (2013). Evaluation of Temporary Ramp Metering for Work Zones. *Transportation Research Record, 2337*(1), 17–24.

124. Transportation Research Board. (2010). *Highway Capacity Manual 2000*, TRB, Washington, D.C.

125. Treiber, M., & Helbing, D. (2002). Reconstructing the Spatio-Temporal Traffic Dynamics from Stationary Detector Data. *Cooper@tive Tr@nsport@tion Dyn@mics,* 24.

126. Treiber, M., Kesting, A., & Wilson, R.E. (2009). Reconstructing the Traffic State by Fusion of Heterogeneous Data. C*omputer-Aided Civil and Infrastructure Engineering, 26*(6), 408–419. arXiv: 0909.4467.

127. Ullman, G. L., Iragavarapu, V., & Brydia, R. E. (2016). Safety Effects of Portable End of-Queue Warning System Deployments at Texas Work Zones. *Transportation Research Record, 2555*(1), 46–52.

128. Vigos, G., Papageorgiou, M. & Wang, Y. (2008). Real-time estimation of vehicle-count within signalized links. *Transportation Research Part C: Emerging Technologies, 16*(1), 18-35.

129. Wang, L., Abdel-Aty, M., & Lee, J. (2017). Implementation of Active Traffic Management Strategies for Safety on Congested Expressway Weaving Segments. *Transportation Research Record, 2635*(1), 28–35.

130. Wang, S.-Y., Cheng, Y.-W., Lin, C.-C., Hong, W.-J., & He, T.-W. (2008). A Vehicle Collision Warning System Employing Vehicle-To-Infrastructure Communications. *2008 IEEE Wireless Communications and Networking Conference,* 3075–3080. ISSN: 1558-2612.

131. Webster, F.V. (1958). *Traffic Signal Settings* (Road Research Technical Paper, 39).

132. Webster, F.V., & Cobbe, B.M. (1966). *Traffic signals*. London: H.M.S.O.

133. Weng, J., & Meng, Q. (2013). Estimating capacity and traffic delay in work zones: An overview. *Transportation Research Part C: Emerging Technologies, 35*, 34-45.

134. Wrapson, W., Harré, N., & Murrell, P. (2006). Reductions in driver speed using posted feedback of speeding information: Social comparison or implied surveillance? *Accident Analysis & Prevention, 38*(6), 1119-1126.

135. Wu, J., Jin, X., & Horowitz, A. (2008). Methodologies for Estimating Vehicle Queue Length at Metered On-Ramps. *Transportation Research Record, 2047*(1), 75-82.

136. Wu, X., & Liu, H.X. (2011). A shockwave profile model for traffic flow on congested urban arterials. *Transportation Research Part B: Methodological, 45*(10), 1768-1786.

137. Xi, J., Guo, H., Tian, J., Liu, L., & Sun, W. (2019). Analysis of influencing factors for rear-end collision on the freeway. *Advances in Mechanical Engineering, 11*(7), 1687814019865079.

138. Yang, G., & Tian, Z. (2019). An exploratory investigation of the impact of ramp metering on driver acceleration behavior. *IATSS Research, 43*(4), 277–285.

139. Zabyshny, A. A., & Ragland, D. R. (2003). False Alarms and Human-Machine Warning Systems. Research Report. UC-Berkeley, Berkeley CA

140. Zheng, Z., Ahn, S., & Monsere, C. M. (2010). Impact of traffic oscillations on freeway crash occurrences. *Accident Analysis and Prevention, 42*(2), 626–636. doi: 10.1016/j.aap.2009.10.009